The basic equipment for pathogen recognition in *Marchantia polymorpha*

Dissertation

der Mathematisch-Naturwissenschaftlichen Fakultät

der Eberhard Karls Universität Tübingen

zur Erlangung des Grades eines

Doktors der Naturwissenschaften

(Dr. rer. nat.)

vorgelegt von

Maike Osterhus

aus Lohne

Tübingen

2022

Gedruckt mit Genehmigung der Mathematisch-Naturwissenschaftlichen Fakultät der Eberhard Karls Universität Tübingen.

Tag der mündlichen Qualifikation:	26.08.2022
Dekan:	Prof. Dr. Thilo Stehle
1. Berichterstatter:	Prof. Dr. Georg Felix
2. Berichterstatterin:	Prof. Dr. Rosa Lozano-Durán

Table of Content

1 Introduction

Plants are exposed to an enormous number of environmental factors and conditions that have impacts on their growth and survival. These factors can be of abiotic or biotic nature. During plant terrestrialization early land plants had to cope with a number of abiotic stresses, like drought and UV-radiation (de Vries and Archibald, 2018). However, also biotic factors were present. Today it is known that already streptophyte algae and early bryophytes are associated with a "suite of N fixers, methanotrophs, cobalamin producers, and early-diverging fungi" (J. J. Knack et al., 2015) but also with pathogenic or parasitic microorganisms (Han, 2019). As a representative of the liverworts, a plant lineage that split from the lineage of vascular plants around 450 MYA, *Marchantia polymorpha* is of interest as a model organism for studying aspects of evolution in land plants (Bowman et al., 2017a). With its phylogenetic position and relatively small genome, *M. polymorpha* is attractive for comparative studies on the conservation and divergence of genes in different land plants during the long separate evolution since terrestrialization.

1.1 Plant-microbe interactions 450 MYA

A mutualistic microbe-plant interaction, which is significant for plant nutrition when growing on soil, is the interaction with mycorrhizal fungi (Rich et al., 2021). Arbuscular mycorrhiza (AM) is already present in 450 MYA old fossils of early bryophytes (Ligrone et al., 2007; Redecker et al., 2000) and *Marchantia paleacea* (Rich et al., 2021). Genome analysis also revealed the presence and conservation of three genes which are evolutionary linked to AM and involved in lipid exchange in all land plant lineages (Radhakrishnan et al., 2020). Evidence for further interactions with microbes was obtained by characterization of the microbiome associated with the non-vascular bryophyte *M. polymorpha* (Nelson and Shaw, 2019; Nelson et al., 2018; Matsui et al., 2020; Alcaraz et al., 2018). This microbiome indicated that *M. polymorpha,* apart from its mutualistic interaction with AM, has to cope also with numerous potentially pathogenic microbes. Thus, *M. polymorpha* might have defense mechanisms such as the ones known from vascular land plants like the model plant *Arabidopsis thaliana* (Yu et al., 2017). The question whether *M. polymorpha* has a defense equipment, comparable with the one of *A. thaliana* stays at the center of this thesis.

Based on the microbiome data, Nelson et al., (2018) predicted the presence of growth-inhibiting fungi, however, experimental data confirming such fungal effects are still in demand and methods to evaluate interactions of microbes with *M. polymorpha* have to be established further. The oomycete *Phytophthora palmivora* is able to grow into the thallus of *M. polymorpha*, as well as to cause transcriptional changes. This represents a first line of evidence that these bryophytes, when attacked by microbial pathogens, respond with activation of defense responses that involve elements known from the immune response of vascular plants (Carella et al., 2017; Carella and Schornack, 2018; Carella et al., 2019). Gimenez-Ibanez et al., (2019) investigated the response of *M. polymorpha* to the well-known bacterial pathogen *Pseudomonas syringae (Pto* DC3000*)*. Inoculation of thallus with high titers of bacteria caused disease symptoms, thallus growth inhibition and marker gene upregulation. The fungal species *Loreleia marchantiae* and *L. postii* have been found in close association with Marchantiaceae (**Figure 1** a; Kost, 1998). Hyphae of *L. postii* were detected in rhizoids of *M. polymorpha* (**Figure 1** b) and resemble an invasive growth of a fungus in specific tissues of bryophytes.

Figure 1: *Loreleia* species associated with *M. polymorpha*. a) *L. marchantiae* growing on *M. polymorpha* (https://swissfungi.wsl.ch). **b)** Rhizoid of *M. polymorpha* with internal hyphae of *Gerronema postii* (synonym of *L. postii*). Microscopic pictures from Kost, (1988). c= clamp connection, p= peg of the rhizoid, scale bar= 10 µM.

In summary, there are several examples of the occurrence of microbes in association with bryophytes. However, whether bryophytes recognize these microbes via immunoprecipitation systems that lead to activation of defense responses as it is well established for vascular plants remains to be elucidated and represents a focus of this thesis.

1.2 *Marchantia polymorpha,* a model bryophyte

M. polymorpha occurs in its dominant gametophytic vegetative plant body, the thallus. The tissue of the thallus can be divided into three layers (**Figure 2**). The upper epidermis, coated by a cuticle and interrupted by air pores, covers an assimilation area with chloroplast-rich cells. A storage region with parenchymal cells connects the upper and the lower epidermis, the latter bearing rhizoids and scales (**Figure 2**; Shimamura, 2016). The pores in the upper layer form air chambers that ensure gas exchange (**Figure 2**). However, these pores are not closable und thus represent potential entry sites for pathogenic organisms to the inner tissue of the plants.

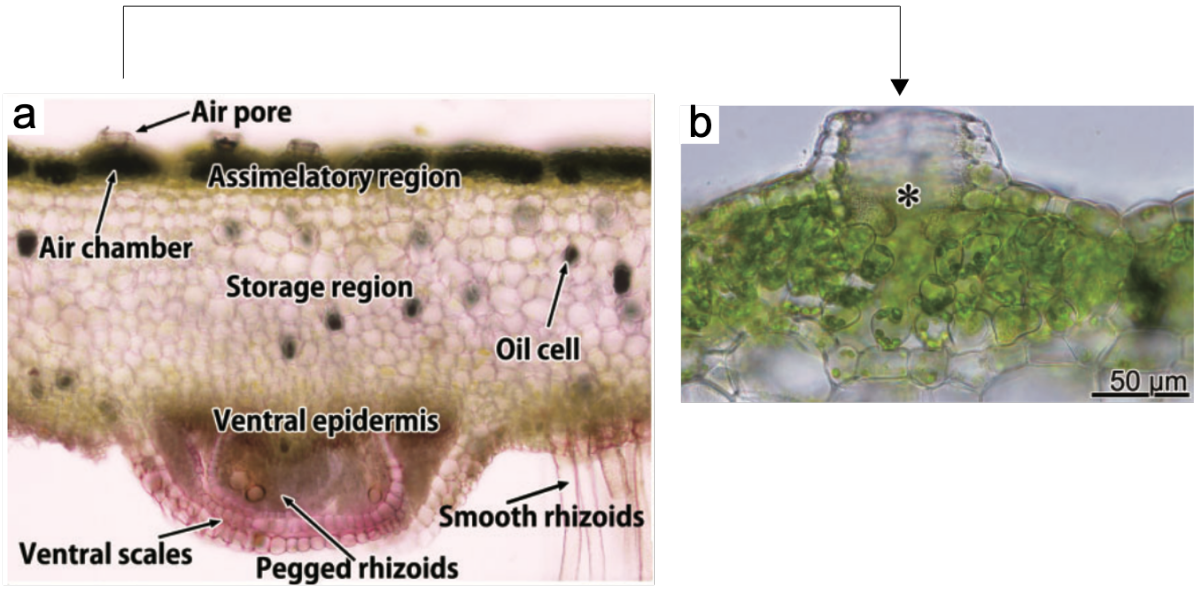

Figure 2: Transverse sections of *M. polymorpha* thallus (Shimamura, 2016). a) Thallus structure consistent of three main regions. **b)** Section of air chamber with air pore (asterisk).

Box 1: *M. polymorpha* propagation

thallus: vegetative plant body

gemmae: vegetative propagules with two apical meristems

gemma cups: cup-shaped organ in which the gemmae develop

gametangiophore: sexual reproductive structure

gametangia: develop in the gametangiophores; umbrella-like archegoniophores with antheridia (female, on which egg cells develop) and disc-shaped antheridiophores with antheridia (male, generating spermatozoids)

The propagation of *M. polymorpha* can be sexual or asexual. The thallus is producing gemma cups which emerge at every dichotomous branching point and produce a high number of gemmae (**Figure 3** a,b). Gemmae are of clonal origin and develop from a single stalk cell until they are mature multicellular gemmae which detach from the

bottom of the gemma cup (**Figure 3** c). The sexual propagation proceeds with the development of gametangiophores (**Figure 3**). The female thallus produces archegoniophores with egg cell-producing archegonia. Male thalli produce antheridiophores with antheridia, which produce spermatozoids. The mobile spermatozoids reach the egg cells by water. After fertilization the zygote develops into a sporophyte (diploid). At its mature stage the sporophyte produces sporangia where meiosis gives rise to haploid spores. Spores are released by opening of the spore capsules and are distributed by wind and water (**Figure 38**, Althoff et al., 2014).

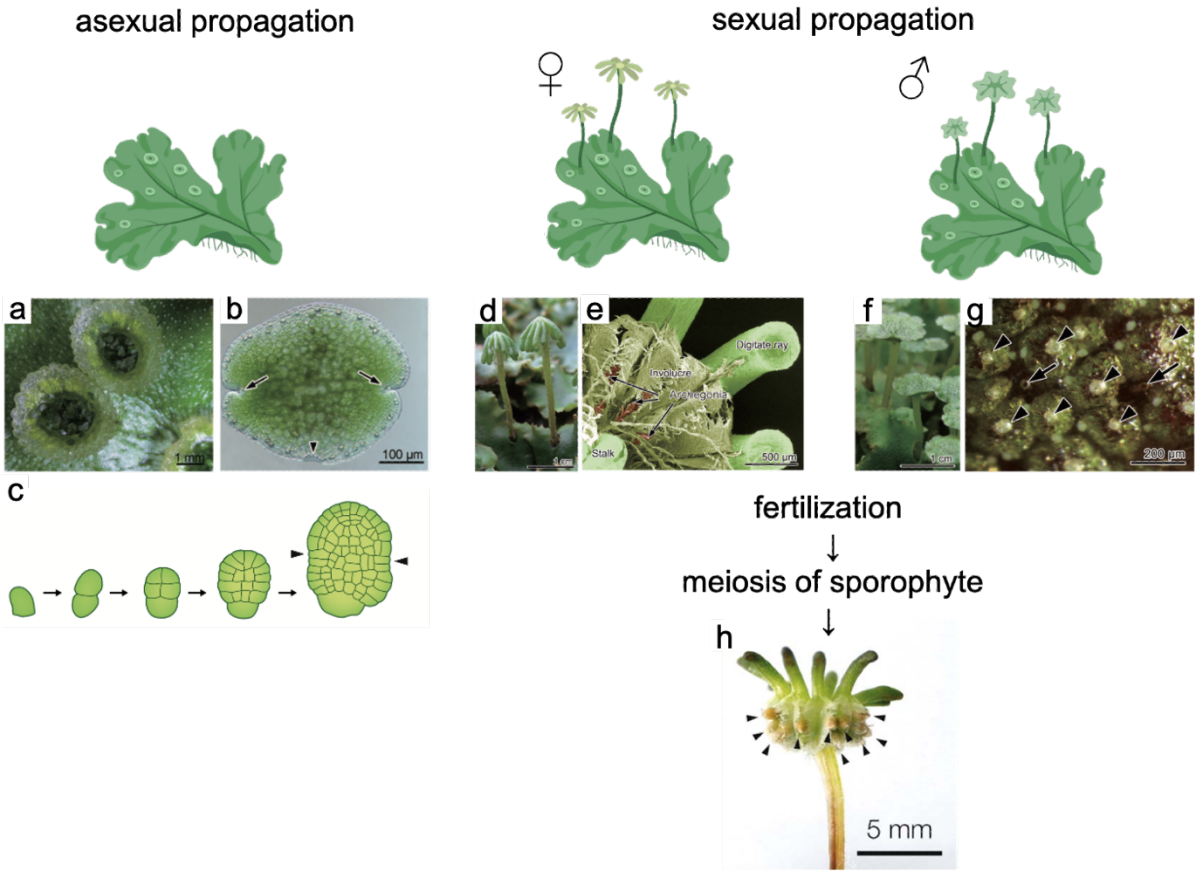

Figure 3: Asexual and sexual propagation of *M. polymorpha*. Figures modified from Biorender, Shimamura (2016), Chiyoda et al. (2008) and Kato et al. (2020). a) Gemma cups filled with gemmae. **b)** Gemma with two apical notches (arrows) and the stalk trace (arrowhead). **c)** Gemmae development from a single cell to multicellular gemmae with apical meristems (arrowhead) **d)** Archegoniophores. **e)** Ventral view on archegoniophore showing the receptacle (scanning electron microscopy (SEM) picture). **f)** Antheridiophores. **g)** Dorsal surface view of an antheridial receptacle with air pores (arrows) and antheridial pores (arrowhead). **h)** Archegoniophore with mature sporangia (arrowhead).

With respect to plant microbe interactions, *M. polymorpha* represents an interesting model not least because of the ecological niche they occupy. Generally, they occur in very moist areas in close proximity to a multitude of microbes. The invasion by putative pathogens is thus very likely. *In vitro*, the successful infection with *P. palmivora*, a broad host-range oomycete pathogen, was shown to be dependent on air chambers. The lack of air chambers as in the *nop1* mutant was causing a reduced pathogen

fitness (Carella et al., 2017). Secondary metabolites with an antimicrobial effect like marchantin A have been described as well (Jensen et al., 2012), but cannot autonomously block infection by pathogens. The lack of sophisticated physiological barriers in combination with the characteristics of the habitat, thus, led to expect that liverworts have to be able to protect themselves against putative pathogenic microbes on various levels.

1.3 Thriving in a changing environment

Fending of pathogenic microbes while allowing interactions with mutualistic partners is essential to maintain plant vitality. Bryophytes are known to possess a constitutive defense via secondary metabolites with antimicrobial activity, like marchantin A (Jensen et al., 2012) or flavonoids (Mewari and Kumar, 2011). However, for the distinction between putative pathogenic and mutualistic microbes a more precise and inducible mechanism is needed. From angiosperms we know sensing mechanisms which provide the ability to react to the presence of specific microbes.

1.3.1 Perceiving the danger

The first, essential, step for activation of plant responses is the perception of a microbe. Specific molecular patterns of microbes, microbe-associated molecular patterns (MAMPs), can be recognized at the plant cell surface and activate a downstream response cascade. These microbe-derived patterns can be, inter alia, peptides, lipophilic substances like sterols and fatty acids or oligosaccharides (Yu et al., 2017). In addition, plants can sense damage-associated molecular patterns (DAMPs), which are plant-derived signals released in the context of pathogen attack (Boller and Felix, 2009).

The detection of MAMPs/DAMPs is ensured by pattern recognition receptors (PRRs) which transmit extracellular signals across the membrane into the cell (Hohmann et al., 2017). The interplay between MAMPs/DAMPs and PRRs is called pathogen-associated molecular pattern (PAMP)-triggered immunity (PTI). A second form or layer of defense is termed effector-triggered immunity (ETI, **Figure 4**). Virulence factors produced by pathogens (effectors), ending up in the cytoplasm of the host cells, will be detected by cytoplasmic immune receptors commonly termed resistance proteins (RP). The main group of R-genes is represented by the nucleotide-binding domain leucine-rich repeat (NLR) receptors. Both, PTI and ETI, are however constantly

evolving by the ongoing selection pressure and are known to act in concert to stop pathogenic infections (**Figure 4**, Pruitt et al., 2021).

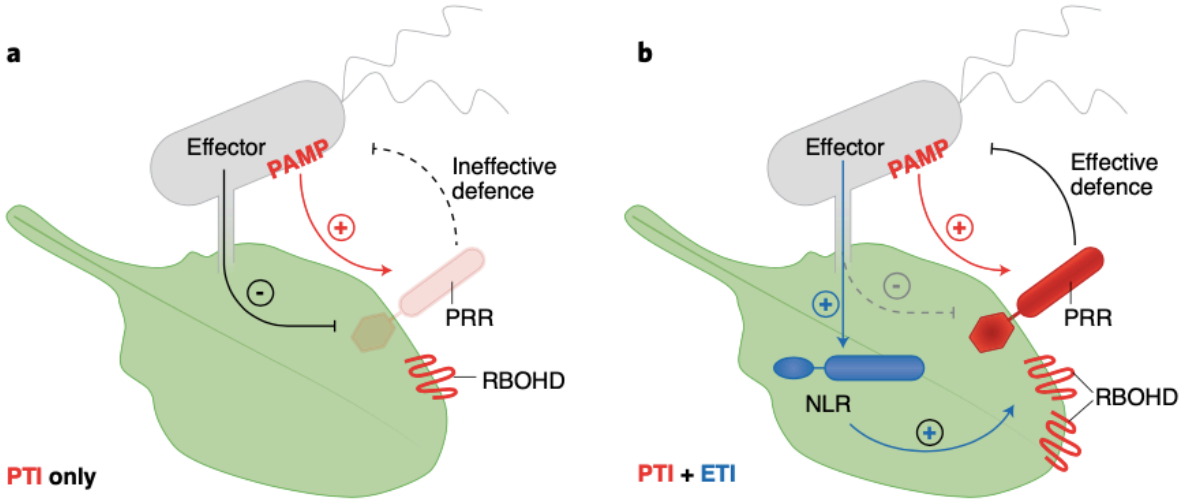

Figure 4: Interplay between PTI and ETI. Pruitt et al., (2021) visualized the interplay between PTI (red) and ETI (blue). **a)** Effectors are pathogen-derived molecules, which are able to block (dotted line) PTI (red line). **b)** However, the plant evolved perception mechanisms via NLR receptors to bypass this effect by perceiving effectors and initiating further responses, which for example result in upregulation of the NADPH oxidase respiratory burst oxidase homolog protein D (RBOHD) (blue line) and thus restore effective defense against invaders.

PRRs can be classified by their ectodomain (ECD). Receptors with leucine-rich repeats (LRR) represent the most common group of PRRs and are present in all kingdoms of life (Kobe and Kajava, 2001). LRRs are organized repeated units with a hydrophobic core and multiple name-giving leucine residues. Further differentiation within the LRR-receptors is caused by the presence or absence of a cytoplasmic kinase domain (**Figure 5**). Receptors with a cytoplasmic kinase are called LRR receptor-like kinases (LRR-RLKs), is the kinase domain missing the receptor is defined as a LRR receptor-like protein (LRR-RLP). Ectodomains of LRR-receptors, within both groups, show further differences, which are caused by the number of LRRs and the presence or absence of an island domain. However, the hydrophobic core of the ectodomain is formed in all cases with a high amount of apolar residues (Kobe and Kajava, 2001). Another group of plasma membrane-associated receptors features instead of a LRR-ECD a domain which is composed of three lysin motifs (LysM) (**Figure 5**) and binds N-acetyl-D-glucosamine-derived carbohydrates (NGA). Other surface receptors have an epidermal growth factor (EGF)- or lectin type ectodomain (**Figure 5**).

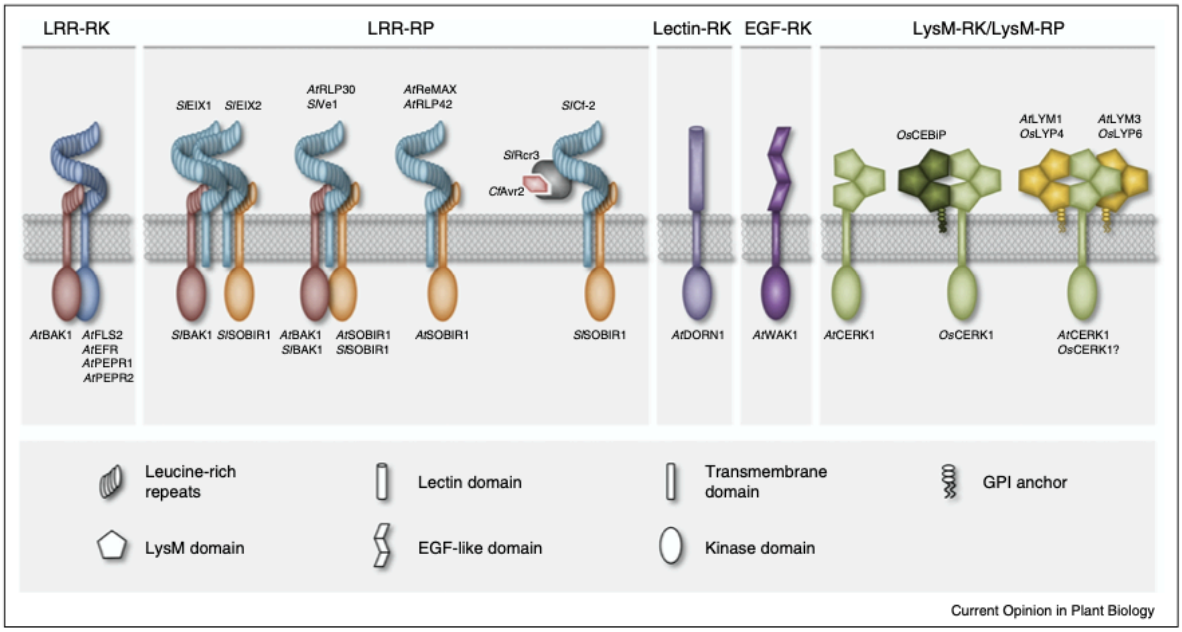

Figure 5: Types of plasma membrane-localized immune receptors (Böhm et al., 2014a). The most common group is represented by leucine-rich repeat (LRR) containing receptors, which can be further differentiated by the presence (LRR-RLK) or the absence (LRR-RLP) of the cytoplasmic kinase domain. Lysin motif (LysM) receptors bind NAG-containing carbohydrates and are known to build hetero- and homodimers leading to an activation of their cytoplasmic kinase domains and thus initiation of an immune response. Epidermal growth factor (EGF)- and lectin receptor kinases (RKs) complete the group of surface-exposed receptor. In most cases the anchoring in the plasma membrane is assured by a transmembrane (TM) domain, however in some cases this TM-domain is substituted by a glycosylphosphatidylinositol (GPI) anchor.

Some receptors are specific to a special microbe whereas others target more common MAMPs. Chitin, a major component of fungal cell walls and the exoskeleton of insects, represents an elicitor which is widely spread (Delaux und Schornack, 2021). The chitin elicitor-binding protein (CEBiP) binds chitin in rice (Kaku et al., 2006). A second receptor was identified working as a co-receptor for OsCEBiP – the chitin elicitor receptor kinase (CERK; Hayafune et al., 2014). Both, CEBiP and CERK contain a LysM domain, with the difference that CEBiP lacks the intracellular domain (**Figure 5**). CEBiP-like LysM-RLPs (LYMs) and CERK-like LysM receptor kinases (LYKs) exist in all angiosperms and function via homo- and heteromeric complex formation (Cao et al., 2014; Liu, Simiao et al., 2016; Liu et al., 2012; Willmann et al., 2011). Another common target is flagellin. Flagella are widely distributed in bacteria, as well as the perception of flagellin-derived epitopes which can thus be found in a large number of plant families (Albert et al., 2010b; Fürst et al., 2020). The LRR-RLK Flagellin Sensing 2 (FLS2) perceives a 22-amino acid long peptide epitope of bacterial flagella (flg22; Felix et al., 1999). Ubiquitously present receptors like CEBiP, CERK, or FLS2 however are not the rule but rather the exception. More like effectors, specific patterns are perceived by diverse surface receptors. An example of a more restricted MAMP

perception is the recognition of a 18-amino acid long peptide epitope of the bacterial elongation factor Tu (EF-TU, elf18), by the EF-Tu receptor (EFR) (Zipfel et al., 2006). Even though EF-Tu is ubiquitously present in bacteria, EFR is restricted to the Brassicaceae (Kunze et al., 2004; Zipfel et al., 2006). The perception of endopolygalacturonases (PG), a fungal protein, by RLP42 is triggering plant defense responses in Brassicaceae species (Zhang et al., 2014, 2021). Numerous examples could be given for specific molecular cues and the knowledge of additional MAMPs/DAMPs and effectors is steadily increasing.

1.3.2 Perceiving endogenous signals

Besides the perception of microbes, plants also perceive internal signals to ensure plant development and reproduction. The same types of surface receptors as in PTI are involved in sensing internal signals. One example of such a ligand-receptor pair is the peptide ligand IDA (inflorescence deficient in abscission) that is detected by the LRR-RLK HAESA (HAE) and HAE-like2 (HSL2) in all flowering plants (Butenko, 2003; Shi et al., 2019). The petals in *ida* knock-out mutants of *A. thaliana* detach later in comparison to the wildtype (Stenvik et al., 2008). This is congruent with the *hae hls2* double mutant, which shows a similar abscission phenotype by delayed floral organ abscission (Stenvik et al., 2008). Overexpression of IDA is causing the opposite effect and induces an earlier loss of these organs (Stenvik et al., 2006). These findings are consistent with the expression pattern of IDA and HAE/HSL2, which are mainly expressed in the abscission zone (AZ) at the base of the sepals, petals and filaments (Butenko, 2003; Cho et al., 2008). *A. thaliana* encodes eight IDA-like (IDL) peptides in addition to IDA (Butenko, 2003). Complexes of IDA/IDL with HAE/HSL2 are also involved in the control of cell separation processes, like root cap sloughing and lateral root emergence (Aalen et al., 2013; Kumpf et al., 2013; Zhu et al., 2019; Shi et al., 2018). Mature IDA peptides have to exhibit several features to be active *in planta*. First, the central proline of the minimal 12-amino acid peptide has to be hydroxylated and second, it has to encode an extended PIP (EPIP) motif (Santiago et al., 2016; Butenko et al., 2014a).

1.3.3 Essential collaboration of LRR-receptors and their co-receptors

Signal perception and transduction is generally performed by receptor complexes. As introduced, FLS2 is perceiving flg22 with its ectodomain. However, this is not sufficient

to activate the cytoplasmic kinase of FLS2. For transmembrane activation of a cytoplasmic response cascade a second LRR-RLK of the somatic embryogenesis receptor kinases (SERKs) family is required (Sun et al., 2013). SERKs are known to act as co-receptors in a multitude of processes involved in development and immunity (Figure 6; aan den Toorn et al., 2015; Fan et al., 2016; Ma et al., 2016; Chinchilla et al., 2009). The knock-out of all SERK proteins in *A. thaliana* is lethal, underlining the key function of these proteins in a multitude of processes (Gao et al., 2009). The single mutant of AtSERK3, also termed BRI1-associated receptor kinase 1 (BAK1), *bak1-4* already shows reduced responsiveness to treatment with flg22 and overexpression results in dwarfism and leaf necrosis (Chinchilla et al., 2007; Domínguez-Ferreras et al., 2015). SERKs also play a role in the sensing of internal signals. HAE/HSL2 is building a heterodimer with a SERK protein after binding of the IDA/IDL ligands. Subsequently, the heterodimer is activating downstream signaling, which results in floral organ abscission. Arabidopsis plants with mutations in several of their SERK genes show delayed abscission of their floral organs much like *ida* and *hae hsl2* double mutants, indicating the involvement of SERKs (Meng et al., 2016).

In contrast to RLKs, RLPs lack a cytoplasmic kinase domain and are thus in need of a second adaptor kinase. The suppressor of BAK1-interacting receptor-like kinase (BIR1) – 1 (SOBIR1) acts as an adaptor kinase and interacts constitutively with RLPs. Upon perception of an appropriate ligand, a SERK protein is recruited and the kinase domains get into close proximity which initiates signaling (**Figure 6**; Gust and Felix, 2014).

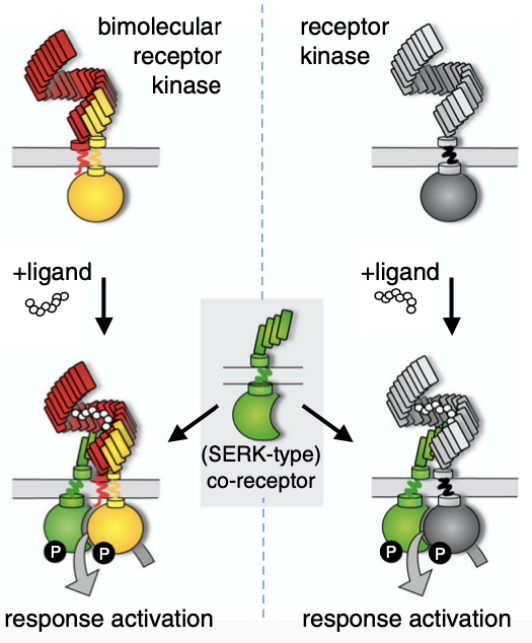

Figure 6: Ligand-induced receptor activation by interaction with co-receptors (figure modified from Gust and Felix, 2014). RLPs (red) constitutively interact with the adaptor kinase SOBIR1 (yellow) and additionally recruit a SERK-type co-receptor (green) after perception of a ligand. RLKs (gray) heterodimerize with SERK-type co-receptors subsequent to ligand binding.

SOBIR1 was initially identified in a suppressor screen of the *bir1-1* mutant. *bir1-1* mutants show an autoimmunity phenotype, loss of function of SOBIR1 in the *bir1-1* mutant background showed wildtype-like growth (Gao et al., 2009). Additionally, SOBIR1 loss of function results in a loss of RLP-mediated immune responses (Albert et al., 2015; Jehle et al., 2013b; Liebrand et al., 2013; Zhang et al., 2013; Postma et al., 2016; Catanzariti et al., 2017; Domazakis et al., 2018).

1.3.3.1 Negative regulators – controlling over-stimulation

The essential role of SERK and SOBIR proteins as adaptor-kinases and co-receptors in LRR-RLK and -RLP-mediated signal transmission was shown for several receptor complexes. However, an overactivation can also be harmful for the plant. Therefore, plants are additionally in need of negative regulatory mechanisms for the fine-tuning of cellular responses. BIRs have been identified in a screen for interactors of BAK1 and were shown to be negative regulators (Halter et al., 2014a). *A. thaliana* has a small gene family encoding four BIR proteins, which can be distinguished by a number of properties. The first difference concerns the activity of the kinase domain. The kinase domain of BIR1 is able to transphosphorylate other kinases and is thus considered active. In contrast, the kinase domains of BIR2, BIR3 and BIR4 are pseudokinases, which do not transphosphorylate. One essential region for kinase activity is the G-loop

which differs between the active and inactive kinase domains of BIR proteins (Blaum et al., 2014). The ectodomain is relevant for binding SERKs with high affinity, however the cytosolic kinase domains seem to be essential for signaling specificity (Hohmann et al., 2018).

The second property concerns the interaction with and release of co-receptors. All BIR proteins interact constitutively with a SERK. Differences between BIR proteins exist in the proteins they release the co-receptor to. BIR1 releases a SERK protein, which is subsequently interacting with a SOBIR/RLP complex after ligand perception by the RLP (**Figure 7** a; Gao et al., 2009; Liu et al., 2016, 1; Ma et al., 2017). In contrast, the pseudokinases BIR2 and BIR3 release the SERK to a RLK protein after binding of a ligand by a RLK (**Figure 7** b; Blaum et al., 2014; Imkampe et al., 2017; Halter et al., 2014; Hohmann et al., 2018). For BIR3 it is additionally reported that it interacts with RLK receptors, like brassinosteroid (BR)-insensitive 1 (BRI1), which perceives the plant hormone brassinosteroid and is involved in developmental processes. BIR3 inhibits BRI1-function until perception of brassinosteroid, by which the dissolution of the BIR3/BRI1 as well as BIR3/SERK complex is induced. Afterwards BRI1 is able to interact with a SERK and to initiate downstream responses (**Figure 7** b; Imkampe et al., 2017; Großeholz et al., 2020).

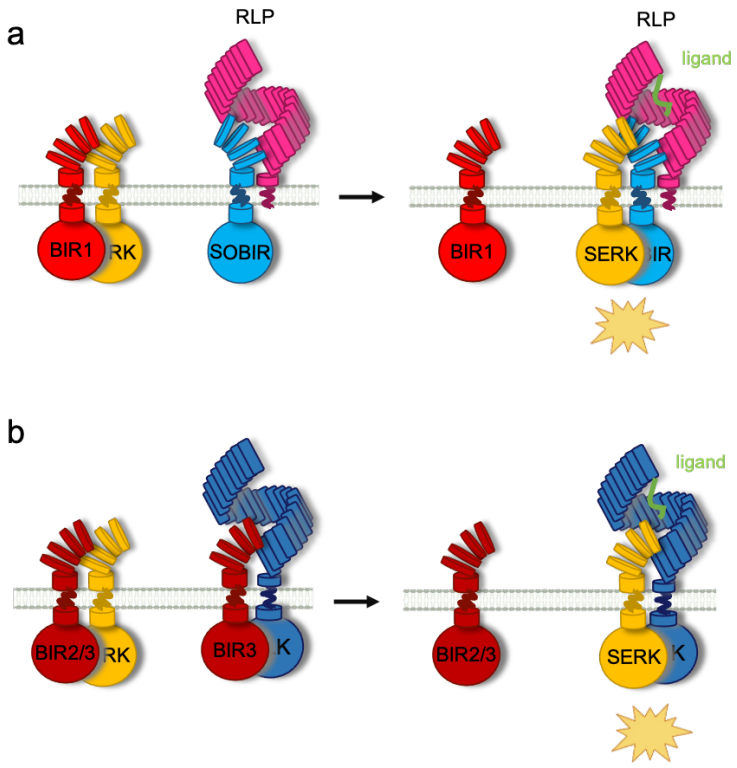

Figure 7: BIR interaction with PRRs is negatively regulating PTI. a) BIR1 is constitutively interacting with a SERK protein and releases SERK after ligand binding to a SOBIR/RLP complex. **b)** The pseudokinases BIR2 or BIR3 are also constitutively interacting with a SERK and release the co-receptor upon ligand binding of a RLK. Additionally, BIR3 is constitutively interacting with BRI1 and also releases BRI1 after perception of brassinosteroids.

All *bir* mutants (*bir1-1, bir2-1* and *bir3*) are hyperresponsive to treatment with MAMPs, (Halter et al., 2014a; Imkampe et al., 2017). In contrast to *bir1-1*, which is lethal, *bir2-1* and *bir3* mutants are however able to grow normally (Gao et al., 2009; Imkampe et al., 2017; Halter et al., 2014a).

1.3.4 Perception mechanisms in bryophytes

Apart from novel receptors to regulate novel developmental processes and plant organs, angiosperms are known to have evolved a multitude of surface receptors as potential immunoreceptors in the arms race between host plants and pathogens (Boller and He, 2009). In contrast, little is known about the arsenal of defense mechanisms and immunoreceptors in non-vascular plants. Genomic data available for the bryophyte *M. polymorpha* allow to identify potential immunoreceptor candidates (Delaux and Schornack, 2021; Han, 2019; Sasaki et al., 2007; Bowman et al., 2017a) and for phylogenetic analysis. LysM-RLKs evolved earlier than LRR-RLKs, which originated with the terrestrialization of plants (**Figure 8,** Delaux and Schornack, 2021). One of the most studied LysM-RLKs is the CERK receptor, which is involved in the perception of chitin. The moss *Physcomitrella patens* encodes a CERK1 ortholog, which is involved in the perception of chitin and other GlcNAC derivatives (Bressendorff et al.,2016). *cerk1-1* mutants showed no growth inhibition or MAPK activation by chitin treatment compared to the wildtype. *M. polymorpha* also encodes a CERK ortholog and treatment of thallus with chitin initiated ROS- and Ca^{2+}-burst (data not shown), two typical responses upon PRR activation (Yu et al., 2017). Interestingly, BAK1-likes are already present in Mesostigmatophyceae (basal green algae) and are thus already part of the equipment bevor terrestrialization (**Figure 8**; Delaux and Schornack, 2021). Considering the key function of the SERK protein family as essential co-receptors in angiosperms, the presence of BAK1-likes supports the hypothesis of potential PRR-mediated processes in early bryophytes.

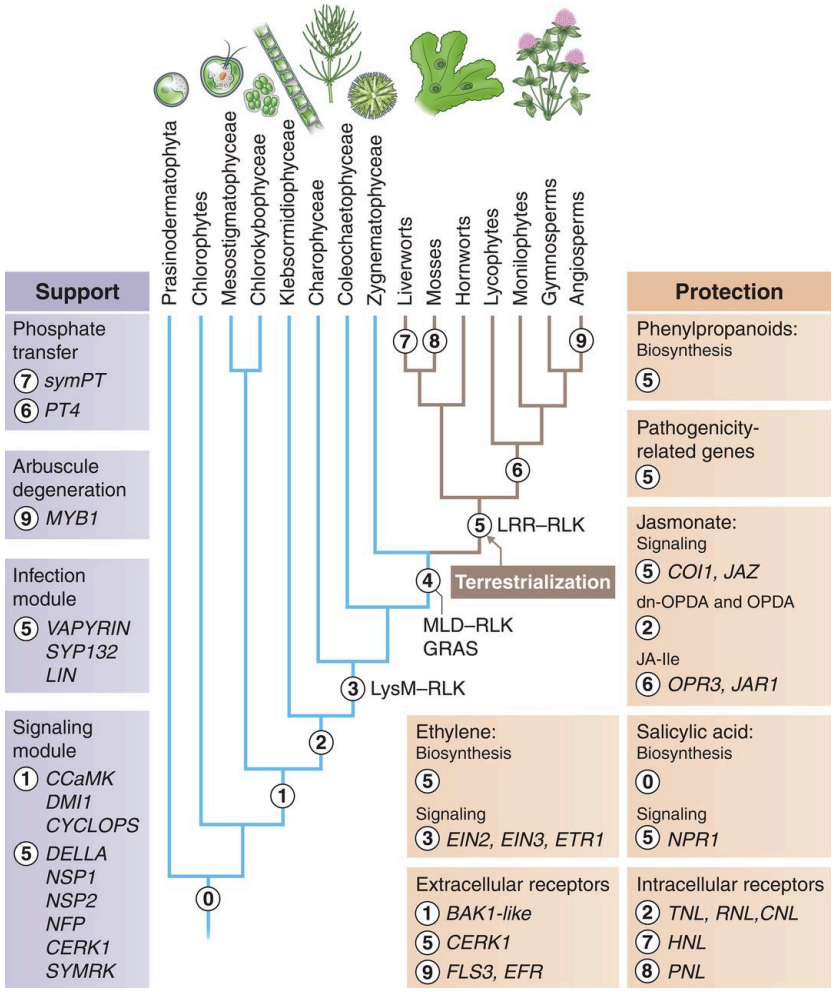

Figure 8: Gain of genes involved in plant microbe associations (Delaux and Schornack, 2021).

Besides perception mechanisms at the cell surface and subsequence activation of downstream response cascades, angiosperms also use structural and chemical barriers such as the cuticula and toxic metabolites (Xie and Lou, 2009; Freeman, 2008), to protect themselves against an infection. Bryophytes do produce antimicrobial metabolites, however do not possess structural barriers like stomata. They do build a cuticula, however stomata evolved in mosses and are thus not existent in liverworts (Bowman, 2011). Liverworts ensure their gas exchange by air pores, which present a direct connection to the inner tissues and thus do not act as a structural barrier for invaders (**Figure 38**), as stomata do in vascular plants (Melotto et al., 2017). By entering the air pores, for example the oomycete *P. palmivora* is able to invade the inner tissues of *M. polymorpha* (Carella et al., 2017). Further, the habitat of *M. polymorpha* has to be considered. Bryophytes mainly emerge in very moist areas in close proximity to fungi and a large number of other microbes (**Figure 1**), making an additional perception mechanism feasible.

It is very likely that, in addition to the chemical and structural barriers against invaders, some of the orthologs of PRRs in *M. polymorpha* are involved in sensing mechanisms to ensure plant health.

1.4 The aim – *M. polymorpha* and its basic equipment in signal perception

The presence of LRR-receptors and BAK1-like proteins in liverworts (Delaux and Schornack, 2021) indicates cell surface perception mechanisms in the ancient land plant *M. polymorpha.* We aimed to elucidate for the first time the function of *M. polymorpha* orthologs of important LRR-receptors, which are known to be essential for perception in angiosperms. *M. polymorpha* gene orthologs were tested in vascular plants for potentially conserved and common functions. Our data will contribute to the understanding of mechanistic aspects as well as the evolution of the multilayered and highly diversified and specified perception mechanism we know from angiosperms.

2 Material and Methods

2.1 Materials

Chemicals, used in this thesis, were purchased from following companies: Duchefa, Carl-Roth, Merck, Sigma-Aldrich, Applichem and Thermo Scientific.

Table 1: *M. polymorpha* cultivation media.

Medium	Components
½ Gamborg	1.528 g Gamborg B5, 14 g Agar Kobe
½ Gamborg + 10% sucrose	1.528 g Gamborg B5, 14 g Agar Kobe, 10 g sucrose
Mp spore medium	1.528 g Gamborg B 5; L-Glutamin; 1 g casamino acids; 10 g sucrose

Table 2: SDS protein gelelectrophoresis media.

Medium	Ingredients	Concentration
Ponceau-S solution	acetic acid	10% (v/v)
	MeOH	40% (v/v)
	Ponceau-S (CI_27195)	0.1% (w/v)
10x Running Buffer	Tris	250 mM pH 8.4
	glycine	1.92 M
	SDS	1% (w/v)
Transfer Buffer	Tris	45 mM
	glycine	39 mM
	MeoH	20% (v/v)
10x PBS-T	NaH_2PO_4	170 mM
	Na_2HPO_4	580 mM
	NaCl	680 mM
	Tween 20	0,5% (v/v)
4x SDS Sample Buffer	Tris	250 mM pH 6.8
	glycerol	40% (v/v)
	SDS	8% (w/v)
	Bromophenol blue	0,04% (w/v)

	β-mercaptoethanol (added immediately before use)	5-10% (v/v)
10x Assay Buffer	Tris	20 mM pH 9.8
	$MgCl_2$	20 mM

Table 3: SDS polyacrylamide gel [8 %(m/v)]; 0.75-1.0 mm thickness, 8.3 cm x 5.5 cm.

Gel	Ingredients	[µl]
Lower (running/separation) gel	H_2O	2400
	Tris [1.5 M, pH 8.8] [to 375 mM]	1250
	Acrylamid/Bisacrylamid [30%, 37.5:1][to 8% (m/v)]	1330
	SDS [20%(m/v)] [to 0.1%(m/v)]	25
	APS [10%(m/v)] [to 0.05% (m/v)]	25
	TEMED [to 0.05%(v/v)]	2.5
Upper (stacking/collection) gel	H_2O	1460
	Tris [0.5 M, pH 6.8] [to 125 mM]	630
	Acrylamid/Bisacrylamid [30%, 37.5:1] [to 5%(m/v)]	420
	SDS [20%(m/v)] [to 0.1%(m/v)]	12.5
	APS [10%(m/v)] [to 0.05%(m/v)]	12.5
	TEMED [to 0.1%(v/v)]	2.5

Table 4: Co-immunoprecipitation media.

Medium	Ingredients	Concentration
Solubilization Buffer	Tris (pH 8 at 4°C)	25 mM
	NaCl	150 mM
	NP40	1%
	Deoxycholate (DOC)	0.5%
Wash Buffer	Tris (pH 8 at 4°C)	25 mM
	NaCl	150 mM

Table 5: Medium for isolation and transient transformation of *A. thaliana* mesophyll protoplats.

Medium	Components	Final concentration
Enzyme solution	Mannitol	0.4 M
	KCl	20 mM
	MES pH 5.7	20 mM

	Cellulase R10	1.5%
	Macerozyme R1	0.4%
	$CaCl_2$	10 mM
	BSA	0.1%
W5-medium	NaCl	154 mM
	$CaCl_2$	125 mM
	KCl	5 mM
	MES pH 5.7	2 mM
MMg	Mannitol	0.4 M
	$MgCl_2$	15 mM
	MES pH 5.7	4 mM
PEG	Mannitol	0.2 M
	$CaCl_2$	0.1 M
	PEG 4000	40%

Table 6: Antibiotics.

Antibiotic	**Final concentration bacteria plates**	**Final concentration plant selection plates**	**Solvent**
Carbenicillin	100 µg/ml	100 ng/ml	water
Chlorosulfuron	100 µg/ml	100 ng/ml	water
Kanamycin	100 µg/ml	100 ng/ml	water
G418	100 µg/ml	100 ng/ml	water
Rifampicin	50 µg/ml	50 ng/ml	methanol
Spectinomycin	100 µg/ml	100 ng/ml	water
Gentamycin	25 µg/ml	/	water
Cefotaxime	100 µg/ml	100 ng/ml	water
Hygromycin	100 µg/ml	10 µg/ml	premixed solution

Table 7: Bacterial strains.

Strain	**Genotype**
E. coli strain Top 10	recA1, endA1, gyrA96, thi-1, hsdR17, supE44, relA1, lac, [F´, proAB, lacIqZ∆M15, Tn10, (Tetr)]; tetR

A. tumefaciens strain GV3101	C58, pTiC58DT-DNA; genR

Table 8: Plasmids.

Plasmid	Reference
pBIN61:35S:P19	Voinnet et al., 2003
pK7FWG2.0:AtFLS2:eGFP	Mueller et al., 2012
pK7FWG2.0:SlFLS2:eGFP	Mueller et al., 2012
pGWB17:BAK1:4xMyc	Mueller et al., 2012
pXpre-K:35SΩ:EFR:GFP	Dr. Judith Fliegmann
BB10:35SΩ:AtFLS2-ECD:MpSERK-KD:GFP:nosT:dy	This thesis
BB10:35SΩ:MpSERK-ECD:AtFLS2-KD:GFP:nosT:dy	This thesis
pGWB20:Ftm-B:10xMyc	Albert et al., 2013
pK7FWG2.0:Btm-F:eGFP	Albert et al., 2013
BB10:35SΩ:FLS2-ECD:MpSERK-KD:4xMyc:nosT:dy	This thesis
BB10:35SΩ:MpSERK-ECD:AtFLS2-KD:GFP:nosT:HygR	This thesis
pK7FWG:MpSERK:4x-Myc	This thesis
BB10:35SΩ:EFR-ECD:BIR1-KD:GFP:nosT:HygR	This thesis
BB10:35SΩ: BIR1:YFP:nosT:dy	Yan Wang
pB7YWG2.0:BIR2	Halter et al., 2014
pB7YWG2.0:BIR4	Halter et al., 2014
BB10:35SΩ:MpBIR:GFP:nosT:pFAST	This thesis
BB10:35SΩ:MpBIR:GFP:nosT:HygR	This thesis
BB10:35SΩ:EFR-ECD:MpBIR-KD:GFP:nosT:HygR	This thesis
BB10:35SΩ:MpSOBIR:GFP:nosT:HygR	This thesis
BB10:35SΩ:EFR-ECD:MpSOBIR-KD:GFP:nosT:HygR	This thesis
BB10:35SΩ:AtSOBIR-ECD:MpSOBIR-KD:GFP:nosT:dy	This thesis
BB10:35SΩ:MpSOBIR-ECD:AtSOBIR-KD:GFP:nosT:dy	This thesis
BB10:35SΩ:AtSOBIR:GFP:nosT:HygR	This thesis
BB10:35SΩ:EFR-ECD:AtSOBIR-KD:GFP:nosT:HygR	This thesis
BB10:35SΩ:MpHSL:GFP:nosT:HygR	This thesis
BB10:35SΩ:EFR-ECD:MpHSL-KD:GFP:nosT:HygR	This thesis
BB10:35SΩ:EFR-ECD:MpLRR-RLK2-KD:GFP:nosT:dy	This thesis
BB10:35SΩ:EFR-ECD:MpLRR-RLK4-KD:GFP:nosT:dy	This thesis

BB10:35SΩ:EFR-ECD:MpLRR-RLK5-KD:GFP:nosT:HygR	This thesis
BB10:35SΩ:EFR-ECD:MpLRR-RLK6-KD:GFP:nosT:dy	This thesis
BB10:35SΩ:EFR-ECD:MpLRR-RLK8-KD:GFP:nosT:dy	This thesis
BB10:35SΩ:EFR-ECD:MpLRR-RLK10-KD:GFP:nosT:HygR	This thesis
BB10:35SΩ:EFR-ECD:MpLRR-RLK11-KD:GFP:nosT:dy	This thesis
BB10:35SΩ:EFR-ECD:MpLRR-RLK12-KD:GFP:nosT:dy	This thesis
BB10:35SΩ:EFR-ECD:MpLRR-RLK13-KD:GFP:nosT:dy	This thesis
BB10:35SΩ:EFR-ECD:MpLRR-RLK14-KD:GFP:nosT:dy	This thesis
BB10:35SΩ:EFR-ECD:MpLRR-RLK15-KD:GFP:nosT:HygR	This thesis
BB10:35SΩ:EFR-ECD:MpLRR-RLK18-KD:GFP:nosT:dy	This thesis
BB10:35SΩ:EFR-ECD:MpLRR-RLK21-KD:GFP:nosT:dy	This thesis
BB10:35SΩ:EFR-ECD:MpLRR-RLK26-KD:GFP:nosT:dy	This thesis
BB10:35SΩ:EFR-ECD:MpLRR-RLK27-KD:GFP:nosT:dy	This thesis
BB10:35SΩ:EFR-ECD:MpLRR-RLK30-KD:GFP:nosT:dy	This thesis
BB10:35SΩ:EFR-ECD:MpLRR-RLK4IM-KD:GFP:nosT:dy	This thesis in collaboration with Dr. Isabel Monte
BB10:35SΩ:EFR-ECD:MpLRR-RLK39IM-KD:GFP:nosT:dy	This thesis in collaboration with Dr. Isabel Monte
BB10:35SΩ:EFR-ECD:MpLRR-RLK72IM-KD:GFP:nosT:dy	This thesis in collaboration with Dr. Isabel Monte
BB10:35SΩ:EFR-ECD:MpLRR-RLK184IM-KD:GFP:nosT:dy	This thesis in collaboration with Dr. Isabel Monte
BB10:35SΩ:EFR-ECD:MpLRR-RLK31-KD:GFP:nosT:dy	This thesis
BB10:35SΩ:MpLRR-RLK5:GFP:nosT:HygR	This thesis
BB10:35SΩ:MpLRR-RLK10:GFP:nosT:HygR	This thesis
BB10:35SΩ:MpLRR-RLK15:GFP:nosT:HygR	This thesis

Table 9: Peptides. Red o indicating hydroxyproline.

Peptide	Sequence	Reference
MpIDA1	FQKLPRSSEVPPQGoSPIHN	Bowman et al., 2017
HBg-MpIDA1	VSGWRLFKKISGFQKLPRSSEVPPQGoSPIHN	This Thesis
MpIDA1-short	EVPPQGoSPIHN	This Thesis
MpIDA2	FERLPRGTTVPDSNoSPVHN	Bowman et al., 2017
MpIDA3	LQRLPRDTPVPPSGoSGPNR	Bowman et al., 2017
MpIDA4	FQMLPRNTRPPPRGoSPGSN	Bowman et al., 2017
MpIDA4-short	RPPPRGoSPGSN	This Thesis
IDA3	PKGVPIPPSAPSKRHN	Prof. Dr. Georg Felix
IDA9 (PiPPo)	PIPPSAoSKRHN	Butenko et al., 2014
flg22	QRLSTGSRINSAKDDAAGLQIA	Felix et al., 1999
elf18	SKEKFERTKPHVNVGTIG	Kunze et al., 2004
systemin	AVQSKPPSKRDPPKMQTD	Pearce et al., 1991

Table 10: Antibodies.

Antibody	Produced in	Stock concentration	Working solution	Company
anti-c-Myc (C3956)	rabbit	approx. 0.5 mg/ml	1:5000 in 5% (1x) PBS-T milk	SIGMA
Rabbit anti GFP (TP401)	rabbit	0.2 mg IgG	1:5000 in 5% (1x) PBS-T milk	Torrey Pines Biolabs Inc
Goat anti rabbit	goat		1:50000 in 5% (1x) PBS-T milk	

Table 11: Agarose beads.

Beads	Company
GFP-Trap Agarose	ChromoTek
GFP-Trap Magnetic Agarose	ChromoTek

Table 12: Plant genotypes.

Genotype	Organism	Properties	Reference
Col-0	*A. thaliana*	wildtype	

fls2 x bak1-4	*A. thaliana*	*fls2* and *bak1-4* mutant in Col-0 background	Zipfel et al., 2004
bak1-4	*A. thaliana*	*bak1* mutant line	Kemmerling et al., 2007
efr-1 x fls2	*A. thaliana*	*efr* and *fls2 mutant*	Felix, pers. communication
fls2	*A. thaliana*	*fls2* single mutant	Zipfel et al., 2004
efr-1	*A. thaliana*	*efr* single mutant	Zipfel et al., 2006)
sobir1-12	*A. thaliana*	*sobir* single mutant	Gao et al., 2009
	N. benthamiana	wildtype	
sobir	*N. benthamiana*	*sobir 2-2*	Huang et al., 2020
TAK1	*M. polymorpha*	Male Wild type	Dr. H. Breuninger
TAK2	*M. polymorpha*	Female Wild type	Dr. H. Breuninger

2.2 Methods

2.2.1 Cloning

In the course of this thesis several plasmid constructs were generated using either GoldenGate (Binder et al., 2014) or Gateway® cloning (Invitrogen). GoldenGate-based assembly of expression plasmids made use of module and vector libraries provided by Dr. R. Morbitzer (Department of General Genetics, ZMBP; Binder et al., 2014) and Dr. J. Fliegmann, Y. Wang, Dr. A. Gust and myself (Department of Plant Biochemistry, ZMBP). The GoldenGate cloning strategy is based on the assembly of DNA fragments by sticky overhangs, generated by Type IIS restriction enzymes and the ligation of the respective fragments by T4 DNA ligase. A multitude of potential overhangs create the possibility to assemble DNA fragments, encoding regulatory and functional domains, in a given order without the addition of extra nucleotides. This cloning technique is especially helpful for chimeric receptor construct cloning. Therefore, the majority of constructs were generated using the GoldenGate cloning strategy. The Gateway® Technology uses recombination events to transfer DNA-fragments into different vectors whilst maintaining the reading frame. Only one plasmid construct – MpSERK:4xMyc – was generated using the Gateway® Technology, because at the timepoint of cloning no 4xMyc tag was available in the module library for GoldenGate cloning.

2.2.1.1 Double reciprocal receptor approach

To validate the interaction of MpSERK and FLS2, a two-hybrid receptor approach – introduced by Albert et al., (2013) – was used. Constructs tested in this thesis were generated according to Albert et al., (2013). The ectodomain-part, including the transmembrane domain (TM) was fused to the kinase domain (KD)-part, including the inner juxtamembrane (iJM) and KD. Constructs FtB and BtF had been generated and validated in Albert et al., (2013). FtB consists of the ectodomain of FLS2 and the kinase domain of BAK1. BtF represents the contrary chimera, with the ectodomain of BAK1 and the kinase domain of FLS2. To test the functionality of MpSERK a new double-reciprocal receptor pair was generated, FtM and MtF. FtM is similar to FtB and contains the ectodomain of FLS2, however paired with the kinase domain of MpSERK. MtF corresponds to the reversed chimera and is composed of the ectodomain of MpSERK and the kinase domain of FLS2 (**Figure 12**).

2.2.2 Polymerase-Chain-Reaction

The Phusion™ High-Fidelity DNA polymerase (Thermo Scientific™) was used for amplification of fragments for further cloning into expression plasmids. Taq DNA polymerase (Thermo Scientific™) was used for colony-PCRs and genotyping was performed using a Phusion polymerase purified in house (Louis-Philippe Maier). The annealing temperature was chosen according to the properties of the used primer pair (Table 13).

step	temperature	time	cycle
	98/95°C	pause	
DNA denaturation	98/95°C	3 min	24-34 repetitions
primer annealing	x	35 sec	
elongation	72/65°C	x	
	72/65°C	5 min	
	8°C	pause	

Table 13: Standard PCR program. The annealing temperature and the time for the elongation was set up individually, depending on the primer pair properties and the size of the amplification product.

If the annealing temperature of the individual primers in one reaction differed from each other drastically, a touchdown PCR was performed. Hence, the program was started at an annealing temperature slightly higher than the highest calculated temperature (more specific, avoiding byproducts), for approximately 12 cycles in which the temperature was decreased 1°C per cycle, followed by additional 25 cycles with an annealing temperature of 55°C (more unspecific). The elongation time was adjusted to the properties of the polymerase and the length of the amplification product. Reactions were performed in the appropriate buffers amended with a mixture of all four dNTPs to a final concentration of 250 µM, each.

2.2.2.1 Colony-PCR

For identification of positive clones, colony PCRs were performed. Particular primers were added to the 2x Allin Red Taq Mastermix (highQu) to a final concentration of 0.4 µM in the final volume (adjusted by adding water). A 10 µl tip was used to pick material of a single colony. By pipetting up and down the bacteria were released into the premixed solution. With the same tip 5 ml LB-medium (with appropriate antibiotics) were inoculated. The PCR program was similar to the normal PCR program.

2.2.3 Gel electrophoresis

20% (v/v) loading dye was added to each PCR sample and loaded onto a 1% agarose gel containing 1:10000 Gel red (Biotium). The agarose gel was applied to 70-100 V until the loading front reached the end of the gel. PCR bands were detected using the Analytik Jena gel imaging system.

2.2.4 DNA purification from agarose gel

Amplified PCR products were cut out of an agarose gel and purified according to the GeneJET Gel-Extraction kit protocol (Thermo Scientific). DNA concentrations were measured using the Nanodrop spectrophotometer. Purified PCR samples were directly used in ligation reactions.

2.2.5 DNA ligation

Amplified PCR products were blunt end ligated using the blunt end vector pJET (Thermo Scientific CloneJET PCR Cloning Kit). The ligation reaction was set up as described in the protocol.

2.2.6 Plasmid DNA isolation

5 ml LB-medium was inoculated with a single colony and grown overnight at 37°C at 200 rpm. *E. coli* cells were harvested from liquid cultures by centrifugation for 2 min and 8000 rpm. DNA isolation was performed according to the protocol of the GeneJET Plasmid Miniprep Kit (Thermo Scientific). DNA concentration was measured using the Nanodrop device.

2.2.7 Restriction digest

For validation of clones, restriction enzymes were used. According to the presence of restriction sites of different enzymes on the respective construct, up to two enzymes were selected. Related buffer and digestion temperatures were chosen to digest the DNA. When using two different enzymes in a double digestion set up the DoubleDigest Calculator of Thermo Scientific™ was used to determine the optimal reaction conditions. After appropriate incubation 20% (v/v) loading dye was added and DNA fragments were separated and visualized using gel electrophoreses (see chapter 2.2.3).

2.2.8 Sequencing

New constructs were validated using the Sanger sequencing service of Microsynth AG.

2.2.9 Transformation of *E. coli* (Top 10)

Aliquots (100 µl) of chemically competent *E. coli* cells (stored at -80°C) were defrosted on ice and subsequently mixed with 1-10 µl plasmid DNA or directly with the cloning reaction (Gateway LR, GoldenGate cut-ligation). After incubation on ice for around 10 min the cells were heat-shocked at 42°C for 30 sec. The cells were then directly placed on ice and incubated for approx. 5 min. 700 µl LB-medium were added followed by an incubation in a 37°C shaker for approx. 30 min. Transformed cells were plated on LB plates containing appropriate antibiotics, and incubated at 37°C overnight.

2.2.10 Transformation of *Agrobacterium tumefaciens*

The *A. tumefaciens* strain GV3101 was used for transient transformation of *N. benthamiana* as well as stable transformation of *A. thaliana* and *M. polymorpha*. To generate recombinant *Agrobacteria*, electro-competent cells (50 µl aliquots, stored at -80°C) were defrosted on ice and mixed with plasmid DNA. The mixture was incubated on ice for 10 min. Precooled 0,1 cm cuvettes were filled with the DNA-cell mixture and electroporated at a setting of 1500 V. Directly after the pulse 700 µl LB-medium were added and cells were incubated at 28°C and 200 rpm for approx. 45 minutes. Cells were plated on LB-medium containing rifampicin and the appropriate antibiotic for selection of the recombinant plasmid and incubated at 28°C for 2 days.

2.2.11 Plant cultivation

2.2.11.1 Cultivation of *Marchantia polymorpha*

Gemmae of wildtype *M. polymorpha* (ecotype TAK1 and TAK2) as well as all transformed lines were cultivated on ½ Gamborg B5 medium + 2% sucrose in long day white light condition (16 h light, 8 h dark) at 22°C.

2.2.11.2 Cultivation of *Arabidopsis thaliana*

Seed were sown on soil (GS90) under short day (8 h/16 h light/dark, 22°C) conditions and separated after two weeks. Plants were kept further in short day for 5-6 weeks and

subsequently used for bioassays. To avoid infestation of black flies, plants were repeatedly watered with Gnatrol and nematodes.

2.2.11.3 Cultivation of *Nicotiana benthamiana*

N. benthamiana plants were grown in the greenhouse under long day conditions (16 h light and 8 h dark) at 22°C and high-power light.

2.2.12 *Agrobacterium*-mediated transient transformation of *N. benthamiana* leaves

For transient expression of proteins of interest 5 ml liquid cultures, with appropriate antibiotics, were inoculated with transformed *A. tumefaciens* (GV3101) and grown over night at 28°C and 180 rpm. Bacteria were harvested by centrifugation (4000 g, 8 min). The bacterial pellet was resuspended in 5 ml 10 mM $MgCl_2$ + 150 µM acetosyringone and incubated for at least one hour at room temperature. The OD of each strain was estimated in a photometer (biowave S2100 Diode Array Spectrophotometer) and adjusted to a final OD of 1. Combinations of constructs were set up and *Agrobacteria* expressing pBIN61:35S:p19, encoding a silencing inhibitor, were added to each transformation (Voinnet et al., 2003). For infiltration the *Agrobacterium* suspension was adjusted to a final OD of 0.1 in 10 mM $MgCl_2$. *N. benthamiana* plants were used for infiltration at an age of approximately six weeks. Plants were properly watered prior to infiltration. Using a 1 ml-syringe the *Agrobacterium* suspension was carefully infiltrated into the leaf by making a little entry using a needle. After 2–3 days leaf material was further processed according to the respective experimental set up.

2.2.13 *Agrobacterium*-mediated transformation of *M. polymorpha* spores

Spore capsules of wildtype *M. polymorpha* were harvested from archegoniophores, dried with silica and stored at -80°C. *M. polymorpha* sporeling transformation was performed as described in Ishizaki et al., (2008), using the *Agrobacteria tumefaciens* strain GV3101. For transformation, 3 spore capsules were sterilized by incubating in a sodiumhypochlorid solution (1:1000 + 10% Triton-X-100) for 2 min while inverting. This was followed by a centrifugation step (13000 g) for 2 min and 3 wash steps with water. Sterilized spores were resuspended in 600 µl “Flüssigmedium”. 100 ml flasks containing 25 ml sterile “Flüssigmedium” were inoculated with 100 µl spore solution. Spores were grown shaking (200 rpm) at 22°C and 16 h white light for seven days. *Agrobacteria* containing the appropriate plasmid were grown for two days on LB plates

containing respective antibiotics. A liquid culture was inoculated with a single colony and grown over night in a 28°C shaker. *Agrobacteria* were harvested by centrifugation (4000 g and 8 minutes) and resuspended in 10 ml “Flüssigmedium” containing 200 µM acetosyringone, and incubated for 6 h at 28°C while shaking (150 rpm). For cocultivation 500 µl (for double transformation) or 1000 µl (single transformation) of the respective *Agrobacteria* suspension were transferred to the flasks containing the spores. A final concentration of 200 µM acetosyringone was added and cocultures were incubated at 22°C under long day conditions, while shaking (150 rpm). After 3 days cocultures were transferred into 50 ml falcon tubes and washed at least 4 times with sterile water. Depending on agrobacteria contamination additional washing steps were added. Washed spores were resuspended in 5 ml water. For selection of transformed spores, ½ Gamborg B5 plates with cefotaxime and appropriate antibiotics were prepared. Spores were transferred with a cut 1000 µl pipet tip onto selection plates (4 plates per transformation). Transformed plates were incubated at 22°C under long day conditions. Surviving pants were directly tested for gene expression and gemmae were transferred on new, appropriate antibiotic containing plates. After the second selection plants were cultivated on ½ Gamborg B5 plates without antibiotics.

2.2.14 *Agrobacterium*-mediated stable transformation of *A. thaliana*

A. thaliana plants were stably transformed using the floral dip method of Zhang et al., 2006. Plants were prepared for the floral dip by removing all too far developed flowers and pods. Resulting seeds were selected by pFAST (Shimada et al., 2010).

2.2.15 Genomic DNA isolation

gDNA from *M. polymorpha* thallus was isolated using an EDWARDS protocol (Edwards et al., 1991) modified by Claudia Gieshold, Universität Osnabrück, 2015 and myself. A small piece of thallus (approx. 0.25 cm^2) was disrupted in 400 µl lysis buffer (20 mM Tris-HCl pH 7.5, 250 mM NaCl, 25 mM EDTA, 0.5% SDS) with 3 metal balls by grinding in a 2 ml eppendorf reaction tube for 2 min with 30 Hz using a Retsch Mill. The processed plant material was centrifuged at 13.000 rpm for 5 min. 350 µl of the supernatant was transferred into a new tube and 350 µl phenol/chloroform-isoamylalcohol (ROTI®Phenol/Chloroform/Isoamylalkohol) was added. The solution was vortexed until no phase separation was visible anymore and centrifuged at 13.000 rpm for 5 min. The upper phase (approx. 300 µl) of the supernatant was

transferred into a new tube and combined with 300 µl isopropanol and 30 µl NaOAc (3 M, pH 4.6) to precipitate the DNA. The solution was inverted several times and afterwards centrifuged at 13.000 rpm for 5 min. The supernatant was discarded, the DNA-pellet was washed with 450 µl 70% EtOH and re-centrifuged (3 min). The DNA was dissolved in 100 µl water after complete removal of EtOH and further drying at room temperature.

2.2.16 Separation and immunological detection of proteins by SDS-polyacrylamide gelelectrophoresis (SDS-PAGE)

Protein samples were prepared according to the purpose of the experiment (**Table 14**) and 10-20 µl each were applied to 8% SDS-PAGE gels (**Table 2**, **Table 3**). Separation was performed by 140 V for approx. 60 min. Semi-dry transfer (Trans-Blot Semi-Dry, Biorad) was performed by assembling first, two layers of thick filter paper (Rotilabo®-Blotting papers, thick 0.75 mm), soaked in transfer buffer, and one prewet sheet of nitrocellulose membrane (0.45 µM) onto the anode plate electrode. The acrylamide gel was equilibrated in transfer buffer and layered on top of the membrane. The setup was completed with another two layers of pre-wet thick filter paper and the cathode electrode. Air bubbles between the layers were rolled out and the transfer was run for 75 min at 17 V. The membrane was stained with Ponceau-S solution to visualize the general protein amount and unspecific binding sites were blocked with 5% milk in PBS-T for 30-60 min at room temperature. After removing the milk, the first antibody (**Table 10**) was added and incubated at room temperature for 1 h or overnight at 4°C. After incubation with the first antibody the membrane was washed two times with PBS-T for 5 min. The secondary antibody (**Table 10**) was added and incubated at room temperature for 45 min-1 h. The membrane was washed again two times for 5 min with PBS-T and equilibrated two times, 2 min each, with assay buffer. The membrane was placed on a foil and covered with nitroblock (Tropix® Nitro-Block II™, applied biosystems, 1:20 in assay buffer) for 5 min. By washing the membrane 2 min with assay buffer excessive nitroblock-solution was removed and the membrane was covered with CDP-star (Roche Diagnostics GmbH, 1:50 in assay buffer), incubated for 5 min, and placed between transparent foils. Protein bands were detected using the Amersham Imager 600.

Table 14: Sample preparation Western blot.

Experiment	Sample preparation	Resuspension per sample
Protoplast – expression control	Harvesting 6 wells of 100 µl protoplasts from 96 well plates, centrifugation, resuspension of cell pellet in SB; Boiling at 95°C for 10 min and centrifugation at 13.000 g for 10 min	60 µl 2x SB (SDS sample buffer with 5% β-mercaptoethanol
Plant material – expression control	Grinding of sample in liquid nitrogen, resuspension in SB, boiling and centrifugation as above	xg plant material plus 2 vol of 2x SB with 5% β-mercaptoethanol
Transiently transformed *N. benthamiana* – expression control	3 frozen leaf discs were ground with a micro-pistol, recovered in SB, boiling and centrifugation as above	3 leaf discs with 100 µl 2x SB with 5% β-mercaptoethanol

2.2.17 Co-immunoprecipitation

Plant material was ground in liquid nitrogen. 230-300 mg of plant material was solubilized in 1.2-1.7 ml solubilization buffer (with DTT and PPI; **Table 4**) for 45-60 min at 4°C and 7 rpm. The solubilized material was ultra-centrifugated (himac CS 120FX) for 30 min and 42.000 rpm (rotor RP45A) at 4°C. A 60 µl aliquot of the supernatant was used as input sample and was mixed with 20 µl 4x SB (10% β-mercaptoethanol). The remaining supernatant of the solubilizate was incubated with 10 µl GFP-Trap beads, equilibrated in solubilization buffer (without DTT and PPI) for 1 h at 4°C and 7 rpm. Incubated beads were washed two times with solubilization buffer (without DTT and PPI) and two times with wash buffer. The washed beads were resuspended in 40 µl 2x SB (5% β-mercaptoethanol). Samples of the input and the incubated beads were boiled (95°C) for 10 min and afterwards centrifugated (13.000 g for 10 min). 10-20 µl of the boiled samples were loaded on an SDS gel. SDS gel electrophoresis was performed as described in chapter 2.2.16.

2.2.18 Peptide-protease-digestion

The immune response upon treatment with MpIDA1 peptide was validated by protease digestion of the peptide. 1 µM MpIDA1 was incubated over night with 200 µM protease (Trypsin or Proteinase K; 1 µg/ml) in Tris buffer (Tris [50 mM, pH 8], $CaCl_2$ [20 mM]) at 60°C or 37°C, respectively. For enzyme inactivation the solutions were heated to 95°C for 20 min. Samples were tested in a ROS assay.

2.2.19 Bioassays

To monitor an immune response upon peptide treatment different bioassays were performed.

2.2.19.1 Detection and quantification of the ROS burst

For the detection of the ROS-burst the protocol of Albert and Fürst, 2017, was used. Leaves were cut in pieces and incubated on water over night. Wells of a 96-well plate were filled with 90 µl water and 10 µl of 10x luminol master mix (200 µM luminol L-012; 10 µg/ml horseradish peroxidase, WAKO). Leaf pieces were transferred into the wells and the background was measured in a luminometer (Centro LB 960; BERTHOLD TECHNOLOGIES) for approx. 10 min. In case the background was stable leaf pieces were treated with respective MAMPs. The response was measured for approximately 30 min.

2.2.19.2 Detection of the plant hormone ethylene

Measurement of ethylene was performed as described in Albert et al., 2010a. Leaves were cut into small pieces and incubated on water over night. 3 leaf pieces were placed into a 6 ml glass-tube containing 250 µl water. Leaf pieces were treated with appropriate amounts of MAMPs and the glass tube was immediately closed with a rubber cap. Samples were incubated for approx. 3 h. 1 ml of the gas-headspace of the tube was injected into a gas chromatograph and ethylene was quantified.

2.2.19.3 pFRK1:Luciferase-reporter assay

The protocol of Yoo et al., 2007 - modified by Dr. Lei Wang - was used for the isolation and transformation of *A. thaliana* mesophyll protoplast of different ecotypes. Leaves of 3-4-week-old plants were cut with a razor blade into small strips and digested in

enzyme solution (**Table 5**) for 20 min in a desiccator and additional approx. 3 h at room temperature and darkness. Protoplasts were released by adding W5-medium (**Table 5**) and swirling movements. Protoplast were filtered through a nylon mesh and centrifuged for 2 min, 100 g, at 4°C. The supernatant was discarded and the sedimented protoplasts were resuspended in 5 ml W5-medium. Protoplasts were rested on ice for approx. 30 min until protoplasts were settling down at the bottom. The supernatant was removed and protoplast were resuspended in 5 ml W5-medium. The number of protoplasts was determined under the microscope using a hemocytometer. To form a pellet, protoplasts were rested on ice for approx. 30 min. The supernatant was removed and protoplasts were resuspended in MMg (**Table 5**) to a final concentration of $4x10^5$ protoplasts per ml. For each transformation 30 µg FRK1 plasmid, 30 µg of plasmid DNA of the respective constructs and 1 ml of protoplasts were combined in a round-bottom tube. After adding 1,1 ml of PEG (**Table 5**) the round-bottom tube was inverted carefully and incubated for 5 min in room temperature. Subsequently, 4,4 ml W5-medium were added and the mixture was inverted carefully. Protoplasts were harvested by centrifugation for 2 min and 100 g at 4°C. The supernatant was removed and the protoplasts were resuspended in 1 ml W5-medium. To each transformation 10 µl 20 mM D-luciferin (Synchem UG & CoKG) was added. 100 µl portions of transformed protoplasts were aliquoted into wells of a 96-well plate. Measurement was performed after approx. 14 h incubation to ensure expression of the pFRK1:Luciferase-reporter and receptors encoded by the respective constructs. The first measurement monitored the background values. After 1 h, protoplasts were treated with respective MAMPs and light emission (RLU) was measured hourly.

2.2.19.4 Gemmae release

TAK2 gemmae were grown on ½ Gamborg B5 medium for two weeks. Gemmae with approximately the same size and normal growth were transferred to a new plate containing +/- peptide (4 gemmae per plate). The thallus was grown for 30 days in long day conditions (white light, 16 h light, 8 h dark, 22°C) until the production of a few gemma cups. Under the clean bench 10 ml of sterile water was added slowly onto the plate, without hitting the thallus. Plates were closed and shaken on a horizontal shaker for 5 min at 150 rpm. The water, containing the released gemmae, was transferred onto a new ½ Gamborg plate. The excessive water was eliminated without removing gemmae and plates were closed with Leukopor adhesive tape (Duchefa Biochemie).

Gemmae were counted after three days and normalized against the number of thalli and gemma cups.

2.2.19.5 Peptide-induced growth inhibition

To test the effect of peptides on the growth of *M. polymorpha* gemmae, a growth inhibition assay was performed. Each well of a 6-well plate was filled with 3 ml water. By using a sterile 1000 ml pipet tip, gemmae were transferred from gemma cups of approximately two-month-old plants to the wells (thallus passed through several dichotomous branching events and thus producing several gemma cups). Only gemmae were considered which were floating on the water surface. Sinking of the gemmae caused growth inhibition by itself. Different concentrations and / or peptides were added. Plates were placed in long day condition (16 h light, 8 h dark, 22°C) for 12 days. The surface area of the gemmae was estimated using imageJ and compared among treatments.

3 Results & Discussion

Plants are able to perceive and to adapt to abiotic and biotic stresses. Biotic stresses include the attack of diverse microorganisms. The crucial inventions for successfully coping with the ever-evolving pathogenic threats can be better understood by comparing present day species of plant lineages like algae, liverworts, or mosses, with vascular plants of which they split early in the evolution of land plants. Concentrating on PRRs, as essential elements in perception systems, holds the possibility to understand the success of the multilayered perception system we know from vascular plants. It additionally gives an insight in the equipment early evolved plant lineages use to cope with cues since 450 MYA.

3.1 PRRs in non-vascular plants

Phylogenetic sequence analysis revealed the occurrence of PRRs, notably those with a LysM ectodomain like the chitin receptor CERK in multicellular green algae (**Figure 8**; Delaux and Schornack, 2021). Receptors with LRR-domains, LRR-RLKs and LRR-RLPs, seem to have evolved concurrent with the plant terrestrialization. *M. polymorpha* encodes >60 LRR-RLKs and >33 LRR-RLPs. However, except for orthologs of TDIF, CLV1 and HSL, which all potentially perceive endogenous ligands, no clear homologs to known PRRs from angiosperms, like for example FLS2 and EFR, were identified (Furumizu et al., 2021; Bowman et al., 2017a; Hirakawa et al., 2019, 2020).

3.2 *Marchantia polymorpha* – a model for plant immunity?

To describe the basic equipment of cell surface receptors in non-vascular plants we selected the liverwort *M. polymorpha* – as representative plant that split from the lineage of angiosperms 450 MYA (Poveda, 2020). We followed two approaches: On the one hand, we introduced PRRs of vascular plants into *M. polymorpha*, to rebuild the perception system of flg22. On the other hand, we tested the functionality of LRR-RLK receptors of *M. polymorpha* by heterologous expression in vascular plants. The successful complementation would indicate a conserved function, however, a negative outcome might also arise from indirect incompatibilities, as, for example, the necessity to form a receptor complex for signaling.

3.2.1 Rebuilding a vascular plant perception system in *M. polymorpha*

Treatment of *M. polymorpha* thallus with elf18, flg22-type peptides or flagellin itself, did not cause a ROS-burst (data not shown) and the genome of *M. polymorpha* encodes no orthologs of EFR and FLS2. Therefore, one initial aim was to introduce AtFLS2, either alone or in combination with its co-receptor AtBAK1, into *M. polymorpha*. This might enable the bryophyte to express a functional binding site for this MAMP or even respond to flg22. Stably transformed *M. polymorpha* plants were generated. None of these transformants did show a ROS-burst upon flg22 treatment (**Figure 9**). Moreover, although PCR analysis demonstrated the integration of the gene expression cassette into the genomic DNA, no accumulation of FLS2 protein could be detected on Western blots (**Figure 9**). This lack of protein accumulation with the AtFLS2 gene under the 35S promoter could hint at a negative or even lethal effect of the AtFLS2 receptor kinase on *M. polymorpha*. In such a situation, the selection for transformants with the antibiotic resistance could go along with a selection for non-expression of the transgenic AtFLS2. Indeed, the number of transformants obtained with the AtFLS2 construct was much lower than expected and observed for transformations with other constructs, notably the co-transformation of MpSERK and the CRISPR genes targeting the endogenous MpSERK (schematic representation in **Figure 9**). Attempts to transform *M. polymorpha* with AtSERK and MpSERK (under the 35S promoter) also resulted in only few or no transformants, indicating that also the overexpression of MpSERK might be detrimental for the plant. Whether this is a phenomenon similar to the severe growth effects observed after overexpression of AtBAK1 in *A. thaliana* (Domínguez-Ferreras et al., 2015), remains to be studied in further experiments. In this series of transformation attempts a high number of transformants was obtained only by co-transformation of MpSERK and the CRISPR genes targeting MpSERK. These transformants also showed accumulation of the transgenic MpSERK detectable via its Myc tag on Western blots (**Figure 28**). Half of these transformants showed a phenotype with multiple branching of the thallus, a phenotype observed also in *Mpserk* knockout mutants (I. Monte, personal communication, **Figure 29**). Dr. Isabel Monte also pursued a similar approach with transfer of EFR into *M. polymorpha*. Microscopic analysis and real-time PCR of her transformants revealed the expression of the protein, however in a very low amount. As observed for AtFLS2, these transformants with EFR did not respond with a ROS-burst when treated with the cognate ligand elf18. Differences between the approach of AtFLS2 and EFR-expression may be caused by different transformation techniques. For the EFR transformants a thallus

transformation (Kubota et al., 2013) was performed, while AtFLS2 was transformed via spore transformation (Ishizaki et al., 2008). If the overexpression of AtFLS2 is negatively influencing the bryophyte, a sporeling may be more sensitive than mature thallus. This could explain why survivor transformants were less in number and show no expression of the AtFLS2 gene (**Figure 9**).

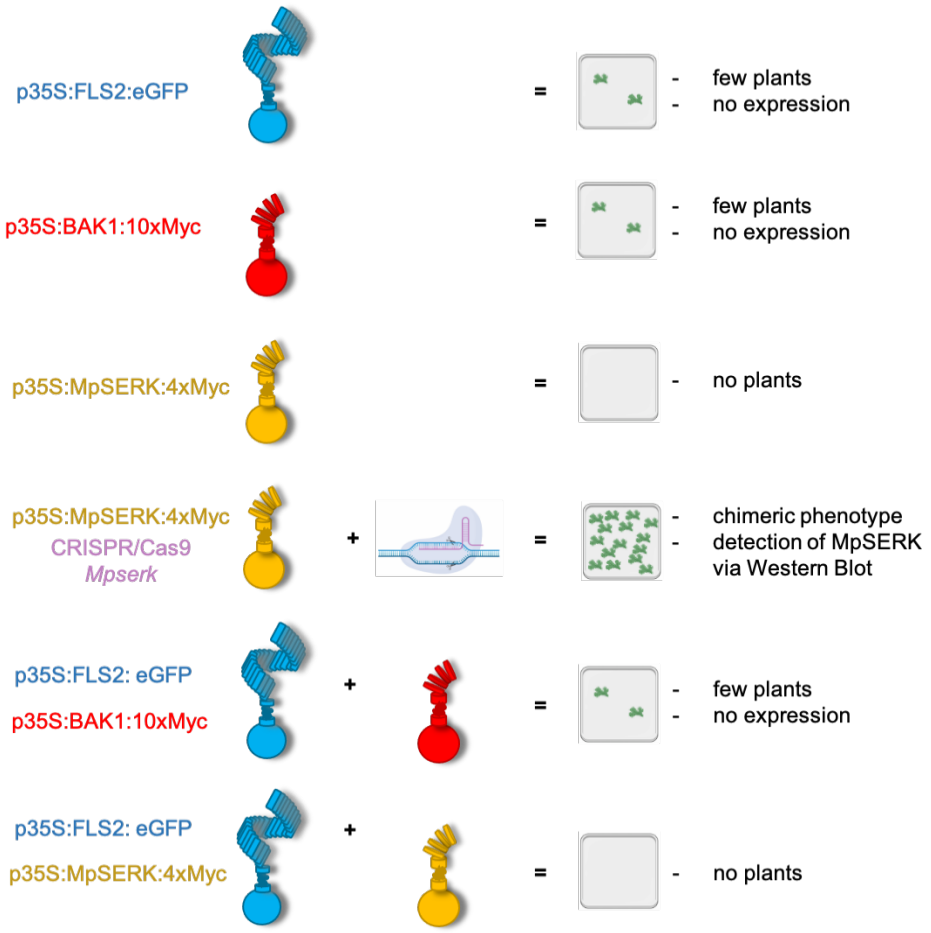

Figure 9: Attempts to generate transgenic *M. polymorpha* over-expressing LRR-RLKs were unsuccessful, except for one. Multiple, independent trials to transform *M. polymorpha* spores with AtFLS2 and/or AtBAK1 or MpSERK. Transformation control was performed via wildtype spores plated out on plates with and without appropriate antibiotics. Only on plates without antibiotics wildtype spores were able to develop, indicating a successful transformation of the resistance cassette in the developing transformed spores.

Future approaches could attempt transformations with an endogenous promotor to avoid overexpression. Another possibility would be the application of inducible promotors to induce expression only after the thallus reaches a mature stage. Several inducible systems have been reported to function also in *M. polymorpha* (Flores-Sandoval et al., 2016; Nishihama et al., 2016; Deveaux et al., 2003; Wachsman and Heidstra, 2010; Flores-Sandoval et al., 2015; Saidi et al., 2005).

3.2.2 Perception of elicitors/MAMPs in *M. polymorpha*

The activation of signaling pathways, like ROS-burst and Ca^{2+}-influx (data not shown), the signaling via phytohormones (Monte et al., 2018), as well as the activation of MAPK (data not shown, Ponce de León and Montesano, 2017) indicate the ability of liverwort to react to pathogens with known stress responses and thus confirms the presence of an innate immune system in the early bryophyte. Immune response in *M. polymorpha* measured by stress response assays are, however, not fully established yet. First studies used altered growth of bryophytes to classify fungi as beneficial, neutral or detrimental (Nelson et al., 2018).

However, the validation of the pathogenicity of a microbe, deduced from growth inhibition of a thallus covered by fungi is a questionable technique. Gimenez-Ibanez et al. (2019) used crude extracts of *P. syringae* with an OD of 1.5 to test for an influence on *M. polymorpha* gemmae growth. This condition, a very high bacterial density, necessitates a careful validation of the effect, by reproducing the results and exclusion of lethal factors like the drowning of gemmae and subsequent impaired gas exchange. An enrichment of the inhibiting factor by purification would support the hypothesis for a *P. syringae*-derived PAMP affecting *M. polymorpha* and would characterize a more defined elicitor for the liverwort. Carella et al. observed that the oomycete *P. palmivora* can enter *M. polymorpha* via its air chambers, where it causes callose deposition (Carella et al., 2017; Carella and Schornack, 2018) and transcriptomic changes (Carella et al., 2019).

These reports demonstrate for the first time the feasibility to perform immune assays in bryophytes, however, they provide no fast and robust screening method for the identification of potential MAMPs.

3.2.2.1 The perception of conserved microbial patterns

Despite methodical problems it was possible to identify chitin, a highly conserved component in fungal cell walls, as a MAMP capable of triggering ROS-burst also in *M. polymorpha* (data not shown). The genome of *M. polymorpha* encodes an ortholog of CERK (Delaux and Schornack, 2021), the chitin receptor in vascular plants and mosses (Bressendorff et al., 2016). Thus, it seems likely that MpCERK functions as a PRR detecting chitin also in bryophytes. Further studies will be needed to demonstrate that MpCERK indeed acts as a chitin receptor. Evidence for this could be obtained by the establishment of *Mpcerk* knock-out mutants in *M. polymorpha* or by successful,

functional complementation of existing *cerk* mutants in angiosperms or *P. patens* with MpCERK.

It can be expected that *M. polymorpha* has perception systems for MAMPs other than chitin. As a first attempt to get evidence for such perception systems, a multitude of crude preparations from diverse microbes and a series of defined MAMP preparations, known to be active in angiosperms, were tested on thallus tissue of *M. polymorpha* using the luminol-peroxidase-based ROS burst assay. However, none of the preparations tested so far, including crude extracts from *Penicillium chrysogenum* (Thuerig et al., 2005) or *Fusarium oxysporum* (extracts provided by Dr. Coleman (Coleman et al., 2021)), bacterial extracts (including peptidoglycan (PGN), ergosterol or pure peptides like elf18, flg22, nlp20, IF1, or pg13 did result in significant and reproducible induction of a ROS burst in *M. polymorpha*. Similarly, a preliminary approach to test *M. polymorpha* extracts for DAMPs or other endogenous stress signals that could activate ROS production remained unsuccessful (data not shown). The ROS-burst assay is based on the oxidation of luminol (see chapter 2.2.19.1) and is strongly dependent on pH and is thus receptive for quenching. Accordingly, it might not be the best suited method for screening certain crude extracts. An extended screen for potential MAMPs of *M. polymorpha* requires therefore an additional technique. ROS-burst assays by staining with 3´-3´-Diaminobenzidine (DAB) or chlorophenol red could represent potential screening methods (Daudi and O'Brien, 2012). However, so far, the ROS-burst assay was the first biochemical assay for *M. polymorpha* with the ability of a fast screening for potential elicitors.

3.3 MpSERK – a functional co-receptor

All ligand-binding LRR-receptors studied so far depend on a co-receptor of the SERK-family (protein kinase family LRR-RLK LII; aan den Toorn et al., 2015). These co-receptors play an outstanding role in a multitude of processes related to immunity and development (Kim and Russinova, 2020). In immune signaling, the co-receptor is crucial for the intracellular transphosphorylation and thus for the conversion of ligand perception at the surface into cellular responses (Wang et al., 2014; Schwessinger et al., 2011). The genome of *M. polymorpha* encodes only one SERK gene. Therefore, we wanted to test whether MpSERK has a redundant function to the SERK genes from angiosperms.

In silico analysis of MpSERK (www.marchantia.info) showed an identity to AtSERK1/2 of 80-82% (AtSERK3= 73,6% and AtSERK4= 72%). Like other SERKs, MpSERK contains five LRR domains (**Figure 10**), resulting in a size similar to AtSERKs.

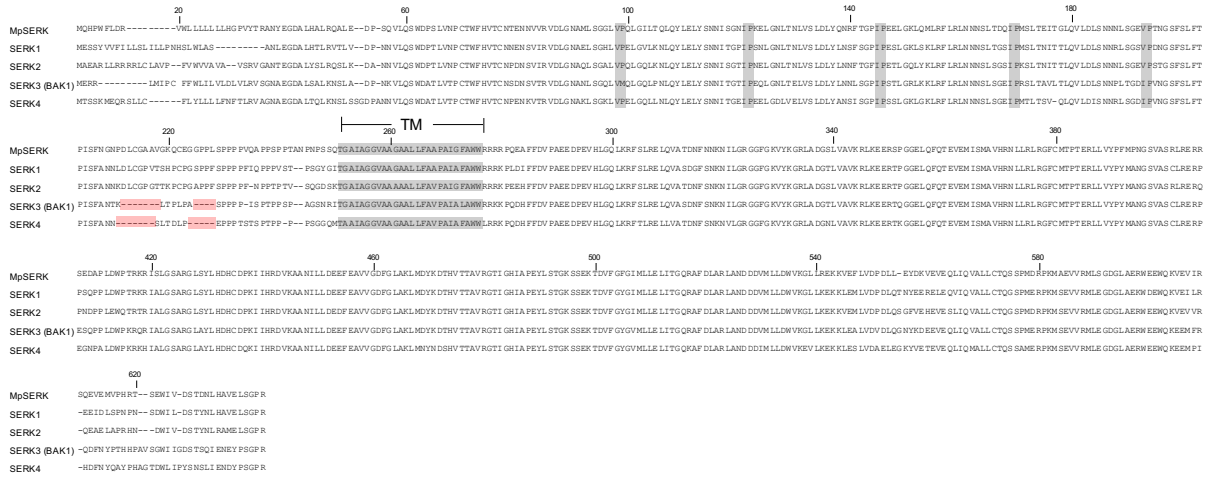

Figure 10: MpSERK is a genuine SERK with highest similarity to AtSERK1/2. Protein size: MpSERK= 627 aa, AtSERK1= 625 aa, AtSERK2= 628 aa; AtSERK3 (BAK1)= 615 aa, AtSERK4= 620 aa. All compared proteins include 5 LRR domains (IP-motifs and transmembrane regions are highlighted in grey). Lack of extra amino acids in SERK3 and SERK4 are highlighted in red.

However, functional studies are missing. A knock-out of this MpSERK gene resulted in a developmental phenotype, with plants exhibiting a fuzzy, multiple branched thallus and reduced production of gemmae (**Figure 29**; Dr. Isabel Monte, pers. communication).

To test if MpSERK can substitute for AtBAK1, the MpSERK gene was co-transformed with a pFRK1:Luciferase-reporter in *A. thaliana* protoplast from *fls2 x bak1-4* mutant plants. These protoplasts, when transformed with the pFRK1:Luciferase-reporter and AtFLS2, showed induced activity of the luciferase reporter when treated with 100 nM flg22, however not to concentrations ≤2.5 nM flg22 (**Figure 11** a). In contrast, protoplasts transformed additionally with AtBAK1 showed a clearly increased sensitivity and responded also to ≤2.5 nM flg22 (**Figure 11** b), confirming earlier observations by Mueller et al. (2011). Protoplasts co-transformed with FLS2 and MpSERK also showed this increase in sensitivity and responded to 2.5 nM flg22, indicating that MpSERK can substitute for AtBAK1 in the *A. thaliana* cells (**Figure 11** c).

To test if MpSERK also physically interacts with LRR-RLKs in a ligand-dependent way, as well documented for AtBAK1 (Chinchilla et al., 2007), tagged versions of the proteins were transiently expressed in *N. benthamiana* leaves and used in co-

immunoprecipitation experiments (**Figure 11** d). Indeed, as for the positive control with AtBAK1, MpSERK was found to co-immunoprecipitate with At- and SlFLS2 (**Figure 13**), as well as with AtEFR (**Figure 15**), but also with the different EFR-ECD:MpLRR-RLK-KD chimeric receptors (**Figure 15**) and with MpHSL (**Figure 18**) in a ligand-dependent way but not in the respective mock-treated control cells. Immunoprecipitation-Mass Spectrometry (IP-MS) data of Dr. Isabel Monte show additionally the interaction of MpSERK with MpBIR (data not shown).

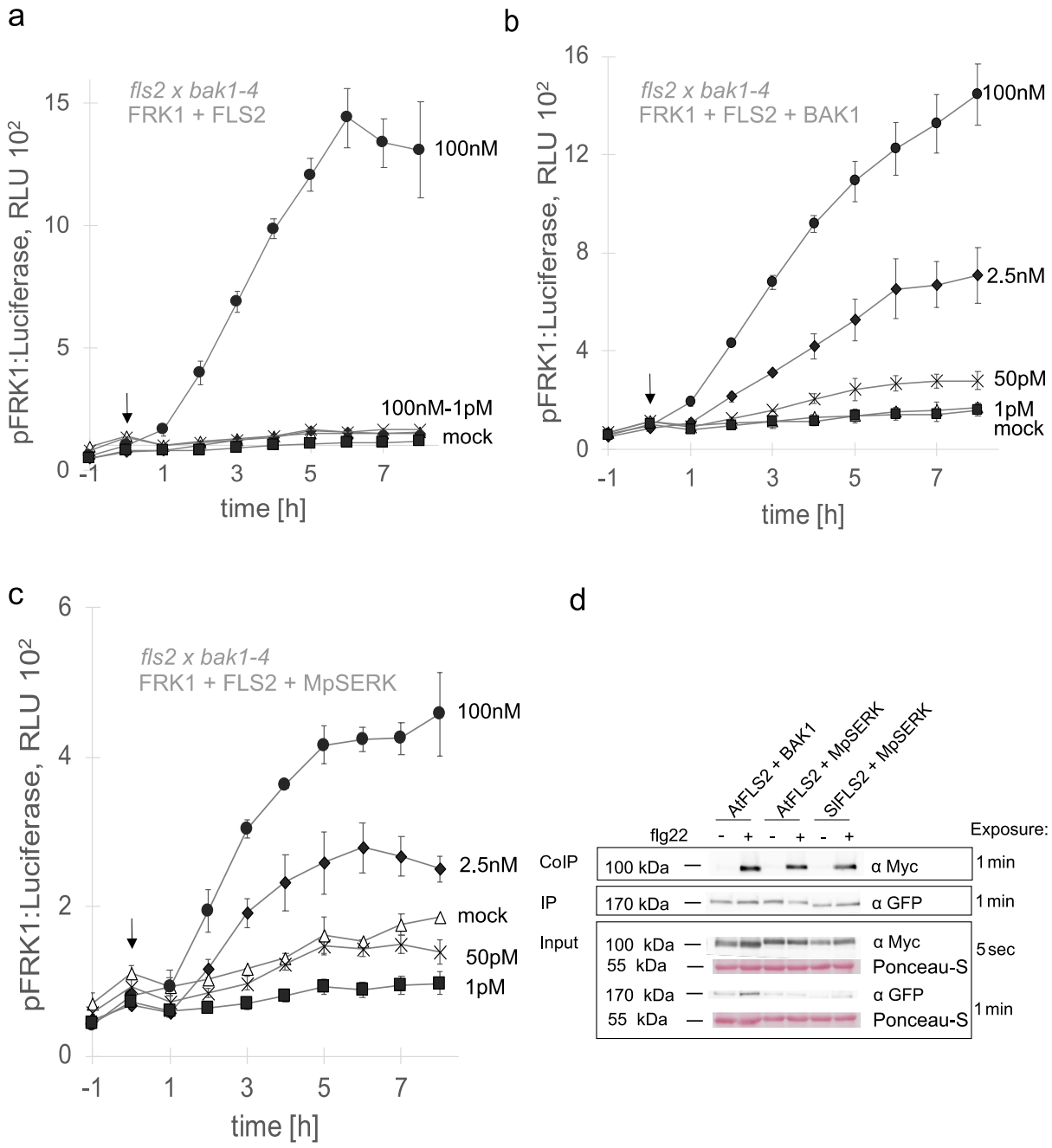

Figure 11: *fls2 x bak1-4 A. thaliana* protoplasts show an improved sensitivity to flg22 when complemented with MpSERK, which is able to interact with FLS2. a-c) pFRK1:Luciferase-reporter assay with *A. thaliana* protoplasts (*fls2 x bak1-4* mutant background) co-expressing AtFLS2 and AtBAK1 or MpSERK, respectively. Arrows indicate the timepoint of mock treatment or addition of flg22

at the concentrations indicated. Error bars indicate the standard deviation of 3 replicates. The experiments were repeated at least three times. mock control=open triangles; 100 nM flg22= circles; 50 pM flg22= crosses; 2,5 nM flg22= diamonds; 1 pM flg22= squares. **a)** Transient expression with AtFLS2 alone. **b)** Protoplasts co-expressing AtFLS2 and AtBAK1. **c)** Co-expression of AtFLS2 and MpSERK. **d)** Ligand dependent interaction of FLS2, either AtFLS2 or SlFLS2 from tomato, with AtBAK1 or MpSERK. Western blot detection of flg22-mediated co-immunoprecipitation of MpSERK:4xMyc by pulling down AtFLS2 or SlFLS2 (GFP-tagged), respectively. Transiently transformed *N. benthamiana* plants, expressing MpSERK and AtFLS2 or SlFLS2, respectively, were infiltrated with mock (-) or 1 µM flg22 (+), respectively. Leaves were harvested after an incubation of approximately 3 minutes. Immunoprecipitation of FLS2:GFP was performed using GFP-trap Agarose beads. Co-immunoprecipitation of MpSERK:4xMyc and AtBAK1:4xMyc, respectively, was detected by using a-myc antibody. Protein input (before IP and CoIP) was controlled by Western blotting and detected by appropriate antibodies. Co-immunoprecipitation of AtBAK1 by pulling down AtFLS2 was used as a positive control. Ponceau-S staining ensured comparable amount of loaded sample.

To corroborate the functionality of MpSERK as a functional co-receptor for AtFLS2 in *A. thaliana* cells, we used an approach with reciprocal swapping of the cytoplasmic kinase domains between MpSERK and AtFLS2. In an earlier study (Albert et al., 2013b), this approach was used to prevent the possible substitution of the AtBAK1 function by other members of the SERK family (**Figure 12**). Thereby, it was found that neither the chimeric FLS2 receptor with the BAK1 kinase, termed FtB, nor the chimeric BAK1 protein with the FLS2 kinase, termed BtF, could confer functional flg22 perception when individually expressed in *A. thaliana* cells. Co-transformation of BtF and FtB, however, did result in functional flg22 perception, demonstrating that the heterologous complex formation of FLS2 with a SERK co-receptor is essential for cytoplasmic signal output. Here, we constructed an AtFLS2 receptor comprising the cytoplasmic kinase domain of MpSERK (FtM) and an MpSERK with the kinase domain of AtFLS2 (MtF), respectively. Expression of the chimeric receptors separately did not initiate reporter gene activation upon flg22 treatment (**Figure 13**, **Figure 31**). Co-expression of the two reciprocal chimeras FtM and MtF, however, did result in a flg22-induced immune response (**Figure 13** b), as for the positive control (FtB, BtF, **Figure 13** a, Albert et al., 2013b).

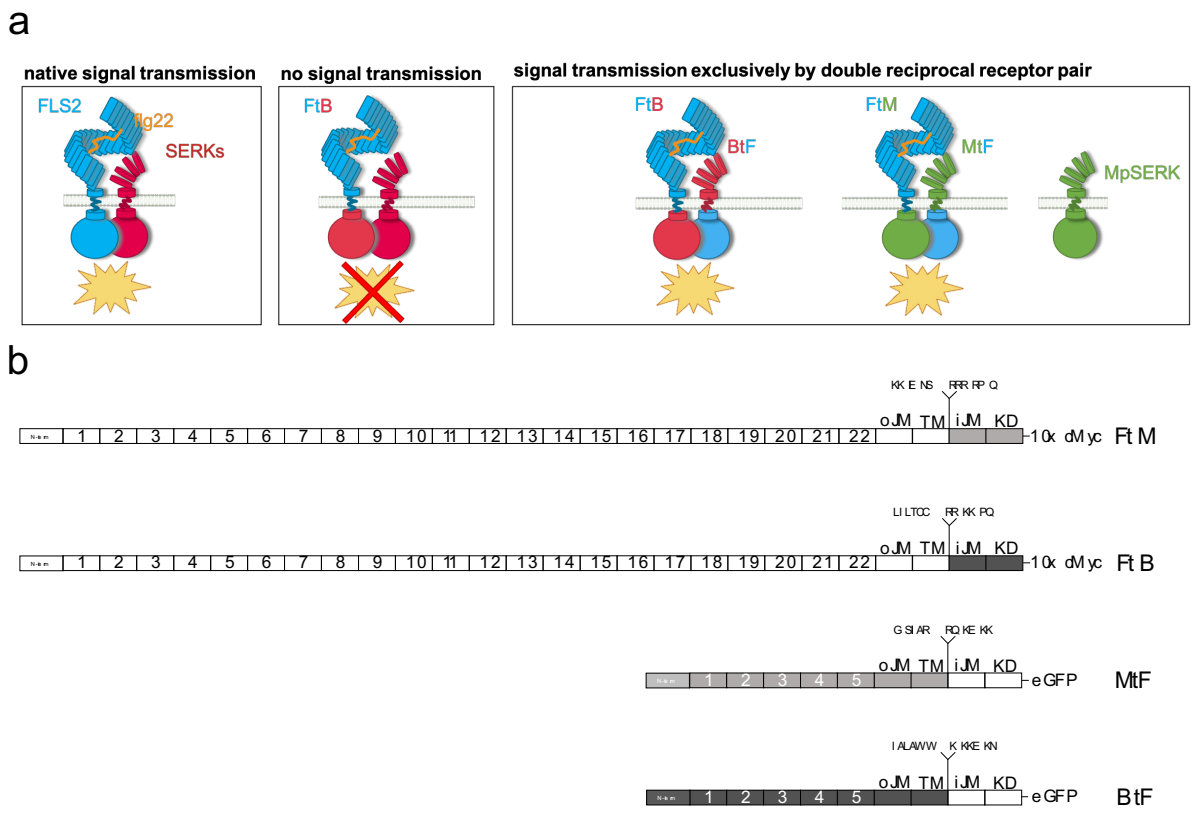

Figure 12: Double reciprocal receptor approach guarantees the exclusive interaction between the two partners. a) Schematic representation of the double reciprocal receptor approach (Albert et al., 2013b). Native AtFLS2 is able to interact with all AtSERK co-receptors (native signal transmission). AtFLS2 with the heterologous kinase of AtBAK1 is non-functional since potential interactions with native SERKs do not provide the heterologous kinase pair required for signal transduction (no signal transmission), unless this is provided by a reciprocal chimeric SERK with a AtFLS2 kinase domain (signal transmission exclusively by double reciprocal receptor pairs, Albert et al., 2013). In this study we replaced the AtBAK1 domains with the respective domains of MpSERK, resulting in FtM and MtF constructs, respectively. **b)** Chimeric constructs consistent of AtFLS2 and AtBAK1 or MpSERK, respectively. White, F= AtFLS2; dark grey, B= AtBAK1; grey, M= MpSERK.

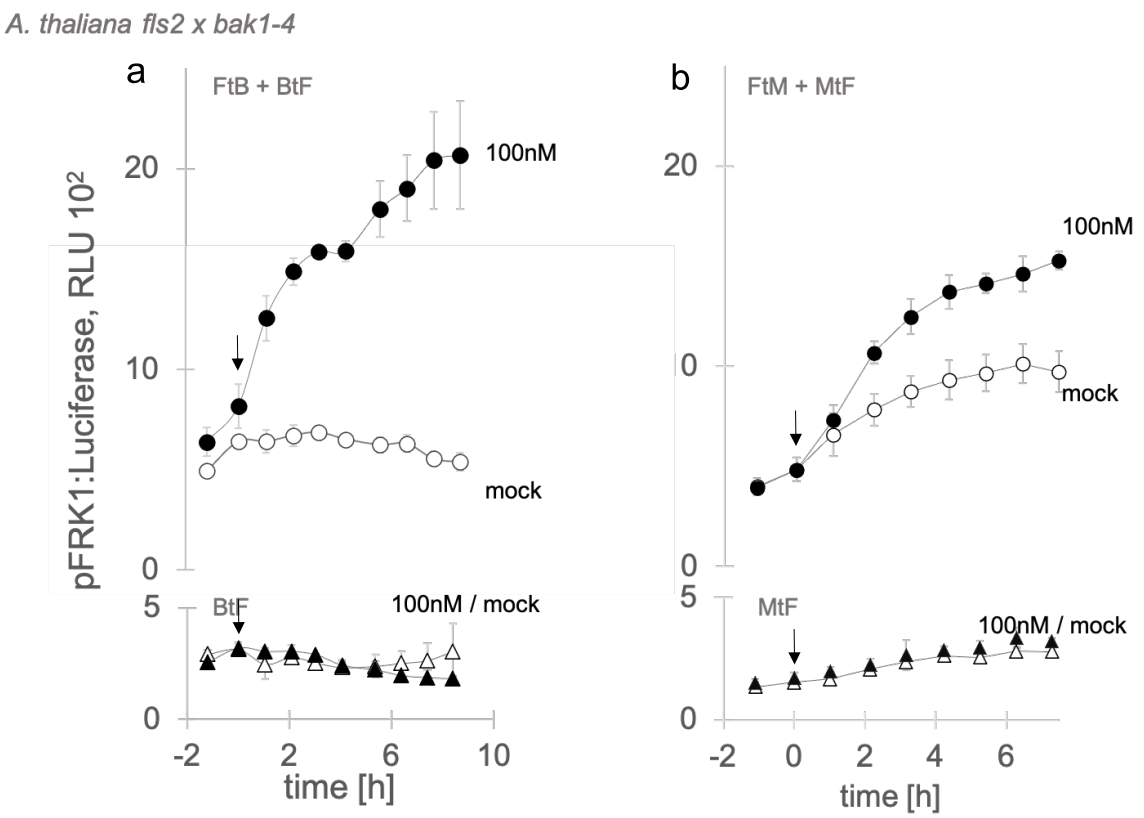

Figure 13: Interaction of MpSERK and FLS2 forms a functional receptor/co-receptor pair, when carrying reciprocal swaps of their cytoplasmic kinase domains. Co-transformation of *A. thaliana* protoplasts (*fls2 x bak1-4* mutant background) with the pFRK1:Luciferase-reporter and the chimeric constructs FtB, BtF (**a**) and FtM, MtF (**b**) as indicated. Arrows indicate the timepoint of treatment with mock solution (solvent for the peptide, open symbols) or 100 nM flg22 (closed symbols). Error bars represent the standard deviation of 3 replicates. The experiment was repeated three times with the same outcome.

The double reciprocal receptor approach supported the finding of MpSERK substitution by unequivocally demonstrating the interaction of the recombinant versions of MpSERK and FLS2 (**Figure 12**).

It is interesting to note that the *Mpserk* mutant is not lethal, as it is the case with the full knock out of the SERK family in *A. thaliana* (Gou et al., 2012). However, it results in a severe negative effect on *M. polymorpha* (Dr. I. Monte, pers. communication). A mutation of *bak1* (SERK3) in *A. thaliana* shows also a negative influence on developmental processes, but also a negative impact on innate immunity (Kemmerling et al., 2007).

To support these observations, the experiments should be repeated using native promoters and in *M. polymorpha* itself. The broad expression of MpSERK in different tissues (**Figure 30**) resembles the expression pattern of BAK1 in *A. thaliana* (Klepiknock-outva et al., 2016). Expression of MpSERK in the thallus, but also in sexual reproductive tissues, corresponds to the extensive involvement of SERKs in diverse processes. MpSERK is important for the development of *M. polymorpha*, as

shown by the multiple branched thallus of *Mpserk* knock-out lines (**Figure 29**, Dr. I. Monte). With respect to a function of MpSERK in innate immunity, our deductions are based on data generated in vascular plants. A major shortcoming for the demonstration of the involvement of MpSERK in innate immunity is the lack of a MAMP or an elicitor preparation that stimulates immune responses in *M. polymorpha* via a LRR-RLKs or LRR-RLPs.

However, the existence of MpSERK hints at the presence of LRR-receptor-mediated processes in non-vascular plants. Sequence analysis showed the presence of a SERK ortholog also in *Closterium*, a unicellular algae, belonging to the conjugates algae (Zygnematales, Sasaki et al., 2007). This indicates an origin of this type of (co-)receptor at times preceding the emergence of land plants and emphasizes the importance of such a co-receptor.

3.4 MpLRR-RLKs with functional kinase domains but orphan function

The previous chapter described a first example of a functional LRR-RLK protein from *M. polymorpha*. However, SERKs act as co-receptors for different LRR-RLKs that function as genuine binding sites for a variety of specific ligands (Hohmann et al., 2017). Thus, it is conceivable that MpSERK acts also as a co-receptor for ligand-binding LRR-RLKs in *M. polymorpha*. Therefore, we identified potential MpLRR-RLKs and tested whether the selected candidates show common features with LRR-RLKs we know from vascular plants.

In silico analysis revealed over 60 genes encoding potential LRR-RLKs in the genome of *M. polymorpha* (G. Felix, P. Chatelain, pers. communication). Apart from MpSERK, additional six of these LRR-RLKs represent orthologs found to be conserved in angiosperms. These were CLAVATA1 (CLV1, Hirakawa et al., 2020), PHLOEM INTERCALATED WITH XYLEM (PXY)-correlated 1 (PXC1), PXC2, EXTRA MICROSPOROCYTES 1 (EMS1), FEI2 (sequence analysis Prof. Dr. Georg Felix), as well as an ortholog of HAE/HSL (see chapter 3.5; Furumizu et al., 2021; Bowman et al., 2017a), but experimental evidence for their role in *M. polymorpha* has not been provided yet. Even less is known for the putative MpLRR-RLKs that have no obvious orthologs in angiosperms. In particular, there is no information about ligands for these MpLRR-RLKs as well as on the physiological output programs that activation of these receptor might have in *M. polymorpha*. In this project, we selected 20 of these MpLRR-

RLKs as candidates, based on the predicted size of their LRR ectodomains as potential ligand-binding sites.

Due to the lack of ligands for these MpLRR-RLKs, we set out to test whether the cytoplasmic kinase domains of these proteins could functionally substitute for the cytoplasmic kinase domain of the well-studied EF-Tu receptor EFR, via a chimeric receptor approach. The chimeric receptors consisted of the ectodomain and transmembrane domain of EFR and the cytosolic part with the kinase domains of the MpLRR-RLKs. The ectodomain of EFR perceives an 18 amino acid long epitope of the elongation factor Tu (elf18) of bacteria (Zipfel et al., 2006). Each of the chimeric receptors was tested for responsiveness to elf18, after heterologous expression in *N. benthamiana* leaves or protoplasts from *A. thaliana* plants with a mutation of the EFR gene (**Table 15**).

When expressed in *N. benthamiana* leaves, hybrid receptors with three out of 20 kinases tested, Mapoly0039s0122 (MpLRR-RLK 5), Mapoly0035s0149 (MpLRR-RLK 10) and Mapoly0065s0076 (MpLRR-RLK 15), respectively, responded to treatment with elf18 with a clear ROS-burst (**Figure 14** a), and a clear induction of ethylene biosynthesis (**Figure 14** b). Similarly, when co-transformed with the pFRK1:Luciferase-reporter in *A. thaliana* protoplasts (*efr x fls2* mutant background), cells expressing the same three chimeric receptors also responded with increased luciferase activity to treatment with elf18 (**Figure 14** c).

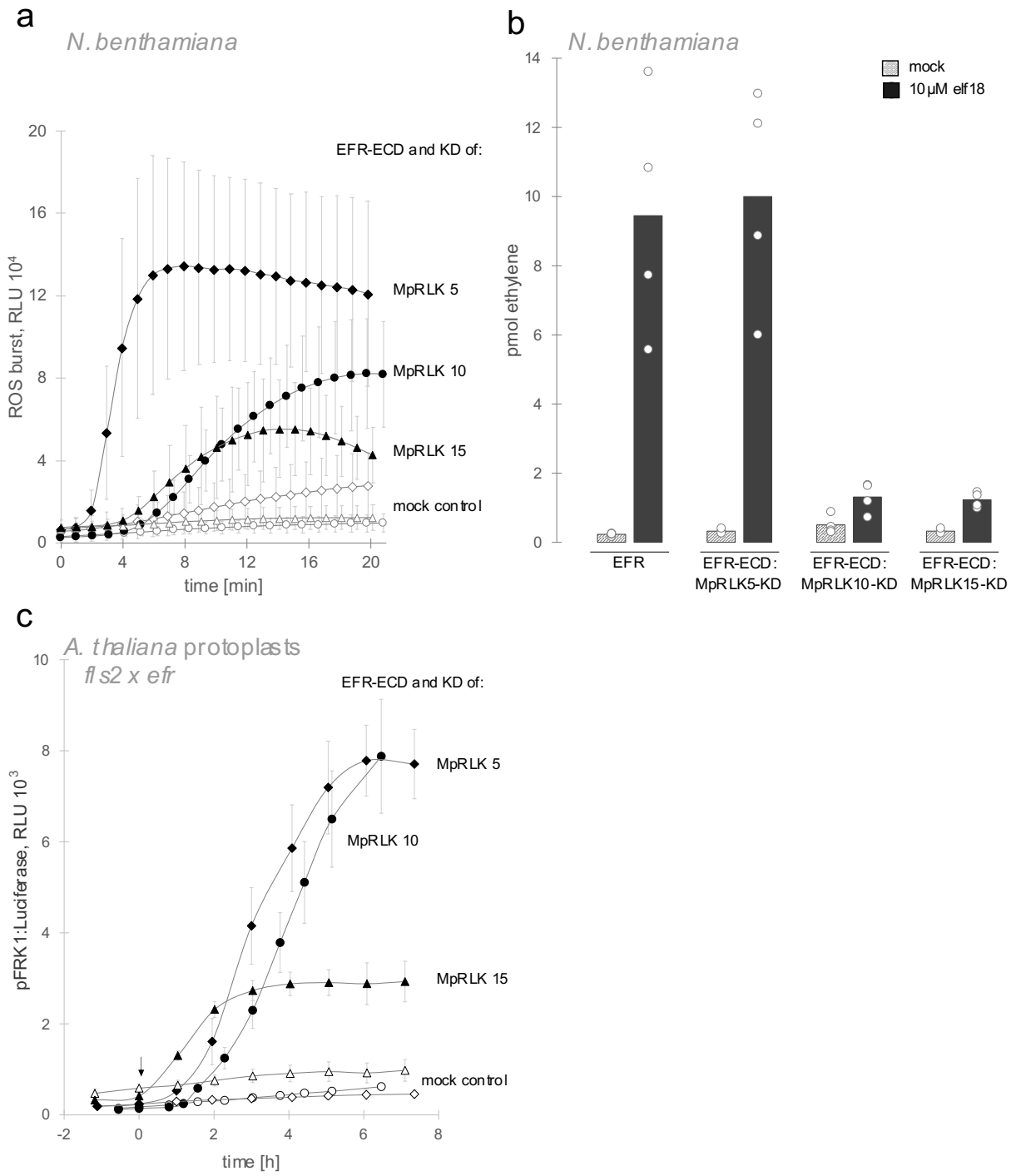

Figure 14: The kinase domains of MpLRR-RLK 5, 10 and 15 can substitute for the kinase domain of EFR. Chimeric EFR receptors with the cytoplasmic kinase domain replaced by the corresponding domains of MpLRR-RLKs were expressed and tested for functionality of elf18 perception in *N. benthamiana* leaves (a and b) or in *A. thaliana* protoplasts (*efr-1 x fls2*) (c). **a)** ROS-burst and **b)** ethylene production after treatment with elf18 in leaf pieces expressing the chimeric receptors indicated. Data represent mean and standard deviation of n=4 replicates. **c)** Luciferase-reporter activity in protoplasts treated with 1 µM elf18 (arrow). Data represent means and standard deviations of three replicates. a), b) and c) All experiments were performed at least three times with the same result.

In contrast, expression of the other 17 chimeric receptors, although leading to detectable accumulation of the proteins in the transformed cells, did not show elf18-dependent induction of the stress responses commonly triggered by activated PRRs

(expression control via Western Blotting, **Figure 34**). These MpLRR-RLK kinases might activate downstream signaling cascades leading to responses different from the stress response tested in our assays. However, a lack of functionality could also arise from a divergent evolution in the 450 MY since the branching of the bryophyte line from the one leading to the angiosperms. This might result in incompatibilities in the interaction of these MpLRR-RLK kinases with cytoplasmic elements relevant for the induction of the stress responses in angiosperms.

In further experiments the active chimeric receptors were tested for their sensitivity to the elf18 ligand. The chimeric receptor with the kinase of MpLRR-RLK 5 showed significant induction of ROS production in transiently transformed *N. benthamiana* leaves down to concentrations of 10 pM elf18. Activation of ROS production via chimeric receptors containing the kinase of MpLRR-RLK 10 was less sensitive and occurred only after treatment with elf18 concentrations ≥ 100 pM. The chimeric receptor containing the MpLRR-RLK 15 kinase domain was even less sensitive and showed a ROS burst response after treatment with ≥ 1 nM. Further, the amplitude of responses to saturating concentrations of elf18 was generally lower with the receptor carrying the kinase of MpLRR-RLK 15 than with receptors comprising the kinases of MpLRR-RLK 5 or MpLRR-RLK 10 (**Figure 33**). Comparing the sensitivity of these chimeric receptors with an authentic EFR (EC_{50}=~ 200 pM; Kunze et al., 2004), they appear less sensitive.

Co-immunoprecipitation of the hybrid receptors, co-expressed with tagged AtBAK1 or MpSERK in *N. benthamiana* leaves, was used to corroborate formation of ligand-dependent complexes between these receptors and co-receptors. Indeed, all of the active chimeric receptors formed a complex with AtBAK1 or MpSERK in a ligand-dependent way, just as the authentic EFR (**Figure 15**).

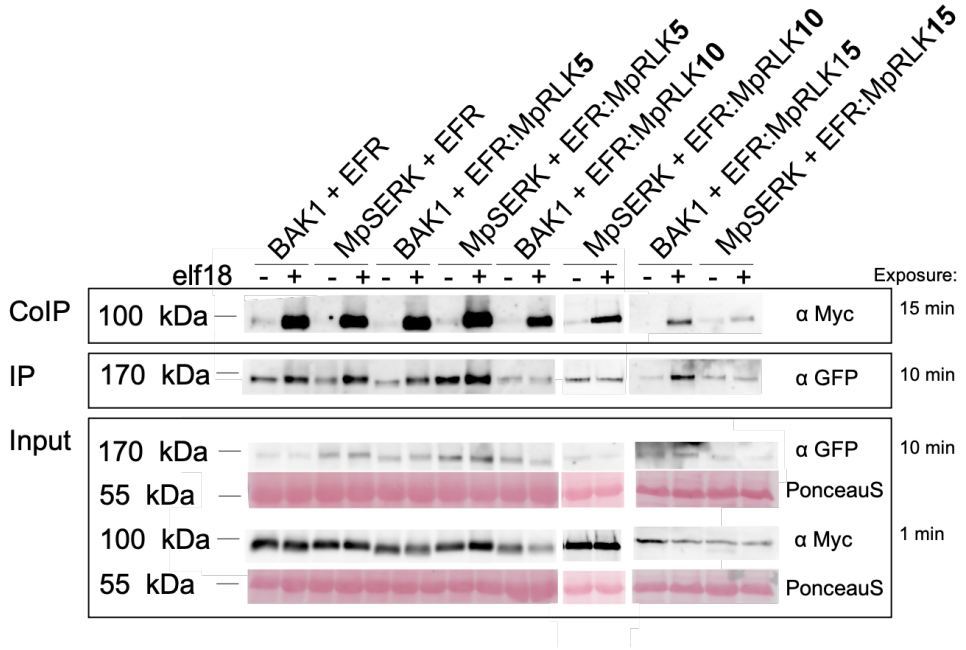

Figure 15: Ligand-dependent complex formation between the chimeric receptors and MpSERK or AtBAK1. Transiently transformed *N. benthamiana* plants, expressing EFR-ECD:MpLRR-RLK-KD chimeras and MpSERK or BAK1, respectively, were infiltrated with mock (-) or 1 µM elf18 (+), respectively. Leaves were harvested after an incubation of approximately 3 minutes. Immunoprecipitation of GFP-tagged chimeric receptors was performed using GFP-trap Agarose beads. Co-immunoprecipitation of MpSERK:4xMyc and BAK1:4xMyc, respectively, was detected by using a-myc antibody. Protein input (before IP and CoIP) was controlled by Western blotting and detected by appropriate antibodies. Ponceau-S staining ensured comparable amount of loaded sample. The experiments were performed three times, with the same outcome, representative data are shown.

The biological functions of these MpLRR-RLKs, notably the ligands they perceive, remain to be elucidated. An indication for the function of a protein could be provided by its expression pattern.

Expression in more specific tissues, for example related to fertilization, can hint towards more specific functions. The main expression of MpLRR-RLK 5 in the sporeling and the sperm (**Figure 35**), could hint towards an involvement in fertilization processes. An example in angiosperms is the involvement and subsequent expression of RLK proteins in the pollen tube. Rapid alkalinization factor 4 (RALF4) and RALF19 are perceived by diverse receptors including *Catharanthus roseus* RLK1-like (*Cr*RLK1L), leucine-rich repeat extension proteins (LRX), ANXUR1/2 (ANX1), BUDDHA´S PAPER SEAL1/2 (BUPS1/2) and LORELEI-like GLYCOLPHOSPHATIDYLINOSITOL (GPI)-ANCHORED PROTEINS (LLGs). These proteins are building complexes with RALFs and adaptor proteins and are curtail to ensure pollen tube growth and integrity (**Figure 16** a; Moussu et al., 2020; Stegmann and Zipfel, 2017; Yu et al., 2021; Johnson et al., 2019). Bryophytes produce a helical shaped sperm cell with and elongated nucleus, and two flagella (Figure 16 b;

Shimamura, 2016). These sperm cells are motile in contrast to angiosperms, where an immotile sperm is transported by the pollen tube to the egg cell (Figure 16 a; Higo et al., 2018). Even though the genome of *M. polymorpha* encodes three RALF peptides (Bowman et al., 2017a; Mecchia et al., 2020), from which two are expressed in the antheridium (Liverwort Atlas eFP Browser at bar.utoronto.ca), none of the RLK proteins involved in the signaling complex in angiosperms show sequence similarity to MpLRR-RLK 5. Due to the lack of sufficient information about the molecular genetics of fertilization of the egg cell by the sperm cell in bryophytes (Minamino et al., 2021) it cannot be excluded that LRR-RLKs are involved in this process. It is however expected that chemotaxis also happens in bryophytes to ensure fertilization, MpLRR-RLK 5 may thus, still play a role in the fertilization process.

To evaluate a potential involvement of MpLRR-RLK 5, knock-out mutants can be analyzed in sperm fertility or swimming velocity (Higo et al., 2018).

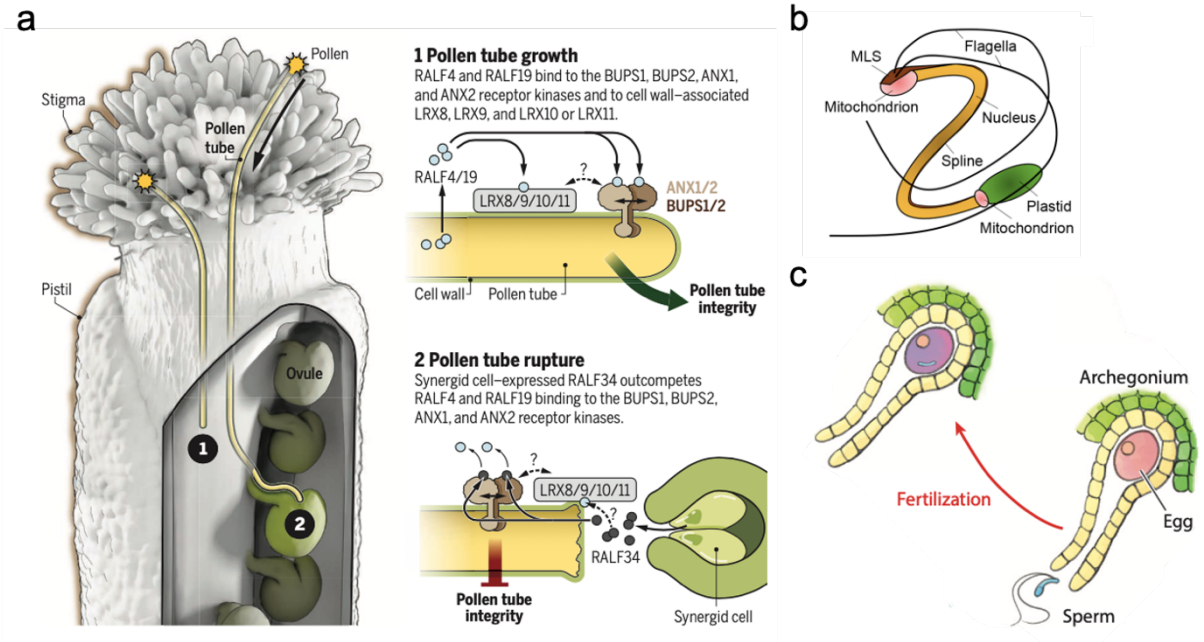

Figure 16: Towards fertilization. Figures modified from Kohchi et al. (2021), Stegmann and Zipfel, (2017) and Minamino et al. (2021). a) After the pollen landed on the stigma of the pistil, the sperm cells are transported in a pollen tube to finally fertilize the egg cell. 1) The signaling complex of RALF4 and RALF19 peptides with LRX, ANX and BUPS proteins is ensuring pollen tube growth. 2) Later, RALF34 is outcompeting RALF4 and RALF19 to initiate pollen tube rupture and release of the sperm cells (Stegmann and Zipfel, 2017). **b)** Spermatozoid of bryophytes consist mainly of an elongated nucleus and two flagella. MLS= multilayered structure (Minamino et al., 2021). **c)** The spermatozoid of bryophytes is motile and is transported to the archegonium by water and further self-locomotes to the egg cells (Kohchi et al., 2021a).

A more broad expression in the thallus is comparable to the expression in the plant body of angiosperms (leaves and stem) and is similar to the expression pattern of

known LRR-RLKs like FLS2 (Klepikova et al., 2016). MpLRR-RLK 10 and 15 are expressed in the thallus and could thus perform comparable functions of known LRR-RLKs.

To further characterize the function of MpLRR-RLKs, knock-out mutants have to be generated and analyzed for developmental phenotypes and altered immune responses. As prerequisite for detecting an effect on immunity in *M. polymorpha*, suitable pathogens have to be found and robust immune response assays, such as defense-related induction of phytohormones, have yet to be established. To identify potential MAMPs/DAMPs an additional approach, in which the receptors MpLRR-RLK 5, 10 and 15 are expressed in *N. benthamiana* and used for screening of potential ligands present in microbial extracts (MAMPs) or plant-derived extracts (DAMPs) with well-established assays like ROS or ethylene biosynthesis, could be performed.

3.5 MpLRR-RLKs in plant development

As mentioned above, few orthologs for LRR-RLKs from vascular plants with known or presumed functions were identified in *M. polymorpha*. One of them is an ortholog of HSL (Furumizo et al., 2021). Additionally, four putative IDA peptides were identified in the genome of *M. polymorpha* (Bowman et al., 2017). However, functional analyses were not reported. In vascular plants, HAE/HSL receptors control floral organ abscission (Stenvik et al., 2008) but are also involved in the cell wall remodeling for the emergence of lateral root primordia (LRP) (Aalen et al., 2013), when perceiving a small secreted protein, IDA (Stø et al., 2015; Santiago et al., 2016; Butenko, 2003).

However, floral organs, fruits or lateral roots are not present in *M. polymorpha*. This led us to ask the questions whether the putative MpHSL receptor indeed perceives the endogenous MpIDA peptides and which biological function such a ligand receptor pair might have in *M. polymorpha*.

Expression of AtHSL in *N. benthamiana* leaves showed that activation of this receptor with its IDA ligand induced stress responses like a ROS burst (Butenko et al., 2014a). Thus, we first tested the kinase domain of MpHSL in the chimeric receptor approach with the EFR-ECD. A ROS-burst assay confirmed the ability of the MpHSL kinase to transmit the immune signal (**Figure 41**).

Next, we wondered whether authentic MpHSL would respond to peptides with the IDA-like sequences found in *M. polymorpha*. For this, MpHSL was transiently expressed in *N. benthamiana* leaves or *A. thaliana* protoplasts and tested for induction of stress

response after treatment with different IDA-type peptides (**Table 9**) as described above for the chimeric EFR receptors. Exclusively cells expressing MpHSL showed a response to two of the four MpIDA peptides, MpIDA1 and MpIDA2, but not MpIDA3 or MpIDA4 (**Figure 18** a, **Figure 43** a-c, Figure 42).

MpHSL showed generally a higher sequence similarity to HSL1 and HAE than to HSL2 (**Table 16**). A specially high conservation between AtHSL/HAE and MpHSL can be observed in the region relevant for binding of the IDA ligand in AtHSL/HAE (**Figure 17**; Stø et al., 2015; Furumizu et al., 2021).

a

LRR	AtHSL1-ECD	LRR	MpHSL-ECD
3	IPSSFGEFRKLESLNLAGNFLSGT	3	IPESYGKFPKLTHLDLSANLLEGS
4	IPASLGNVTTLKELKLAYNLFSPSQ	4	IPSHIGNVSTLVLFEAHMNTFNSS
5	IPSQLGNLTELQVLWLAGCNLVGP	5	LPVELGNLKHLEVL GSWCLLQGN
6	IPPSLSRLTSLVNLDLTFNQLTGS	6	IPASLGE TNLTAYL EDNSLAGS
7	IPSWITQLKTVEQIEFNNNSFSGE	7	IPPELGKLKRLVVLDLSNNSLTGG
8	LPESMGNMTTLKRFDASMNKLTGK	8	IPRELMFLPNLRELQLYQNKLSGQ
9	IPDNLNLL NLESLNLFENMLEGP	9	IPAEFGNLTSLVEIDLSENQLVGP
10	LPESITRSKTLSELKLFNNRLTGV	10	IPESVSFLTSLELIHFHTNSLNGS
11	LPSQLGANSPLQYVDLSYNRFSGE	11	IPTGIGSLPGLYDLKLFNNLLTGQ
12	IPANVCGEGKLEYLILIDNSFSGE	12	IPARLGEPSRLQTLDVSSNSLVGL
13	ISNNLGKCKSLTRVRLSNNKLSGQ	13	IPRGLCTGGALDTLILFDNELSGD
14	IPHGFWGLPRLSLLELSDNSFTGS	14	IPEDLGSCPSLQRIRLQNNKLNGS
15	IPKTIIGAKNLSNLRISKNRFSGS	15	VPVGLWSYPLVKHVDLSNNELDGD
16	IPNEIGSLNGIIEISGAENDFSGE	16	ITFEKVTTSMLEALYVNNNLFSGS
17	IPESLVKLKQLSRLDLSKNQLSGE	17	FPTQVGSLANLIILIASNNNFHGE
18	IPRELRGWKNLNELNLANNHLSGE	18	LPKELGDLNFLTKLELANNDLTGP
19	IPKEVGILPVLNYLDLSSNQFSGE	19	IPTSLSQCERLSTLNLSGNQLVGE
20	IPLELQNLK LNVLNLSYNHLSGK	20	IPSVLGSLPALNVLDLSHNKLSGP

b

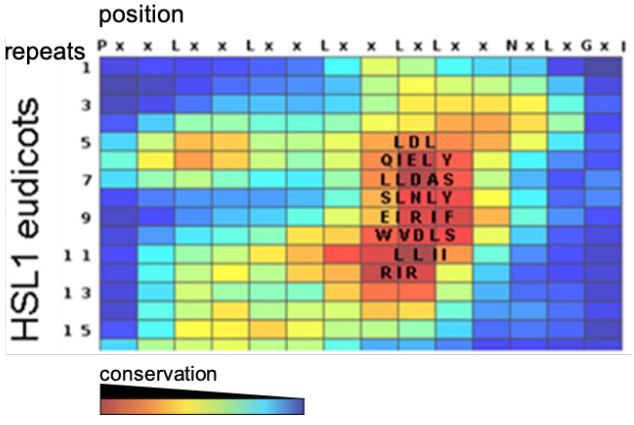

Figure 17: MpHSL encodes a conserved binding pocket and provides thus a potential ligand binding site. a) Sequence comparison between AtHSL1-ECD and MpHSL-ECD, highlighting the conserved residues of the ligand-binding pocket, as defined by comparing HSL1 orthologs from

eudicotyledons (Stø et al., 2015). Using a heatmap, based on Repeat Conservation Mapping (RCM), Stø et al., (2015) identified identical and highly similar residues in the LRR domains of HSL1 orthologs of eudicots. The highest conservation corresponds to the residues Santiago et al., (2016) later identified as the binding pocket. Peptide binding was indicated via isothermal titration calorimetry (ITC) and the binding pocket further characterized via crystals of HAE and the HAE /IDA complex (Santiago et al., 2016). Residues which are part of the ligand-binding pocket of AtHSL1, and the equivalent position in MpHSL, are depicted in bold. Furthermore, identical residues are printed in red, similar residues in green, unrelated residues in blue Residues which provide the helical structure of LRRs are printed in gray. **b)** Modified heat map of Stø et al., (2015) highlighting the conserved residues in the ectodomain of HSL1 orthologs of eudicots.

Furumizu et al., (2021) postulated in their paper the compatibility of MpIDA1 and 2, to fit into the binding pocket of MpHSL, based of sequence models. By testing different versions of the MpIDA peptides for activity, we tried to identify the necessary properties of the peptide which are needed to fit into the binding pocket of MpHSL and thus activate the receptor (**Figure 43**, **Table 17**). Our results showed a loss of activity when truncating the N-term of MpIDA1 (MpIDA1-short, **Figure 43** c). Indicating the need of a specific length of the IDA/IDL peptide to be perceived. Santiago et al., (2016) showed the importance of the Arg-His-Asn-motif at the C-term of the peptide for interaction with a SERK. Even though MpIDA peptides do not encode an Arg the His-Asn-motif at the end of the C-term has to be present for activation. If the His-Asn-motif is also decisive for co-receptor binding has to be elucidated, however is expected considering its effect in *A. thaliana*.

A hydroxyproline at the position of the central proline acts as an anchor and improves peptide binding in angiosperms (Santiago et al., 2016). Based on the sequence model, Furumizu et al., (2021) also postulate a positive effect of a hydroxyproline at the central proline of MpIDA. However, this hypothesis has to be confirmed by activity assays. For this, peptides lacking the hydroxyprolination on the central proline have to be synthesized and tested on MpHSL. A hydroxyproline at the most C-terminal proline, however, seems to be harmful.

Furthermore, we tested whether MpHSL is dependent on a co-receptor of the SERK family by expressing MpHSL in *A. thaliana* protoplasts derived either from the *fls2 x bak1-4* background or the *efr x fls2* background. Only protoplasts expressing endogenous AtBAK1 were able to respond to MpIDA1, confirming the BAK1 dependency (**Figure 18** b). Complex formation of MpHSL with AtBAK1 or MpSERK was tested by co-immunoprecipitation. After pulling down GFP-tagged MpHSL, BAK1:4xMyc was co-immunoprecipitated in a ligand-dependent manner, as was MpSERK:4xMyc (**Figure 18** c).

These results demonstrate that MpHSL is recruiting a SERK as a co-receptor for activation and signal transmission like orthologs in angiosperm (Meng et al., 2016; Zhu et al., 2019; Butenko, 2003; Cho et al., 2008). Additionally, we demonstrated that MpHSL is forming a complex with MpSERK in a ligand-dependent manner. To further validate the functionality of the MpHSL/MpSERK complex the *A. thaliana bak1-4* mutant would have to be complemented with both, MpHSL and MpSERK, which should lead to an enhanced response to MpIDA.

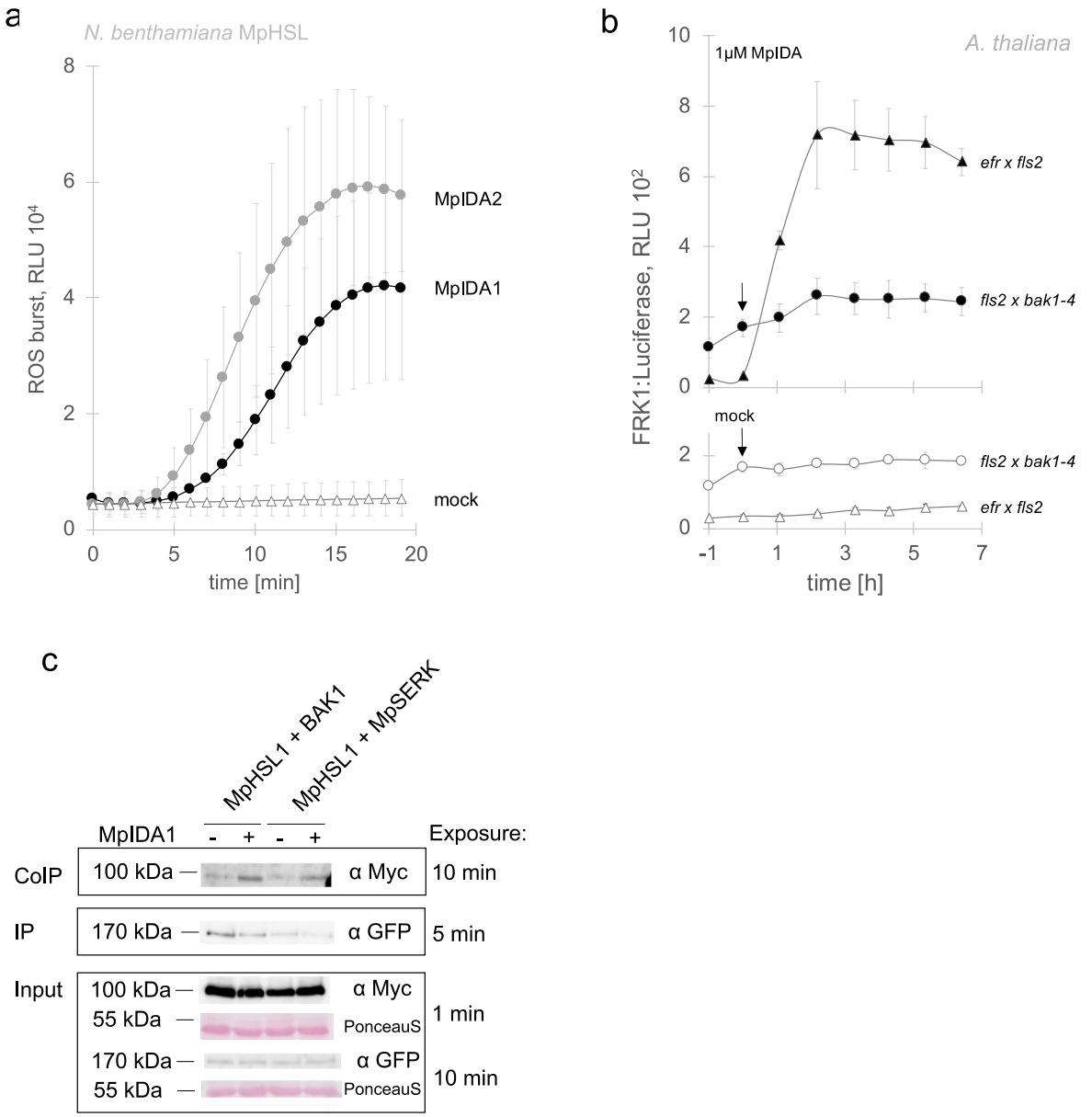

Figure 18: MpHSL and MpIDA form a functional receptor-ligand pair. a) ROS-burst in leaf pieces of *N. benthamiana* plants, expressing MpHSL, to treatment with mock solution, 100 nM MpIDA1 or MpIDA2, respectively (see **Figure 42** for control transformation with p19 only). Data points represent the average of three/four replicates. Error bars indicate the standard deviation of three/four replicates. **b)** *A. thaliana* protoplasts co-expressing MpHSL and pFRK1:Luciferase-reporter treated with 1 µM MpIDA1 (filled symbols) in the *efr-1 x fls2* background (triangles) or *fls2 x bak1-4* background (round

symbols). Arrows indicate timepoint of elicitation. **c)** Ligand-dependent co-immunoprecipitation of 4xcMyc-tagged MpSERK or BAK1, respectively, after pulling down MpHSL:GFP. Transiently transformed *N. benthamiana* plants, expressing MpHSL and MpSERK or BAK1, respectively, were infiltrated with mock (-) or 1 µM MpIDA1 (+), respectively. Leaves were harvested after an incubation of approximately 3 minutes. Immunoprecipitation of MpHSL:GFP was performed using GFP-trap Agarose beads. Co-immunoprecipitation of MpSERK:4xMyc and BAK1:4xMyc, respectively, was detected by using a-myc antibody. Protein input (before IP and CoIP) was controlled by Western blotting and detected by appropriate antibodies. Ponceau-S staining ensured comparable amount of loaded sample. Each experiment was performed at least 3 times and each data point is the average of three or four replicates. Error bars represent the standard deviation.

Having identified a matching peptide/receptor pair, we further focused on potential functions in *M. polymorpha*. To test the influence of the peptide on *M. polymorpha* directly, we applied 1 µM MpIDA to Marchantia gemmae, which caused growth inhibition of the thallus tissue (**Figure 19**).

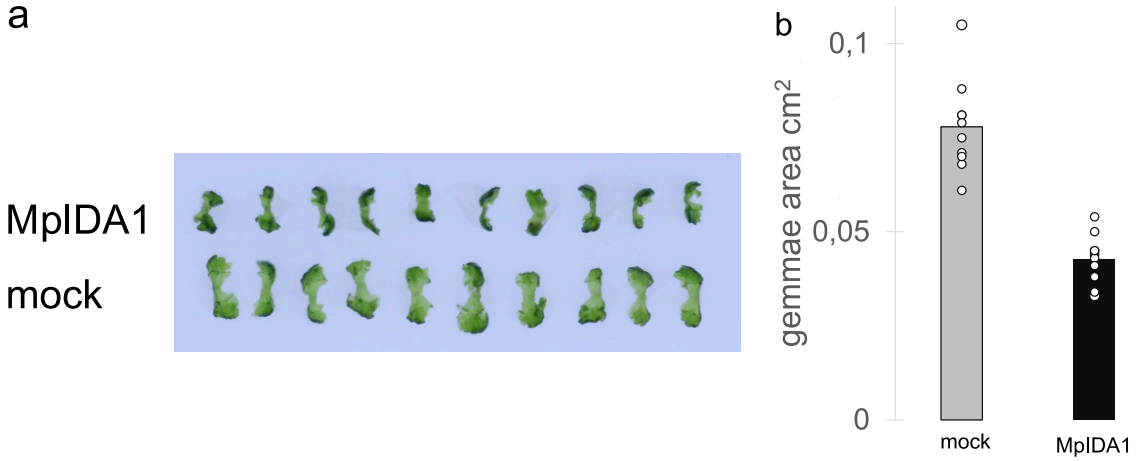

Figure 19: MpIDA1 inhibits the growth of *M. polymorpha* gemmae. a) Growth inhibition of gemmae, after 12 days in liquid medium containing mock solution or 1 µM MpIDA1. **b)** Quantification of gemmae size in cm^2. Bars represent the average surface area. Datapoints represent individual replicates. The experiment was repeated three times with the same outcome. Inactive peptides did not inhibit the growth of gemmae (**Figure 44**).

Floral organ abscission is an important function of the HAE/HSL/IDA signaling complex in vascular plants, however does not exist in bryophytes. Nevertheless, the life cycle of *M. polymorpha* entails two stages which could involve abscission processes. First, sexual propagation involves the development of sex-specific gametangiophores (**Figure 3**; Kohchi et al., 2021). After successful fusion of the sperm and the egg cell, a spore-containing sporangiophore is built. To release the spores, the spore capsules open up (Kohchi et al., 2021a), this opening of the spore capsules could be equivalent to the process of abscission. To validate this hypothesis archegoniophores could first be pollinated with sperm cells and subsequently treated with MpIDA peptide and mock, respectively. When harvesting the spores with water drops (harvesting solution),

differences in spore release could be determined via differences in OD of the harvesting solution. Second, asexual propagation of *M. polymorpha* is ensured by the production of gemmae. Gemma development starts with a single gemma cup floor cell protruding from the base of the gemma cup. The emerging gemma is dividing and detaches from the gemma cup floor after reaching its mature stage (Kato et al., 2020; Kohchi et al., 2021;**Figure 3**, **Figure 38**). The detaching of the mature gemma from the gemma cup floor, at the stalk cell, could hence involve a form of abscission.

To test whether MpIDA has an influence on the amount and timing of gemmae release, a release assay was performed (see chapter 2.2.19.4). However, despite attempts with several experimental set ups, no clear and reproducible effect of MpIDA treatment could be observed (**Figure 45**). Future approaches could try to improve the timing of the peptide treatment as well as to use different application techniques. Another possibility could be the addition of a surface tension reducing agent like silwet, to improve the supply of the peptide to the floor of the gemma cup, when treating directly with peptide. An addition of peptide into solid medium bears the risk of degradation of the peptide over time, due to instability, or a limited supply reliability due to immobilization.

To further identify the function of MpHLS/MpIDA, knock-out lines could be generated and tested for interference in gemmae and spore release. Heterologous complementation of the *hae/hsl2* or *ida* knock-out mutants in *A. thaliana* represents another possibility to validate the functionality of either or both the *M. polymorpha* receptor and peptides. A similar function in *M. polymorpha* would be plausible if MpHSL/MpIDA were able to complement the delayed loss of floral organs of the *A. thaliana* mutants (Stenvik et al., 2008).

The location of receptors and peptides is often linked to protein function. Localization of the MpHSL receptor and MpIDA peptides is thus expected to indicate protein function. Therefore, we compared the expression data of MpHSL and MpIDA with the expression pattern of AtHSL and AtIDA.

The expression database of *M. polymorpha* genes (Liverwort Atlas eFP Browser at bar.utoronto.ca) shows solid expression of MpHSL in all tissues and under all conditions (**Figure 39**). MpIDA1 shows rather low overall expression with clearly elevated levels in the gametophores and the gemma cups. MpIDA2 is generally higher expressed but does not show specificity with respect to an organ or tissue. The expression in propagation-related tissues of both active MpIDA peptides supports the hypothesis of potential areas of abscission associated with spore and gemmae

release. This would resemble the situation in *A. thaliana,* in which both, the HSL receptor as well as the IDA peptide, are expressed directly at the abscission zone (Butenko, 2003; Stø et al., 2015).

MpIDA3 is expressed exclusively in the sperm, but at low levels. MpIDA4 is as highly expressed as MpIDA2, however mainly in the thallus and under abiotic stress conditions (**Figure 40**). However, MpIDA4 does not show activation of the ROS burst in combination with MpHSL (**Figure 43** c).

For the confirmation of expression Atlas data, as well as for monitoring protein locations during different developmental stages or different treatments, reporter lines are useful. GUS-reporter constructs were used in several studies including the localization of IDA in *A. thaliana* (Butenko, 2003), but also for localization in *M. polymorpha* (Althoff et al., 2014).

3.6 MpSOBIR – as an adaptor kinase for RLPs in vascular plants?

Besides RLKs, a second multimembered family of cell surface receptors in plants is formed by RLPs. RLPs have a LRR ectodomain like RLKs but lack cytoplasmic kinase domains. Therefore, they depend on an additional RLK, the adaptor-kinase SOBIR. In *A. thaliana*, AtSOBIR1 associates with all the RLPs acting as PRRs (Albert et al., 2015; Zhang et al., 2021; Domazakis et al., 2018; Fan et al., 2022). The RLP-SOBIR1 dimers can be considered as bi-molecular equivalents of RLKs. As observed for the activation of RLKs, ligand binding to the RLP-SOBIR dimer recruits a SERK into a tri-partite complex that is essential for activation of cytoplasmic responses (Gust and Felix, 2014).

In silico analyses revealed the presence of ≥33 genes encoding potential LRR-RLPs in the genome of *M. polymorpha* as well as >60 LRR-RLKs (sequence analysis G. Felix and P. Guillaume Chatelain), including one gene (Mapoly0115s0067) encoding a potential SOBIR ortholog. The amino acid sequence of this presumptive MpSOBIR protein, however, is only 38.1% identical with AtSOBIR1. Due to two insertions in the third and in the last LRR domain, MpSOBIR (772 aa) is larger than AtSOBIR (641 aa) (**Figure 20**). Interestingly, these insertions are also present in the SOBIR ortholog of *P. patens*, which represents a member of the mosses which are also a family separated from the lineage of angiosperms 450 MYA. *Amborella trichiopoda,* representing the only member of a monophyletic group of early angiosperms (Amborella Genome

Project et al., 2013), also encodes a SOBIR with an additional sequence in the last LRR, however with fewer amino acids (**Figure 20**).

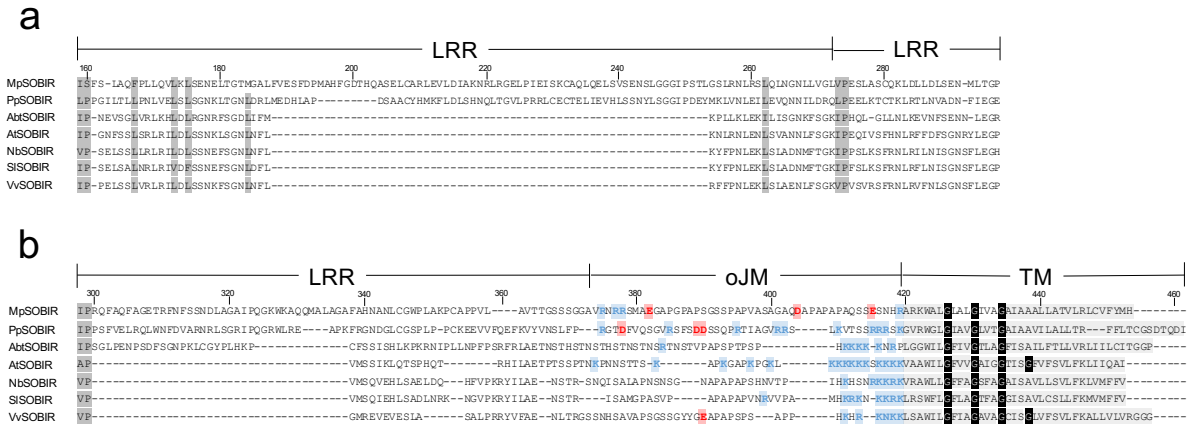

Figure 20: The amino acid sequence of MpSOBIR differs from other SOBIR orthologs. SOBIR orthologs are organized from most ancient to youngest in terms of evolution from top down. **a)** SOBIR proteins of *M. polymorpha* and *P. patens* (PpSOBIR) have insertions in the third LRR of about ~66 aa. SOBIR orthologs of *M. polymorpha* and *P. patens*, as well as *Amborella trichopoda* (AbtSOBIR) show an enlarged fifth LRR domain due to a further insertion. An enrichment of positively charged amino acids (blue) C-terminal to the oJM is present in all compared species, except for *M. polymorpha*. On the contrary, *M. polymorpha* as well as *P. patens* encode a few negatively charged residues (red). The GxxxG motif (bolt black, Gust and Felix, 2014; Bi et al., 2016) of the TM (light grey), as well as the structural ensuring residues (gray) are present in all compared species. (AtSOBIR= *A. thaliana*, NbSOBIR= *N. benthamiana*, SlSOBIR= S*. lycopersicum*, VvSOBIR: *Vitis vinifera*).

Due to the accordance to SOBIR genes of angiosperms we set out to test whether MpSOBIR is able to functionally substitute for angiosperm SOBIRs.

First, the chimeric approach with the EFR-ECD was used to test the activity of the MpSOBIR kinase domain. *N. benthamiana* leaf pieces expressing the hybrid EFR-receptor with the MpSOBIR kinase exhibited a clear ROS-burst response when treated with elf18 at concentrations >0.1 nM (**Figure 21** a). Also, the biosynthesis of ethylene was activated upon treatment of the chimeric MpSOBIR-KD receptor (**Figure 21** b). These results demonstrated the activity of the kinase domain.

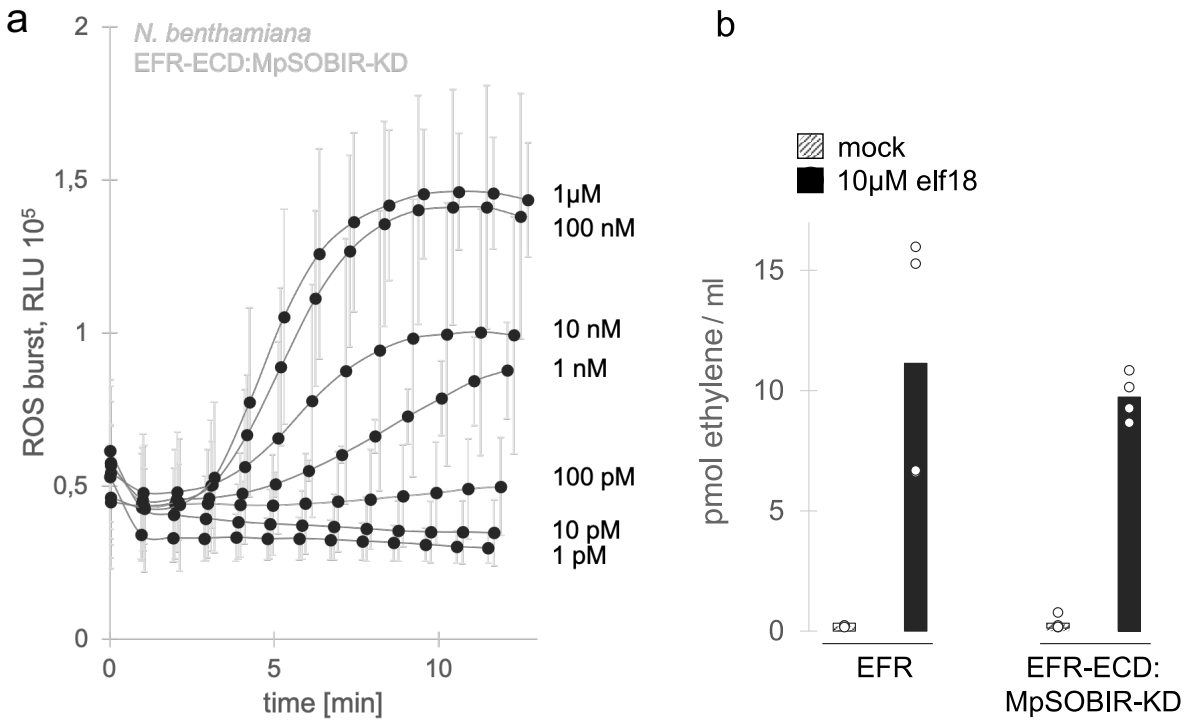

Figure 21: The kinase domain of MpSOBIR is able to transmit the peptide signal. **a)** ROS-burst dose-response to elf18 of *N. benthamiana* leaf pieces transiently expressing EFR-ECD:MpSOBIR-KD (EC_{50}=25 nM). Data points represent the average of three/four replicates. Error bars indicate the standard deviation of three/four replicates. **b)** Ethylene biosynthesis of *N. benthamiana* leaf pieces, expressing EFR-ECD:MpSOBIR-KD or EFR, after treatment with 10 µM elf18. Each experiment was performed at least 3 times with a similar result and each bar is the average of four replicates (circles).

To validate the functionality of MpSOBIR, complementation studies were performed. Leaf pieces of the *N. benthamiana sobir* mutant were transiently co-transformed with MpSOBIR and selected RLPs from *A. thaliana*. The selection of the receptors was based on the absence of such perception systems in *N. benthamiana* and the availability of cognate ligands: we used AtRLP42, the receptor for pg13 (Zhang et al., 2021), AtRLP32, the receptor for IF1 (Fan et al., 2022) and AtRPL23, the receptor for nlp20 (Böhm et al., 2014b). To confirm a clear background transformants with either MpSOBIR or RLPs alone were also generated and tested.

Indeed, the co-expression of MpSOBIR with AtRLP42 conferred pg13-responsiveness to the *N. benthamiana* tissue, as evidenced by a strongly increased biosynthesis of ethylene after treatment with this peptide (**Figure 22** a). However, similar attempts to demonstrate functionality of MpSOBIR when co-expressed with either AtRLP23 or AtRLP32 were unsuccessful (**Figure 22** a and **Figure 48**). Co-immunoprecipitation studies confirmed the ligand-independent interaction of the full-length MpSOBIR with RLP42, however, no such interaction between MpSOBIR and AtRLP23 or AtRLP32 was observed (**Figure 23**).

In order to test whether the lack of functionality in the combination of MpSOBIR with AtRLP23 can be attributed to either the ectodomain or the kinase domain of MpSOBIR, hybrid versions of MpSOBIR and AtSOBIR1 with swapped cytoplasmic domains were constructed. The SOBIR hybrid with the AtSOBIR ectodomain and the cytoplasmic kinase domain from MpSOBIR (**Figure 47**) did lead to a functional RLP23/SOBIR complex while the reciprocal construct, with the ectodomain of MpSOBIR and the kinase of AtSOBIR1, did not restore responsiveness to nlp20 (**Figure 22** b). Thus, at least in the case of AtRLP23, the ectodomain of MpSOBIR cannot substitute for the ectodomain of AtSOBIR1 (Albert et al., 2015).

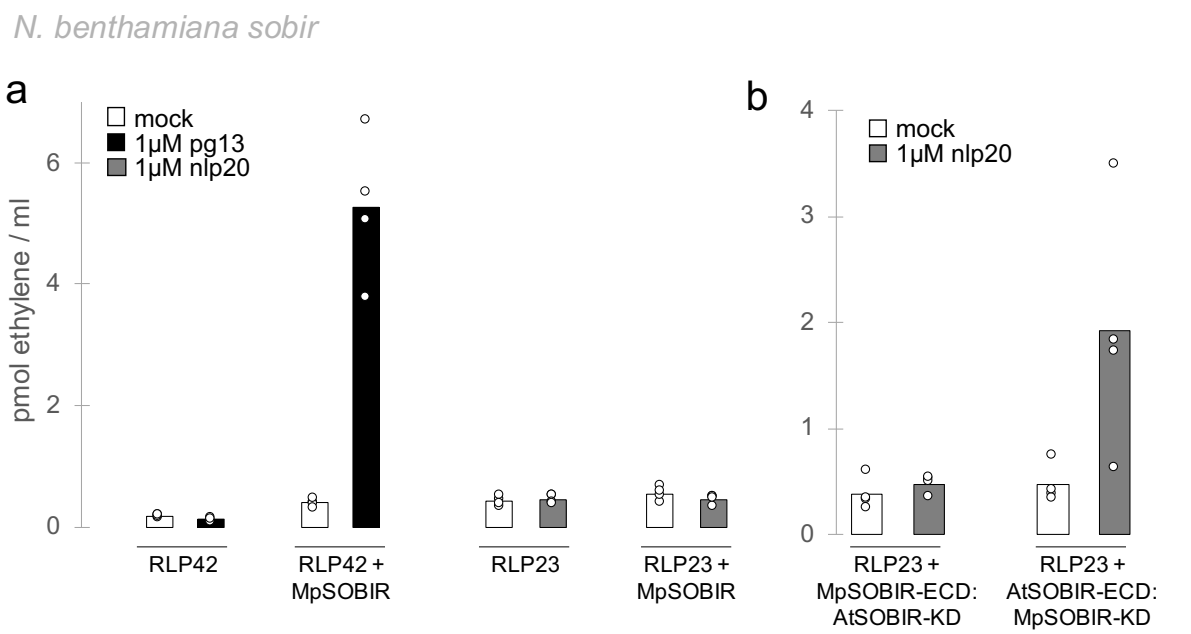

Figure 22: MpSOBIR is able to substitute for NbSOBIR in co-transformation with RLP42 and, as a chimera, with RLP23. a) Co-expression of RLP42 and MpSOBIR complemented the *sobir* mutant of *N. benthamiana* for the induction of ethylene after peptide treatment. RLP42 or RLP23 alone, or RLP23 in co-expression with MpSOBIR, did not. **b)** Co-expression of RLP23 with a chimeric version consisting of the ectodomain of AtSOBIR fused to the kinase domain of MpSOBIR, but not with the reciprocal version, complemented the nlp20-dependent ethylene induction. Displayed is a representative experiment. Each experiment was performed at least 3 times and each bar is the average of four replicates (circles).

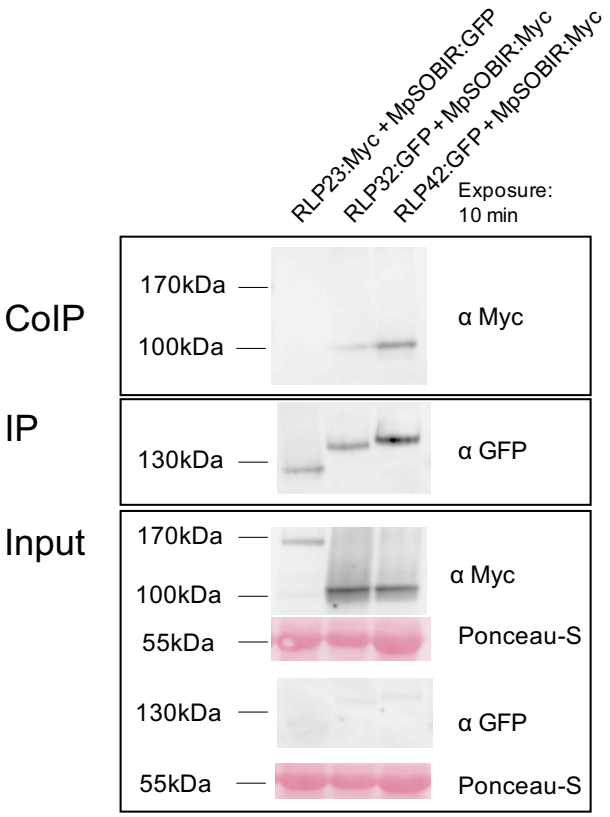

Figure 23: Co-immunoprecipitation confirms the interaction between MpSOBIR and RLP42. Transiently transformed *N. benthamiana sobir* plants, expressing MpSOBIR and RLP23, RLP32 or RLP42, respectively. Immunoprecipitation of GFP-tagged proteins was performed using GFP-trap agarose beads. Co-immunoprecipitation of MpSOBIR:4xMyc and RLP23:4xMyc, respectively, was detected by using a-myc antibody. Protein input (before IP and CoIP) was controlled by Western blotting and detected by appropriate antibodies. Ponceau-S staining ensured comparable amount of loaded sample. The experiment was repeated two times with the same result. The weak band in RLP32+ MpSERK was not observed in additional experiments and resulted probably from spillover of the RLP42+MpSERK sample. Additional repetitions have to be performed to validate the missing interaction.

An incapability of MpSOBIR to form a signaling-competent complex with RLP23 and RLP32 may be caused by a size or charge difference. Compared to SOBIR orthologs of vascular plants, MpSOBIR, as well as PpSOBIR, have a bigger ectodomain, caused by two insertions in the LRR-region (**Figure 20**) and have a more negatively charged inner juxtamembrane region. A non-functional SOBIR/RLP pairing has been described previously for another RLP from *A. thaliana,* RLP1 (also named ReMAX), which perceives an enigmatic MAMP of Xanthomonas (eMax). RLP1 expressed in *N. benthamiana* did not enable the perception of eMax, probably due to incompatibilities with adaptor proteins and co-receptors (Jehle et al., 2013a). Signal transduction was however restored when the C-terminal part (including the extracellular juxtamembrane region, the transmembrane domain, and the intracellular juxtamembrane region) of RLP1 were replaced with the corresponding domains from

ethylene-inducing xylanase (Eix2), the binding protein for xylanase (Ron and Avni, 2004; Jehle et al., 2013).

An active chimera of the EFR ectodomain and the kinase domain of MpSOBIR, as well as the chimeric receptor AtSOBIR ectodomain and MpSOBIR kinase (**Figure 21**), demonstrate the general function of the MpSOBIR kinase domain. The ectodomain however, seems to be obstructive. As shown for Eix2 the C-tail of RLPs seem to be functionally important, however the interaction between RLPs and SOBIR is probably also taking place at the apoplastic part, the transmembrane domain or/and the inner juxtamembrane. The GxxxGxxxG motif in the transmembrane domain of SOBIR proteins is described to be critical for the RLP-SOBIR interaction (Bi et al., 2016). MpSOBIR also encodes a GxxxGxxxG motif (**Figure 20**), which is why an unsuccessful substitution cannot be explained by the lack of this motif. To map the specific region which causes the incompatibility in the ectodomain of MpSOBIR, chimeric constructs encompassing smaller domain swaps could be generated. Also, point mutations in RLP42, mainly in the transmembrane domain could be tested with MpSOBIR to narrow down important residues, which should be compared to the non-functional interaction partners RLP23 and RLP32. To further evaluate the interaction between MpSOBIR with RLP23 and RLP32, respectively, different interaction approaches could be performed, aiming a direct interaction, like bimolecular complementation assay (BiFC). Further *in vivo* analyses in *M. polymorpha* in form of *Mpsobir* knock-out mutants can be additionally useful to reveal protein function. Also, interactions with MpLRR-RLP proteins can be tested via co-immunoprecipitation, due to the constitutive interaction between RLPs and SOBIR and thus no need of a specific elicitor.

3.7 MpBIR – a potential negative regulator

With MpSERK and MpSOBIR we identified two proteins which act, like their orthologs in vascular plants, as positive regulators when heterologously expressed in *A. thaliana* and *N. benthamiana*. The presence of a tremendous number of signaling-initiating molecules in the surrounding can, however, cause a constant and strong activation of stress responses. Negative regulators help to prevent overactivation of immune responses that could cause severe damage to the plant. Known negative regulators of plant immunity are RLKs with small LRR domains of the BIR family (Gao et al., 2009; Liu et al., 2016; Halter et al., 2014a; Blaum et al., 2014). In *A. thaliana,* this family has four members, which differ with respect to their kinase activity. BIR1 was described as

an active kinase, whereas the kinase domains of BIR2, 3 and 4 seem to be inactive (Blaum et al., 2014). BIR2, 3 and 4 inhibit, when overexpressed, the response to elicitors like flg22 (Halter et al., 2014a). In contrast, BIR1 does not show an inhibitory effect (Liu et al., 2016). Thus, the absence of kinase activity seems to be decisive for an inhibitory effect for RLK-mediated immune responses.

In silico analysis revealed a BIR ortholog in the genome of *M. polymorpha* (Mapoly0028s0071), with an identity of 49.4% compared to AtBIR1 (identity to AtBIR2: 41.9%). Amongst other sequence similarities with AtBIR1, MpBIR also shows an Ala in the G-loop (Blaum et al., 2014), compared to AtBIR2, 3 and 4, which encode a Val at this position (**Figure 24**).

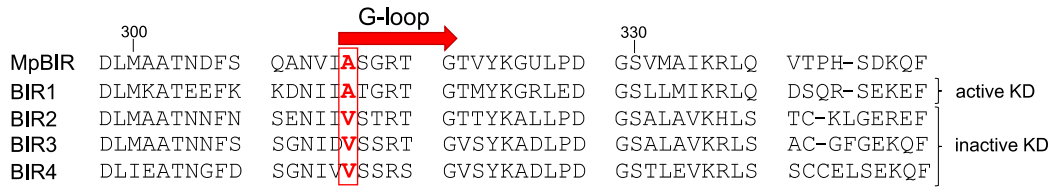

Figure 24: MpBIR is more similar to BIR1 than to BIR2, BIR3 or BIR4 of *A. thaliana*. The G-loop, which is critical for kinase activity (Blaum et al., 2014), is highlighted in red. The accordance of the G-loop between MpBIR and BIR1 is exemplary and goes along with other matching residues. KD= kinase domain.

To examine if MpBIR behaves like AtBIR1 or like AtBIR2, AtBIR3 and AtBIR4, overexpressing protoplasts were tested for an inhibition effect on flg22-treatment. Wildtype *A. thaliana* protoplasts were co-transformed with the Luciferase-reporter gene under the inducible FRK1 promotor and either MpBIR, AtBIR1, AtBIR2 or AtBIR3 under the strong 35S promotor, respectively. In contrast to the overexpression of AtBIR2 and AtBIR3, the overexpression of MpBIR or AtBIR1 did not inhibit the response to 100 nM flg22 (**Figure 25**).

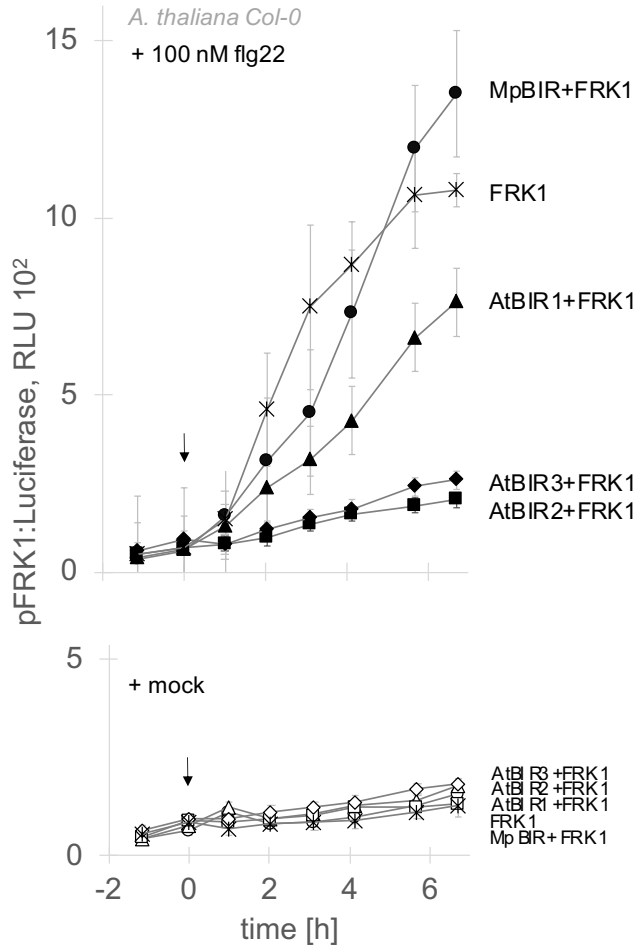

Figure 25: MpBIR behaves like BIR1 from *A. thaliana*. Co-expression of pFRK1:Luciferase-reporter gene with AtBIR1 (triangles), MpBIR (circles), AtBIR2 (squares) or AtBIR3 (diamonds), respectively, in wildtype *A. thaliana* protoplasts, treated with 100 nM flg22 (filled symbols) or mock solution (open symbols). Arrows indicate the timepoint of mock treatment or addition of 100 nM flg22. The experiment was repeated three times, each symbol represents the average of four replicates in a representative experiment. Error bars represent the standard deviation. The expression of the proteins was confirmed by Western blotting (data not shown).

MpBIR seems to lack the inhibitory effect of AtBIR2 and AtBIR3, and the sequence of its kinase domain shares features with AtBIR1. We thus tested whether MpBIR can complement for AtBIR1 in *A. thaliana* plants. The loss of AtBIR1 in *A. thaliana* (*bir1-1)* is lethal (Liu et al., 2016). Therefore, heterozygous *BIR1/bir1-1* plants were used for stable transformation with MpBIR. Transformed seeds of the T0 generation were selected by the fluorescence-accumulating seed technology (pFAST; Shimada et al., 2010) and grown in soil. One quarter of the T1 plants are expected to be homozygous for *bir1-1* and would not survive unless the transgene MpBIR would complement for the AtBIR1 function. Thus, in case of a successful complementation by MpBIR, none of the progeny, or at least a clearly smaller percentage than 25%, would show a lethal phenotype (**Figure 26**).

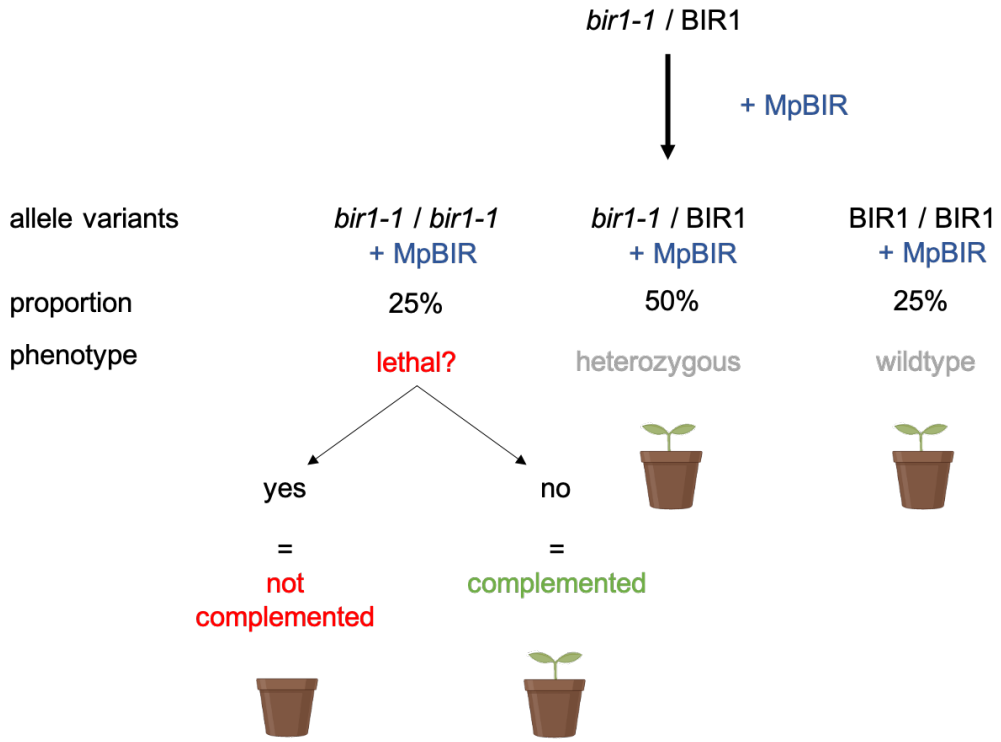

Figure 26: Expected outcomes of *bir1-1* complementation with MpBIR. Transformation was validated by pFAST. Only transformed seeds were propagated.

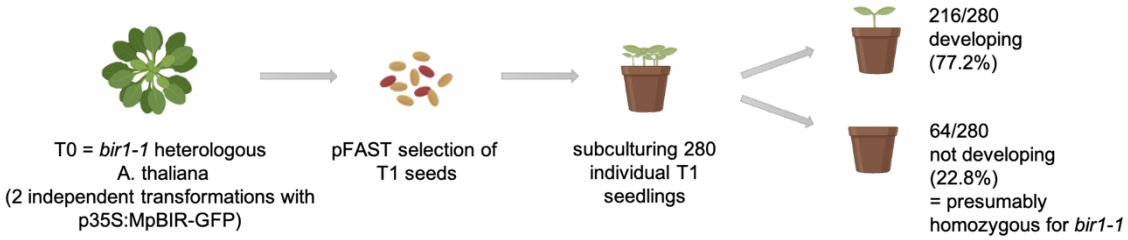

Figure 27: MpBIR is not able to complement the bir1-1 phenotype in *A. thaliana*. Stable transformation of MpBIR in the heterozygous *bir1-1* T-DNA-insertion mutant background did not rescue the mutant phenotype (n=280). Transformed seeds were selected via pFAST and expression of MpBIR:GFP was confirmed by Western blotting (**Figure 49**).

However, 22.8% of the transgenic seeds did not grow and develop, suggesting that MpBIR cannot functionally substitute for AtBIR1 (**Figure 26**). As a further control, 66 of the growing transformants were genotyped for the presence of wildtype AtBIR1 and mutated AtBIR1 with the T-DNA insertion (**Figure 49**). None of these surviving transformants was homozygous for the mutant version of AtBIR1 containing the T-DNA insertion. Genotyping also revealed an unexpected distribution of heterozygous and homozygous (wildtype) plants, which was inverted compared to the expected percentual distribution of the allele variants (**Figure 49**). This could indicate a negative influence of the *bir1* mutation also in the heterozygous lines. To validate this effect

untransformed heterologous *bir1-1 A. thaliana* seed have to be analyzed, as well as complemented with the endogenous AtBIR1.

To further elucidate the function of MpBIR experimental approaches could aim to confirm the function of the MpBIR kinase domain in a chimeric version with the ectodomain of EFR. An active chimeric protein would indicate another commonality with AtBIR1 (no pseudokinase). Furthermore, a chimeric version of the ectodomain of MpBIR and the kinase domain of AtBIR2 could be tested in the inhibition assay in *A. thaliana* protoplasts. An inhibitory effect of this chimeric protein could indicate the functionality of the ectodomain of MpBIR. Furthermore, detailed domain swapping between AtBIR1 or AtBIR2 with MpBIR, respectively, could reveal potential compatibility problems.

The interaction with a co-receptor of the SERK family is a clear characteristic of the BIR proteins (**Figure 7**), thus MpBIR was also tested in interaction with MpSERK. Results of IP-MS data indeed showed an interaction between MpSERK and MpBIR (personal communication of Dr. Isabel Monte). Additional interaction studies could validate the interaction with SERK orthologs of vascular plants. The interaction with BIR proteins, however, seems to be instable (Halter et al., 2014a), thus, potentially negative results have to be evaluated carefully.

3.8 Final discussion – the basic equipment for pathogen recognition in *M. polymorpha*

During the evolution of land plants, multiple perception systems for signals evolved that ensure the communication within different cells and tissues of the plant and the interaction of plants with their surroundings. How bryophytes are able to perceive their biotic environment remained so far unanswered. *In silico* analyses indicated the existence of orthologs involved in perception mechanisms known from more extensively studied vascular plants. However, experimental evidence for the functioning of these mechanisms in bryophytes are still missing. Here we provide first examples for the substitution of LRR-receptor function in angiosperms by orthologous genes from *M. polymorpha*.

In summary, we can postulate the presence of proteins that share the function they have in vascular plants. This includes a functional co-receptor, MpSERK, which is able to substitute for SERK function in vascular plants and form signaling-competent complexes. Another functional MpLRR-RLK is represented by MpSOBIR, which is able to substitute for NbSOBIR and restore pg13 perception by interacting with RLP42,

implying an important role in complex formation and perception of MAMPs/DAMPs as in vascular plants. Moreover, we identified immune signaling-competent MpLRR-RLKs, since their cytoplasmic domains are able to transmit an immune signal, when combined with the EFR ectodomain. Finally, with MpHSL and its ligand MpIDA we identified an active receptor-ligand pair which is forming a ligand-dependent signaling complex with a co-receptor of the SERK protein family.

Deciphering the physiological and developmental behavior as a status quo in early land plants is a promising tool to understand the evolution of specific traits. However, one has to take into account the ongoing evolution of bryophytes. Bryophytes separated 450 MYA from the lineage leading to present day angiosperms, and, like angiosperms, are under constant selection pressure, resulting in evolutionary changes which might, or might not, follow a similar course. However, we were able to show that some of the principles we know from vascular plants are present as a basic equipment of signal perception in bryophytes. Above all, this pertains to the necessity to form a ligand-induced complex between signal-perceiving LRR-receptors and co-receptors (and adapter kinases, if necessary) to activate a signaling cascade, resulting in the ability of the plant to respond to its environment.

4 Outlook

The ability of bryophytes to perceive their surrounding and thereby maintain vitality, is barely elucidated. Accordingly, there is a long list of questions to be answered concerning the evolution of plant-microbe-interactions. First, one would need to identify other molecular cues (in addition to chitin) which would trigger defense reactions in the bryophyte, for a more comprehensive description of the repertoire of MAMPs. With that knowledge (from this, as well as from other model plants), we could try to answer the question when the receptors for the highly diverse collection of external signals, which we observe in present day angiosperms, evolved. Second, we would like to know if signaling and defense mechanisms like the hypersensitive response (HR), ROS burst, phytohormone and phytoalexin biosynthesis play a role in *M. polymorpha*, or if there are other, yet unknown systems (in addition to calcium- and MAPK-signaling, which seem to be very early inventions).

However, we were able to demonstrate, for some of the studied candidate receptors from *M. polymorpha*, a functional conservation in angiosperms. The identification of functional orthologs of SERK and SOBIR1, and the first description of a ligand/receptor pair in *M. polymorpha* now provides unprecedented opportunities to trace the evolutionary trajectory and common principles of LRR-mediated signaling, like, for example, an early emergence of the necessity to form ligand-induced receptor complexes for sensitive and specific perception of endogenous and exogenous signals.

As Delaux et al., (2019) nicely described “Comparison of functional data gathered in model angiosperms, mosses, liverworts as well as multiple representatives of the major plant clades will allow the plant community to paint a more comprehensive picture of the evolutionary mechanisms that have led to the diversity observed in extant species”. Therefore, our data add on to this collection and to the understanding of signaling mechanism evolution.

5 Summary

The aim of this thesis was to discover ancient principles of signaling mechanisms in the liverwort *M. polymorpha* by identifying orthologs involved in perception systems in angiosperms and elucidation of the function of the respective proteins.

By heterologous expression of *M. polymorpha* genes in the angiosperm model plants *A. thaliana* and *N. benthamiana* we were able to use established methods to test for protein or protein subdomain function in terms of complex formation, activation and signal transmission. Our proteins of interest included core regulators of signaling mechanisms, SERK, SOBIR and BIR, as well as a selection of MpLRR-RLKs, resembling the well-established cell surface receptors in vascular plants. We were able to demonstrate (i) that MpSERK is able to substitute for BAK1 in vascular plants and shows interaction with known LRR-RLKs, (ii) that the MpSOBIR ortholog is functional and able to build a signaling-competent complex with RLP42, (iii) that MpBIR bears sequence and conceptual similarity to BIR1, but not BIR2 or BIR3, from *A. thaliana*, (iv) that three of the selected MpLRR-RLK kinase domains are able to feed into higher plant signaling cascades, and (v) that MpHSL and MpIDA form a signaling-competent complex with dependency on a co-receptor of the SERK family.

These results contribute to the understanding of the basic equipment of signaling mechanisms in bryophytes and built the basis for further approaches to gain information about the evolution of pattern recognition.

6 Zusammenfassung

Ziel dieser Arbeit war es, alte Prinzipien von Signalmechanismen in dem Lebermoos *M. polymorpha* zu entdecken, indem Orthologe identifiziert wurden, die an Wahrnehmungssystemen in Angiospermen beteiligt sind, und die Funktion der jeweiligen Proteine aufzuklären.

Durch heterologe Expression von *M. polymorpha*-Genen in den Angiospermen-Modellpflanzen *A. thaliana* und *N. benthamiana* konnten wir mit Hilfe etablierter Methoden die Funktion von Proteinen oder Protein-Subdomänen im Hinblick auf Komplexbildung, Aktivierung und Signalübertragung testen. Zu den Proteinen, die uns interessierten, gehörten zentrale Regulatoren von Signalmechanismen, SERK, SOBIR und BIR, sowie eine Auswahl von MpLRR-RLKs, die den bekannten Zelloberflächenrezeptoren in Gefäßpflanzen ähneln. Wir konnten zeigen, (i) dass MpSERK in der Lage ist, BAK1 in Gefäßpflanzen zu ersetzen und Interaktion mit bekannten LRR-RLKs zeigt, (ii) dass das MpSOBIR-Ortholog funktionell und in der Lage ist, einen signaltechnisch kompetenten Komplex mit RLP42 zu bilden, (iii) dass MpBIR Sequenz- und konzeptionelle Ähnlichkeit mit BIR1, aber nicht mit BIR2 oder BIR3, aus *A. thaliana* aufweist, (iv) dass drei der ausgewählten MpLRR-RLK-Kinase-domänen in der Lage sind, sich in höhere pflanzliche Signalkaskaden einzuschalten, und (v) dass MpHSL und MpIDA einen signal-kompetenten Komplex bilden, der von einem Co-Rezeptor der SERK-Familie abhängig ist.

Diese Ergebnisse tragen zum Verständnis der Grundausstattung von Signalmechanismen in Bryophyten bei und bilden die Grundlage für weitere Ansätze, um Informationen über die Evolution der Mustererkennung zu gewinnen.

7 Supplementary Data

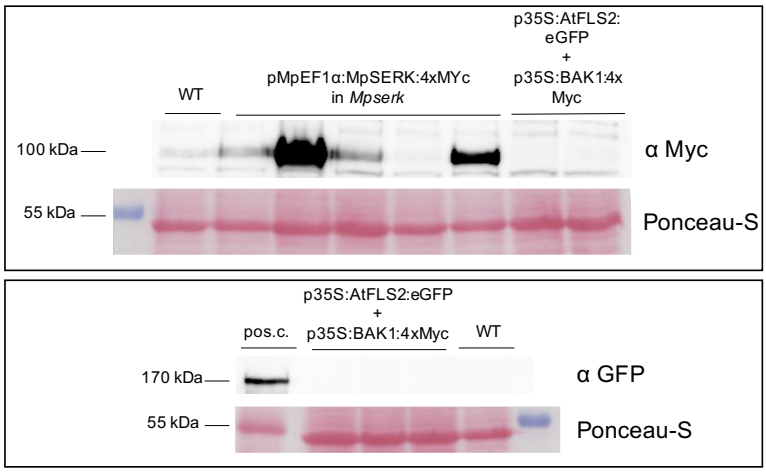

Figure 28: Confirmation of the expression of transformed genes in *M. polymorpha* via Western Blot using crude thallus material. High amount of background signal I n crude samples including the WT control. FLS2:eGFP~170 kDa, BAK1:4xMyc~100 kDa, MpSERK:4xMyc~100 kDa. Pos c. = crude material of *N. benthamiana* expressing p35S:EFR:eGFP.

7.1 MpSERK – a functional co-receptor

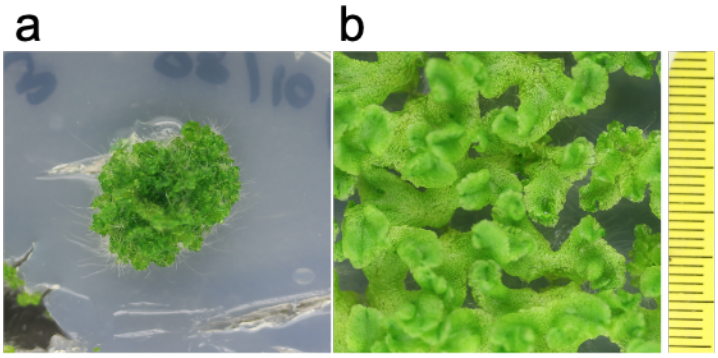

Figure 29: *Mpserk* mutant shows fuzzy multiple branched thallus and overall growth reduction (pictures form Dr. Isabel Monté). a) *Mpserk* mutant. **b)** Corresponding WT.

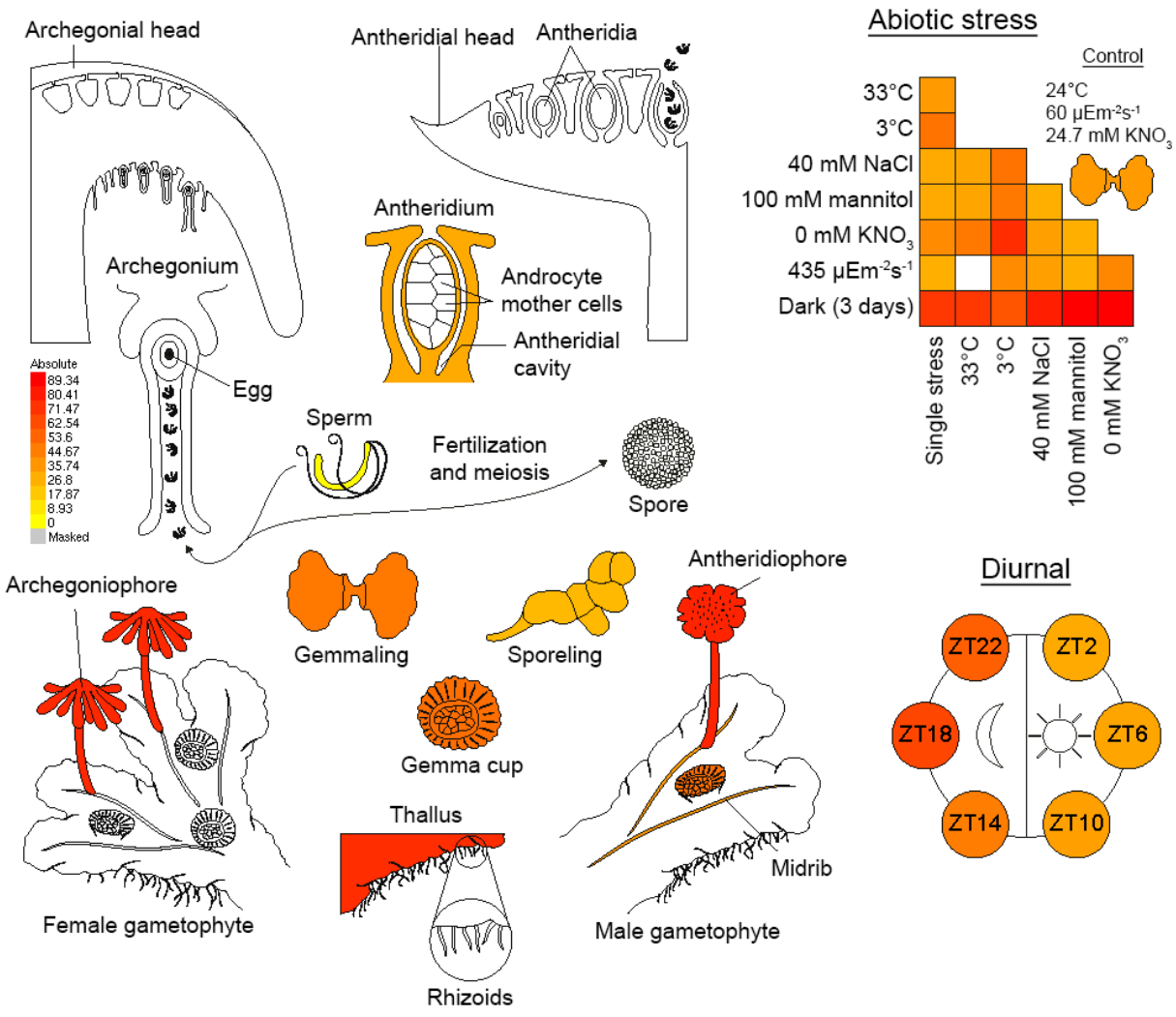

Figure 30: MpSERK is broadly expressed in all plant tissues and organs, but not in the sperm (Liverwort Atlas eFP Browser at bar.utoronto.ca).

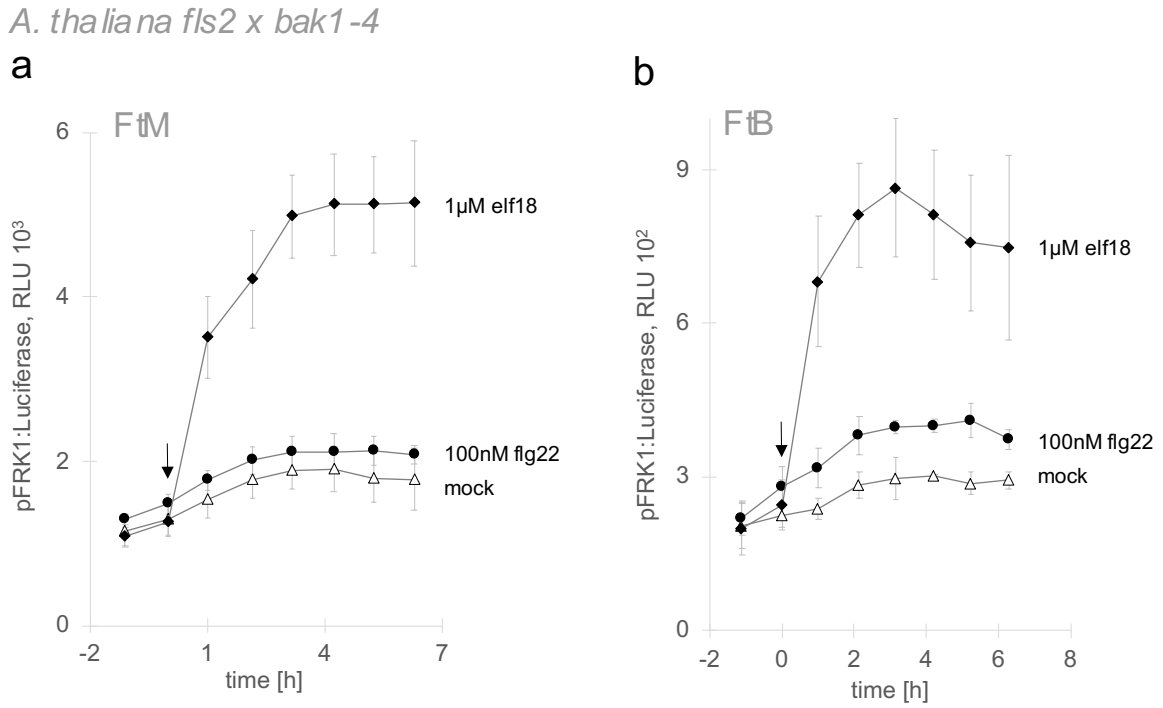

Figure 31: Single transformation of FtM or FtB, respectively, did not restore the immune response to flg22. a) *A. thaliana* protoplasts of the background *fls2 x bak1-4* were transformed with the pFRK1 reporter gene and FtM. In the pFRK1:Luciferase-reporter assay the transformed protoplast did not show light emission to flg22 (filled circles), however to elf18 (filled diamonds), which confirms the vitality of the protoplasts however the non-responsiveness to flg22. The expression of FtM was confirmed by Western blotting. **b)** FtB was also not able to activate the reporter gene upon flg22 treatment. The vitality of the protoplasts was confirmed by a response to elf18 and expression was controlled by Western blotting. Error bars indicate the standard deviation of three/four replicates. Datapoints represent the average of replicates. Arrows indicate the timepoint of elicitation. The experiment was repeated at least three times with the same outcome.

7.2 MpLRR-RLK with functional kinase domains but orphan function

		assay		
Mapoly ID	**name**	**ROS**	**ethylene**	**pFRK1:Luciferase**
Mapoly0012s0045	MpLRR-RLK 2	X	X	X
Mapoly0081s0043	MpLRR-RLK 4	X	X	X
Mapoly0039s0122	MpLRR-RLK 5	✓	✓	✓
Mapoly0039s0089	MpLRR-RLK 6	X	X	X
Mapoly0039s0121	MpLRR-RLK 8	X	X	X
Mapoly0035s0149	MpLRR-RLK 10	✓	✓	✓
Mapoly0106s0043	MpLRR-RLK 11	X	X	X
Mapoly0141s0029	MpLRR-RLK 12	X	X	X
Mapoly0008s0216	MpLRR-RLK 13	X	X	X
Mapoly0049s0132	MpLRR-RLK 14	X	X	X
Mapoly0065s0076	MpLRR-RLK 15	✓	✓	✓
Mapoly0042s0003	MpLRR-RLK 18	X	X	X
Mapoly0097s0050	MpLRR-RLK 21	X	X	X
Mapoly0218s0005	MpLRR-RLK 26	X	X	X
Mapoly0041s0120	MpLRR-RLK 27	X	X	X
Mapoly0011s0079	MpLRR-RLK 30	X	X	X
Mapoly0182s0011	MpLRR-RLK 31	X	X	X
Mapoly0004s0263	MpLRR-RLK 4 IM	X	X	X
Mapoly0039s0031	MpLRR-RLK 39 IM	X	X	X
Mapoly0184s0024	MpLRR-RLK 184 IM	X	X	X

Table 15: Three out of 20 kinase domains are able to transfer the perception of a ligand at the surface into a cellular response. Kinase domains were tested in three different immune assays, covering a wide timespan of known stress responses in plants (synthesis of reactive oxygen species (minutes), gene activation (> 1 hour), ethylene biosynthesis (>3 hours) (Yu et al., 2017)). Genes with the abbreviation IM were selected by Dr. Isabel Monte. Candidates were selected based on their ectodomain size and the presence of a signal peptide and a hydrophobic transmembrane domain, predicted by Phobius analysis (https://phobius.sbc.su.se).

gene	sequence	position overhang	size [aa]	activity
MpLRR-RLK 2	TSGVIGIILVGIGVTIWYCL**FT**KVIEYHRKTLGPEMPH	946/947	1292	×
MpLRR-RLK 4	VGCGGIGLILLAIYALGVVF**FI**RGDRRQESEAVP	777/778	1111	×
MpLRR-RLK 5	LVATVFAITLALILAGVFIY**YR**RRTRFESDESSAKL	828/829	1174	✓
MpLRR-RLK 6	SVASASVLALALIIIGIVAC**RR**RGRTYEDSDQSVGK	829/830	1184	×
MpLRR-RLK 8	GYAISALVGALALIFFGVGL**YR**LRSRRLDRRGAEGCLEVWS	814/815	1136	×
MpLRR-RLK 10	ATVPSAIILGVAVYLWWLIL**FS**GRFKPESSTVKMHFGP	808/809	1135	✓
MpLRR-RLK 11	LIGGCTVGAALVVGICLFVY**FR**SVAKSNDTSPGSEFG	701/702	1167	×
MpLRR-RLK 12	VGAGAMTAFIFIASLVAWSC**IG**RCRRRNSCLVSHSCDL	764/765	1125	×
MpLRR-RLK13	VVSGAAGFVLALVGLGIFLW**MS**GEKKKCVTSTRKELGIYTTQ	698/699	1078	×
MpLRR-RLK 14	ILGISIVSTLLVLIVVGIAC**YA**STRRTYVRNENGATSPD	775/776	1132	×
MpLRR-RLK 15	ILIVAGVLIPFMCSLSMCLC**IR**STRFKQYIAKKEANNWSM	685/647	1063	✓
MpLRR-RLK 18	IIIASSVLVPQASCLVVCWR**WR**VYKDKHQHDADMIAT	646/647	1026	×
MpLRR-RLK 21	ALVGGLLLAIITAVVCIFVC**RR**RRKRKNRFHHSEFS	615/616	1211	×
MpLRR-RLK 26	GIIAGGVAVFVIVLLIGFYA**FR**QKRRADRAEV	630/631	1003	×
MpLRR-RLK 27	AIGGVVVVLLILGLLLFLYC**RR**RRRPPSVPTAMSEI	562/563	983	×
MpLRR-RLK 30	ISVVAGVAATFFLIVIGTFG**FF**LSKKKNKFPESPRKNFY	558/559	945	×
MpLRR-RLK 31	GVAIGAFIILAILAVALFLW**CR**SPYPMGQPQGHNRGS	1039/1040	1384	×
MpLRR-RLK 4 IM	VALGTLIVGIVALSASIWCT**WK**KKKSTARLAPILEMSNFT	546/547	871	×
MpLRR-RLK 39 IM	TIILTVDGLLALVDAYALLL**YW**RVRKPKKEKNEPVSMCEPS	464/465	838	×
MpLRR-RLK 184 IM	KSVAGVSAVLGAFVVVVGAF**VW**RERRFRRTRVHVQGPET	402/403	771	×

overhang:

F K aa
TTC **A**A$\frac{A}{G}$ bp

Figure 32: Chimeric constructs are seamlessly combined at a position directly after the transmembrane region. EFR-ECD:MpLRR-RLK chimeras were generated by changing the residues (upper part: highlighted in red) adjacent to the transmembrane domain (highlighted in green/black) into phenylalanine (F) and lysine (K) due to the design of the K-overhang (lower part: bold, black). Hydrophilic residues of the outer juxtamembrane region are colored in blue. The size corresponds to the original size of the MpLRR-RLK gene. The last column summarizes the outcome of the bioassays, in which the chimeric receptors were tested for signal transmission conveyed by the kinase domains of MpLRR-RLKs.

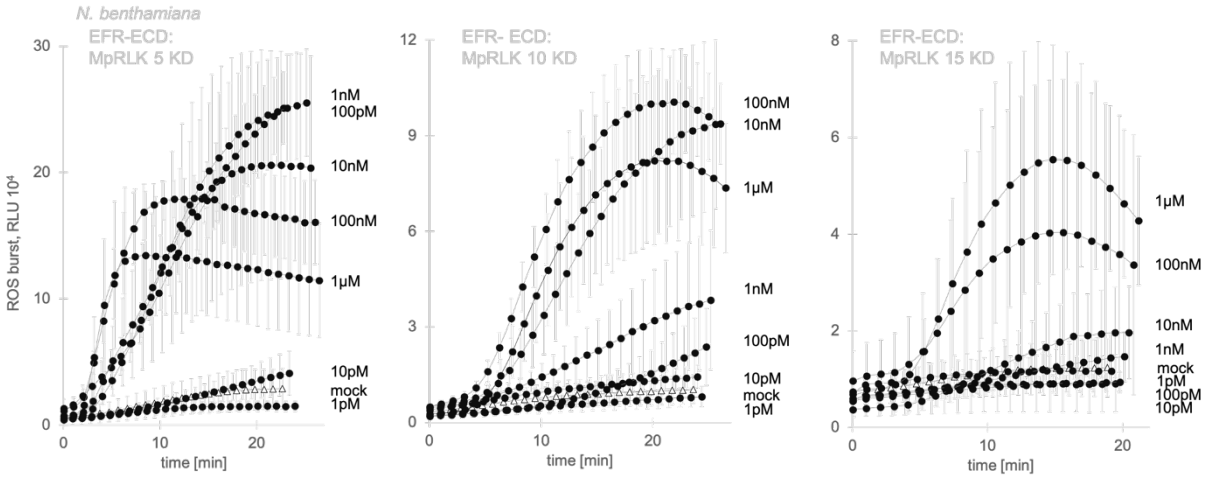

Figure 33: The kinase domains of three MpLRR-RLKs confer sensitivities to elf18 in the nanomolar range, when tested as EFR-ECD chimeras. EFR-ECD:MpLRR-RLK-KD chimeric receptors were transiently expressed in *N. benthamiana* leaves and tested in a dose dependent-manner for the ROS-burst response after treatment with elf18. Data points represent the average of three/four replicates. Error bars indicate the standard deviation of three/four replicates.

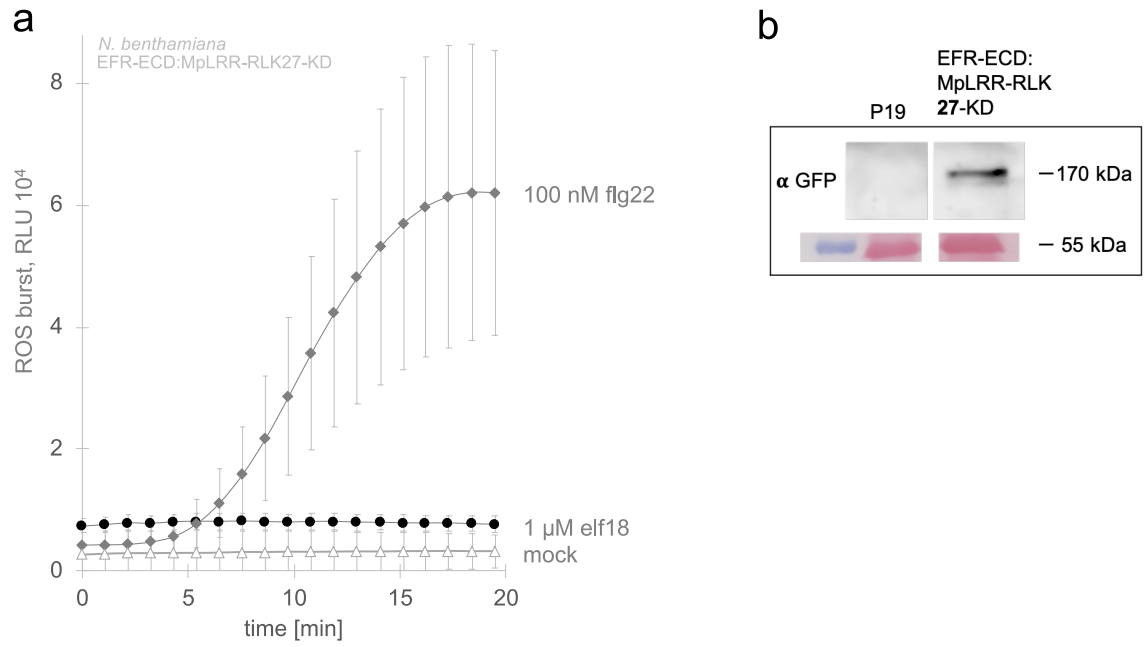

Figure 34: Example of an inactive MpLRR-RLK kinase domain (MpLRR-RLK 27). a) The chimeric receptor, consistent of the ectodomain of EFR and the kinase domain of MpLRR-RLK 27, did not show a ROS-burst after treatment with 1 µM elf18 (filled circles), when expressed transiently in *N. benthamiana* leaves. Leaf pieces were able to respond to 100 nM flg22 (filled diamonds), which confirmed the general ability to initiate a ROS-burst. Error bars represent the standard deviation of three replicates. Data points represent the average of replicates. **b)** Expression was confirmed by Western blotting. Each experiment was repeated three times with the same results.

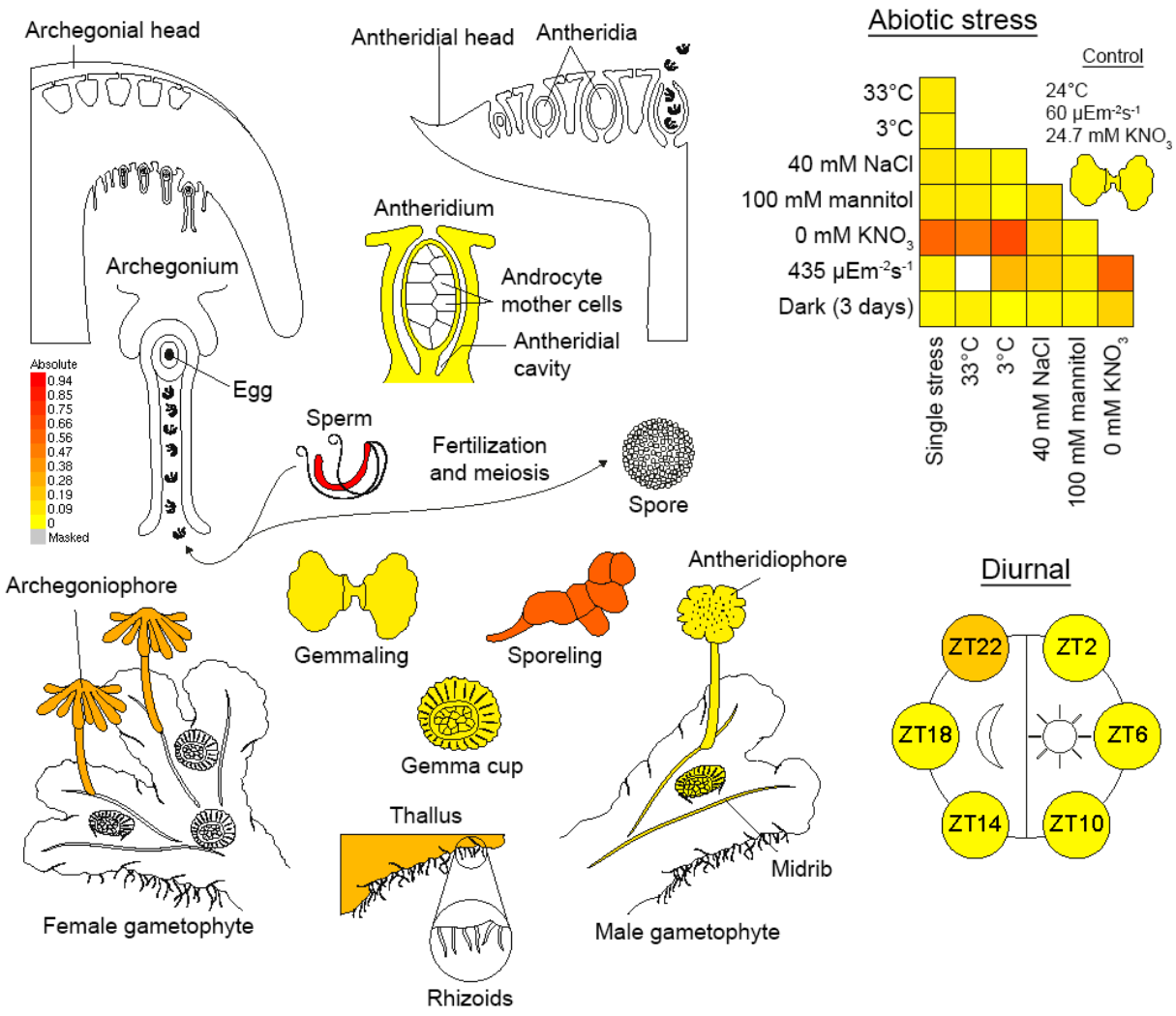

Figure 35: MpLRR-RLK 5 is generally little expressed in *M. polymorpha* (Liverwort Atlas eFP Browser at bar.utoronto.ca). The sperm, sporeling and abiotic stress conditions show the highest expression. Lower expression in indicated for the archegoniophore and the thallus. in Comparison to MpLRR-RLK10 and 15, MpLRR-RLK5 shows the lowest expression.

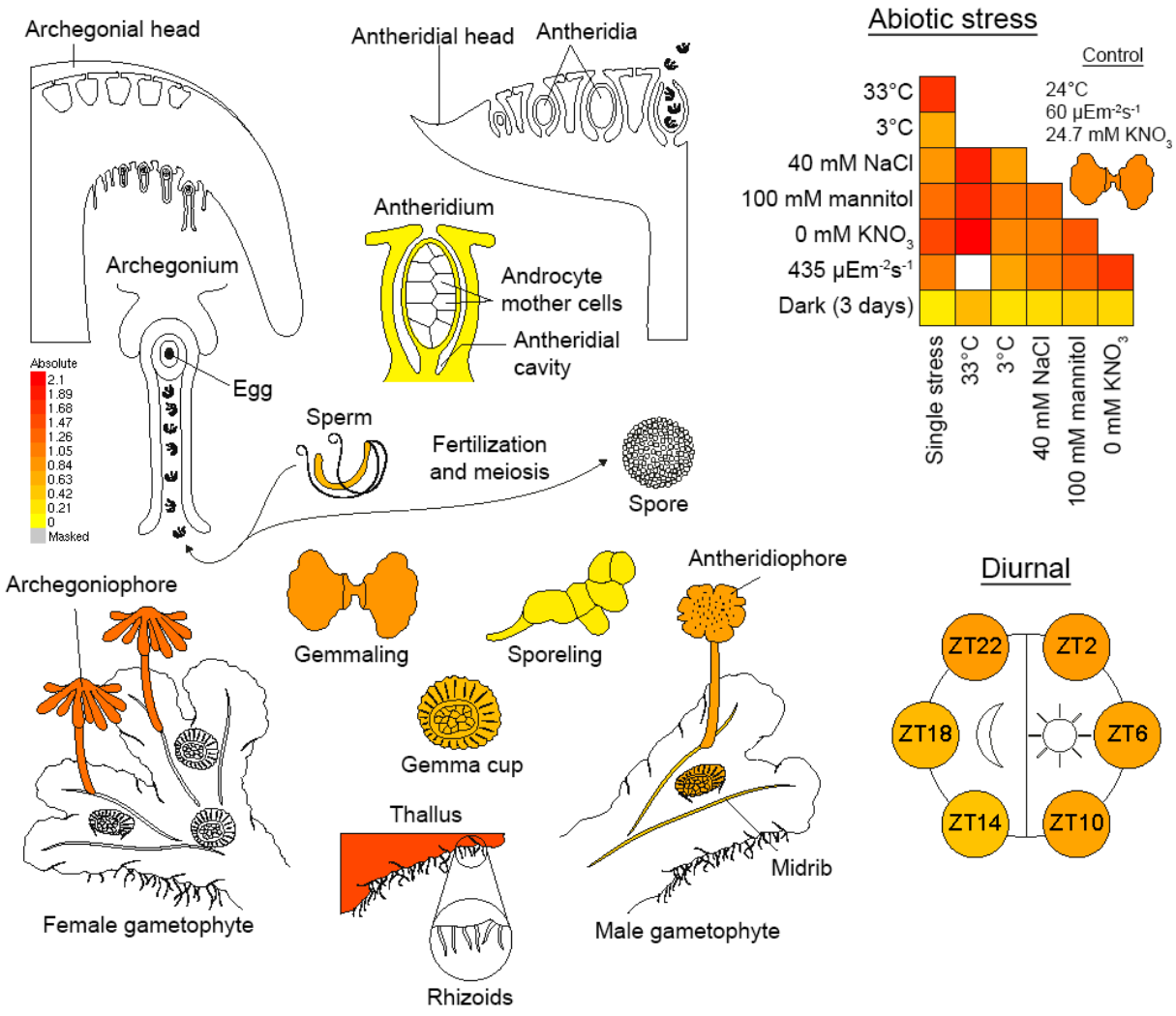

Figure 36: MpLRR-RLK10 is mainly expressed in the thallus (Liverwort Atlas eFP Browser at bar.utoronto.ca). Increased expression upon abiotic stress. In contrast to MpLRR-RLK 5, MpLRR-RLJ10 is not expressed in the sporeling. Generally, the expression is lower compared to MpLRR-RLK15.

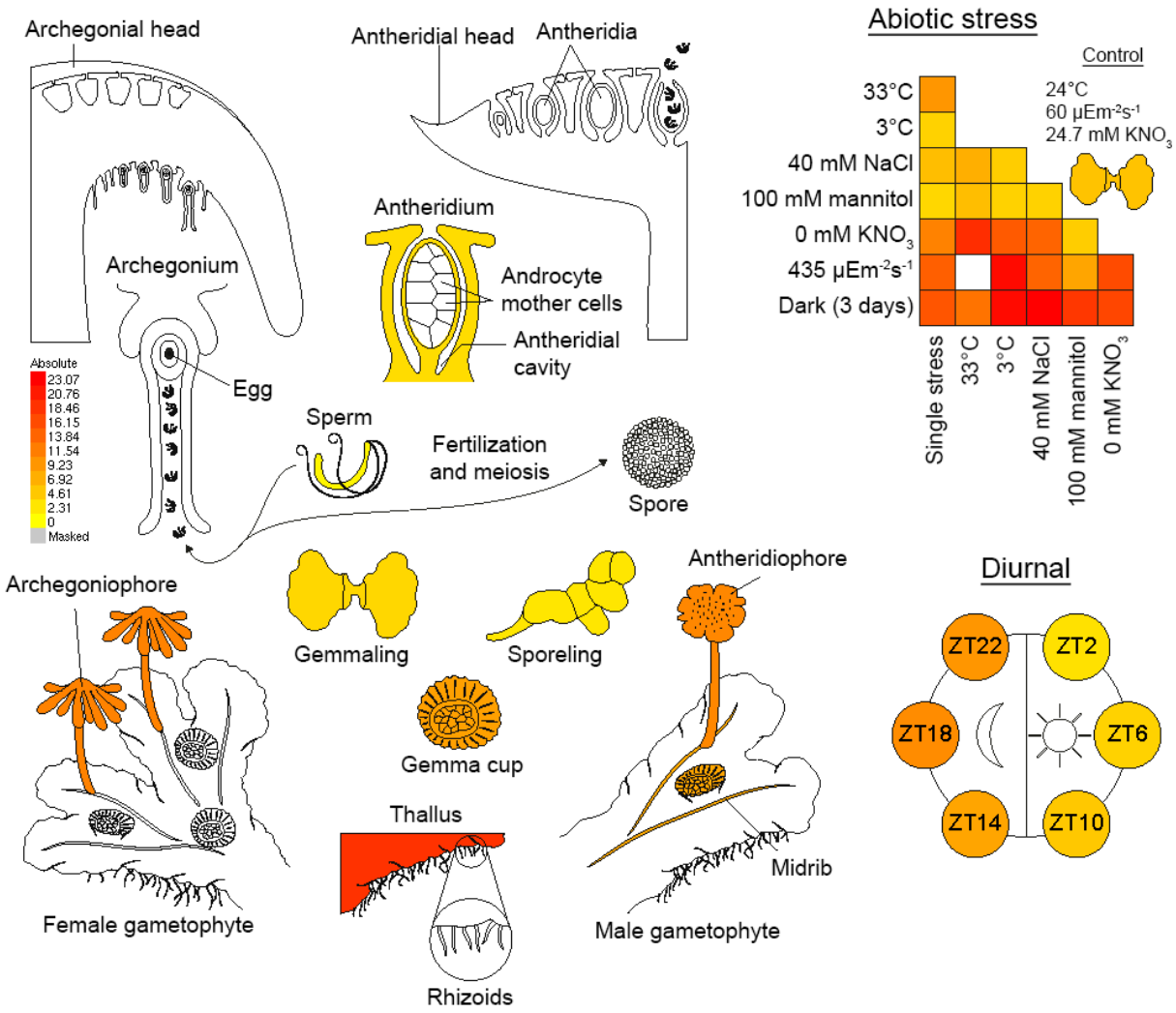

Figure 37: MpLRR-RLK15 is expressed in the thallus and less in reproductive tissues (Liverwort Atlas eFP Browser at bar.utoronto.ca). Like MpLRR-RLK 10, MpLRR-RLK15 is not expressed in the sporeling and the sperm. The main expression can be found in the thallus. Expression increased upon abiotic stress, related to light intensity. MpLRR-RLK15 shows the highest expression compared to MpLRR-RLK5 and 10.

7.3 MpHSL-MpIDA – a functional receptor-ligand pair

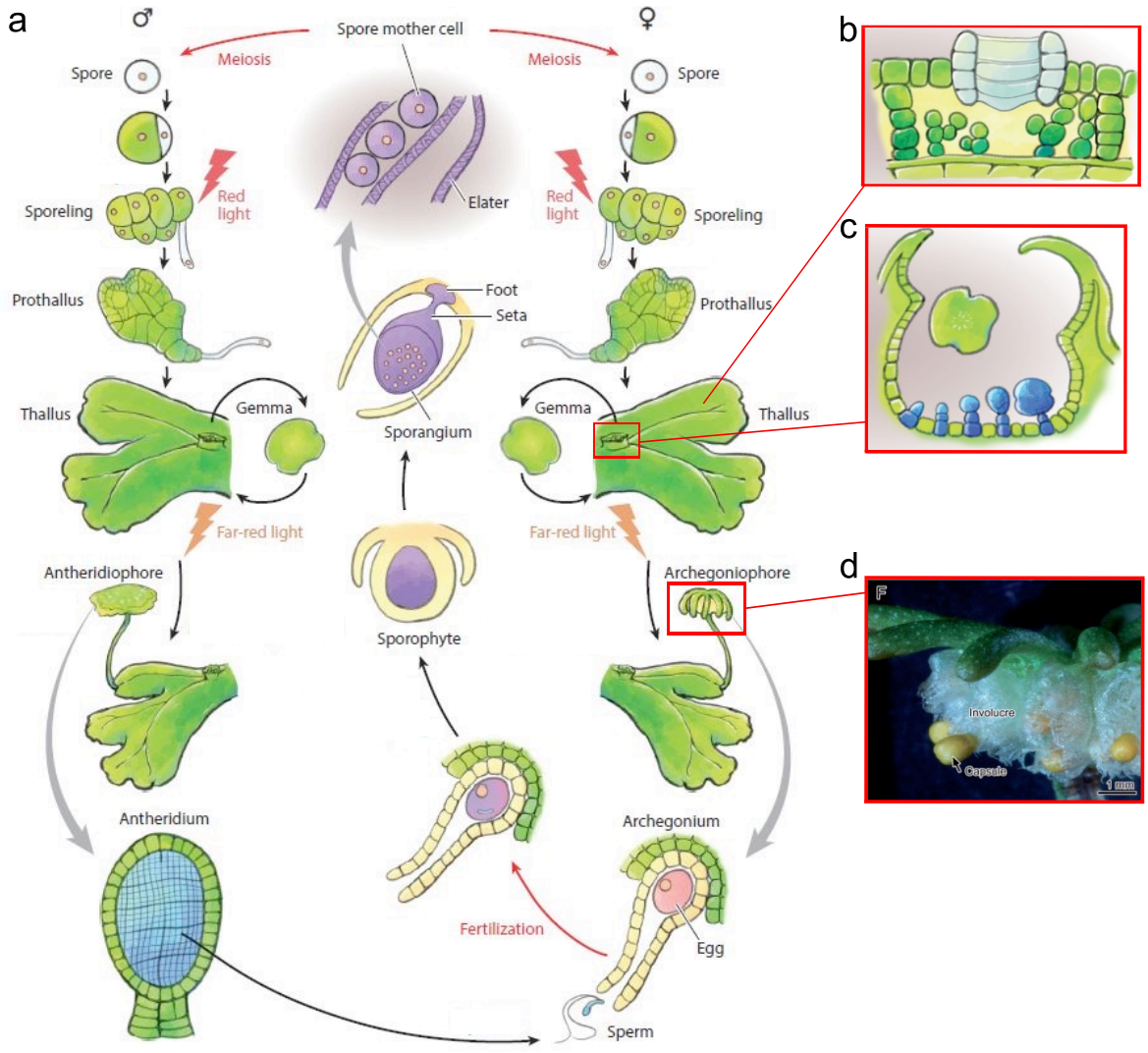

Figure 38: The life cycle of M. polymorpha highlighting air pores as openings into inner tissues, as well as potential areas of abscission. a) Sexual and vegetative reproduction of M. polymorpha. b) Cartoon of a transverse section of thallus with an air pore. c) Depiction of a transverse section of a gemma cup and gemmae development (shaded in blue), Release of a matured gemmae from the gemma cup floor cells, displaying a potential “abscission” process. (Cartoon modified from Kohchi et al., 2021). d) Spore capsules, which will release spores, potentially with the help of abscission processes, are exposed to the outside (Shimamura, 2016). Cartoons by Kohchi et al., 2021 and image by Shimamura, 2016.

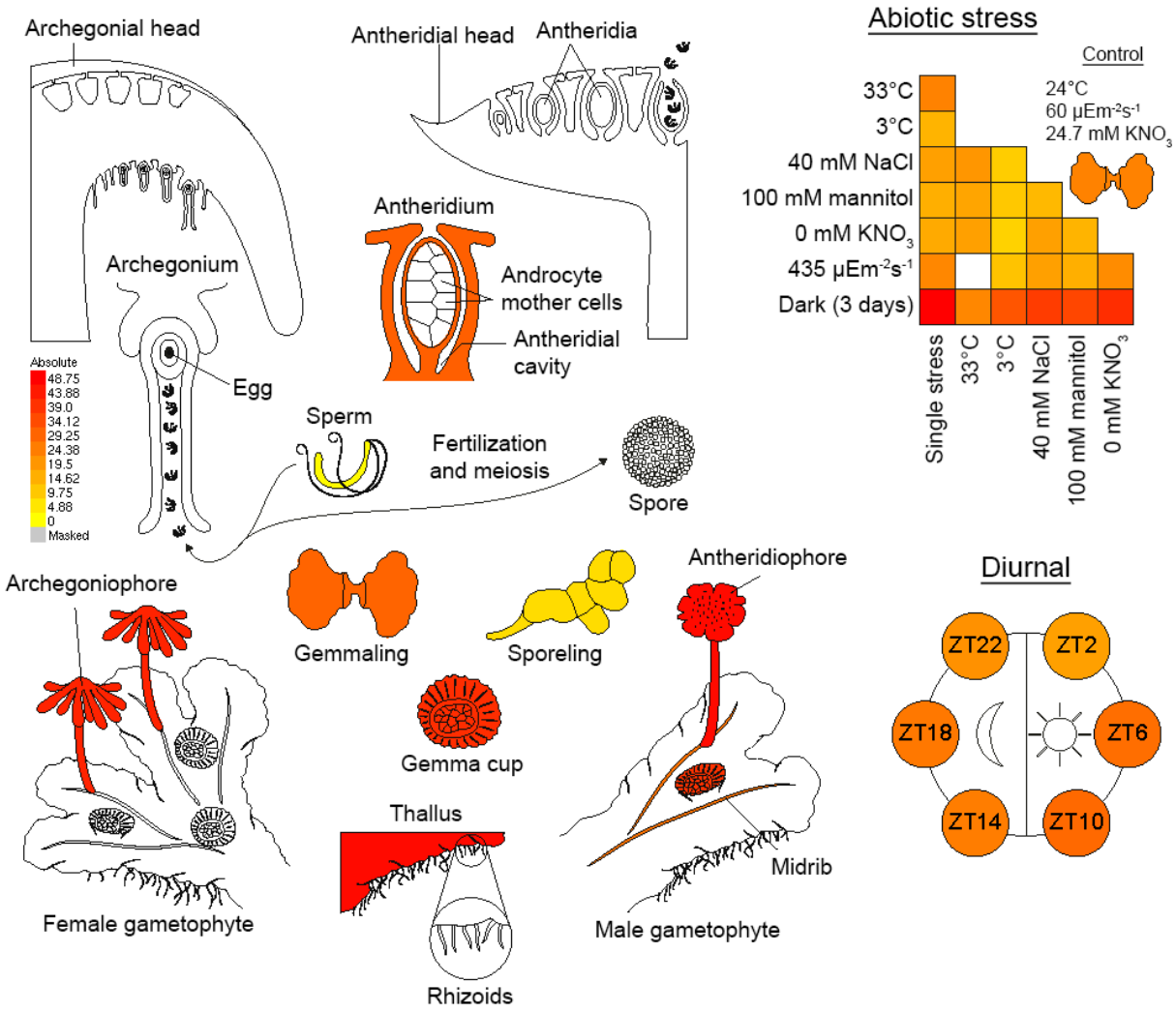

Figure 39: MpHSL is overall well expressed (Liverwort Atlas eFP Browser at bar.utoronto.ca). Generally expression in all tissues, except for the sporeling and sperm. Darkness increases the expression.

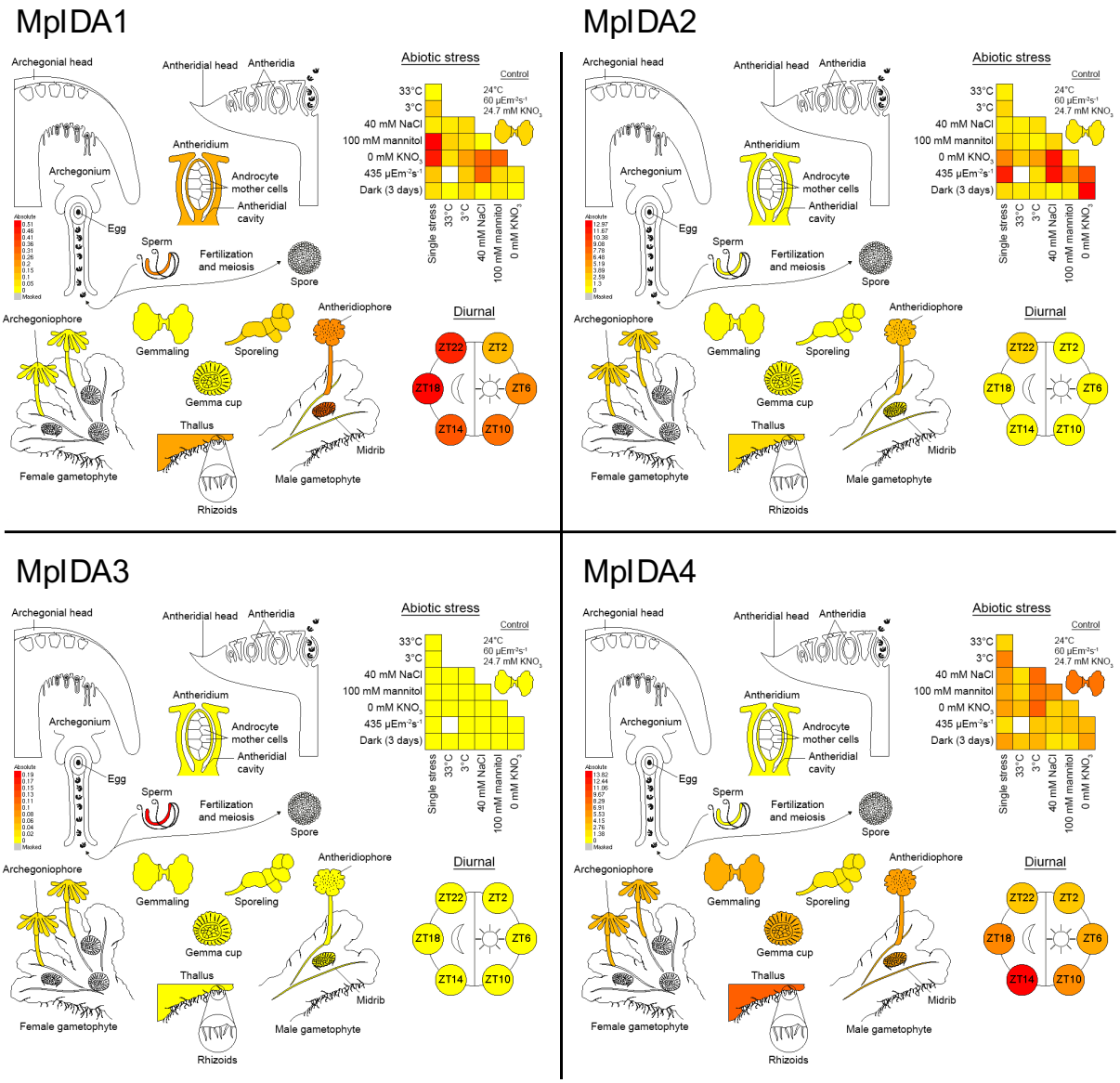

Figure 40: Differential expression of the four MpIDA genes (Liverwort Atlas eFP Browser at bar.utoronto.ca). MpIDA2 and 4 show a higher expression compared to MpIDA1 and 3. MpIDA1 is mainly expressed in the antheridiophore, antheridium, the gemma cup and the thallus. MpIDA2 is exclusively expressed in the antheridiophore and upregulated upon abiotic stress. MpIDA3 is only present in the sperm, albeit at a very low level. The expression is not influenced by abiotic stresses. MpIDA4 is mainly expressed in the thallus, but also in the gametophores, gemma cup and in gemmalings.

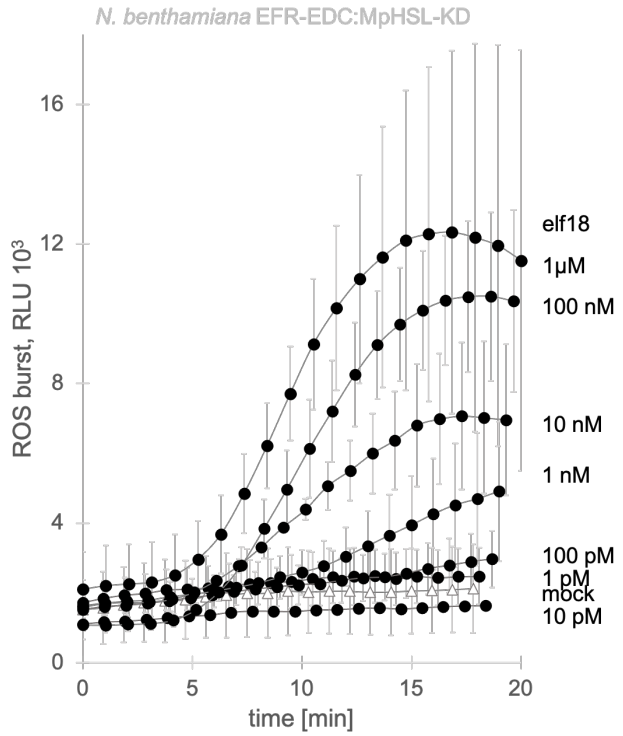

Figure 41: The kinase domain of MpHSL is able to transfer the perception of a ligand at the surface into a cellular response. A chimeric receptor consisting of the ectodomain of EFR and the kinase domain of MpHSL triggered a ROS-burst upon treatment of the leaf tissue with elf18; EC_{50}= 25 nM. Thus, the kinase domain of MpHSL was validated as active. Data points represent the average of four replicates. Error bars indicate the standard deviation of three/four replicates.

	% identity		
domain	**MpHSL/HSL1**	**MpHSL/HLS2**	**MpHSL/HAE**
LRR	44	40	44
structure	63	60	63
surface	25	19	24
kinase	64	60	62

Table 16: Amino acid sequence comparison of MpHSL with AtHSL1/2 and HAE by Prof. Dr. Georg Felix. According to the percentual identity of different domains between MpHSL and the HAE/HSL genes in *A. thaliana*, MpHSL shows the highest similarity to AtHAE and HLS1.

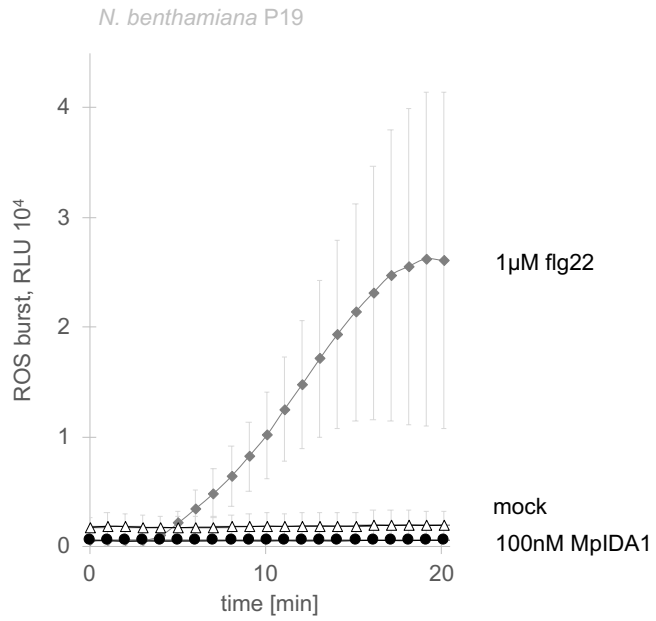

Figure 42: MpIDA1 does not initiate a ROS burst in *N. benthamiana* plants transformed with P19. Data points represent the average of four replicates. Error bars indicate the standard deviation of three/four replicates.

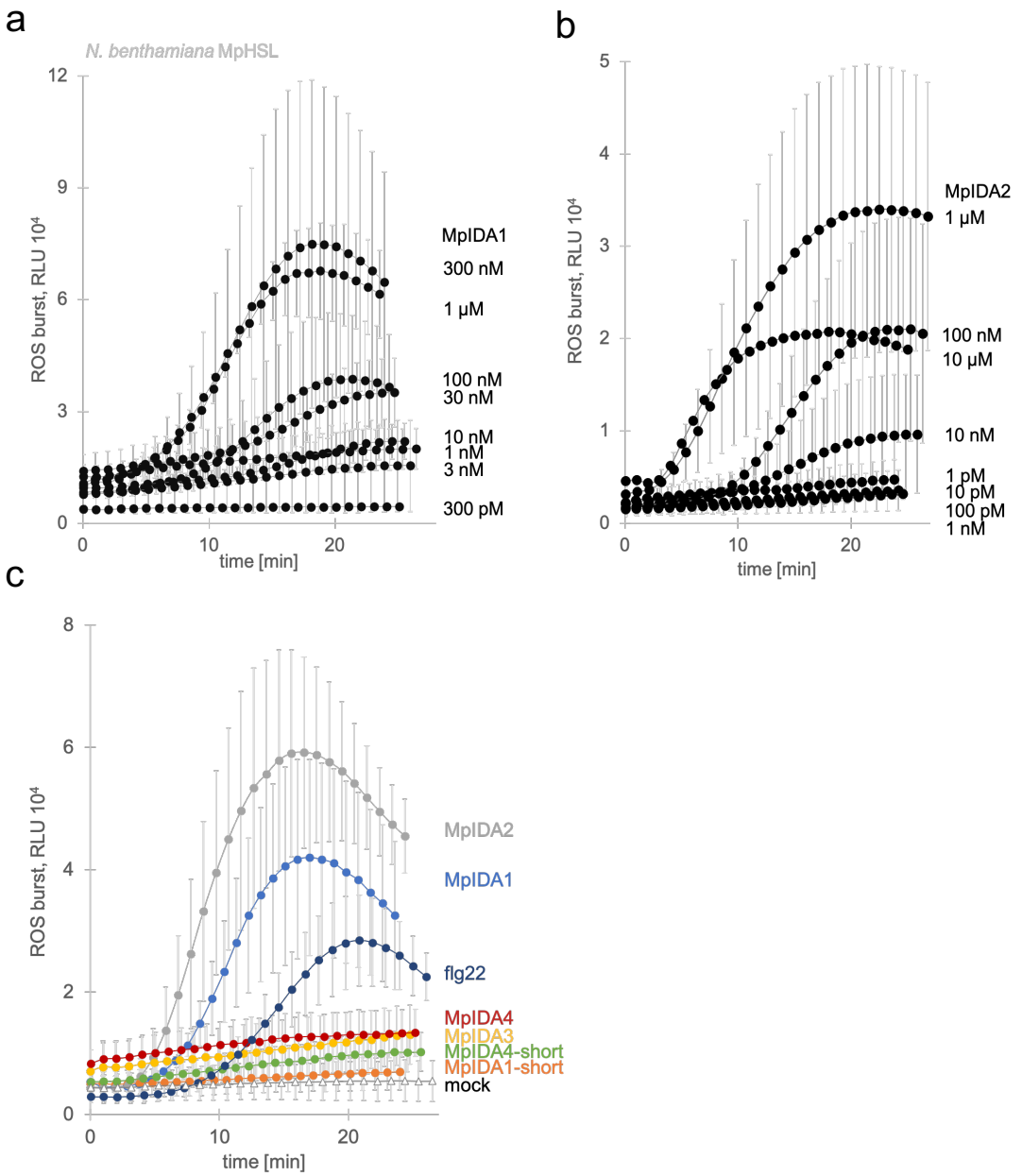

Figure 43: MpHSL and MpIDA1 behave like a functional ligand-receptor pair. ROS burst response of MpHSL, expressed in *N. benthamiana* leaves after treatment with different concentrations of **a)** MpIDA1 and **b)** MpIDA2. Datapoint represent the average of 4 replicates. Error bars indicate the standard deviation of three/four replicates. **c)** *N. benthamiana* leaf pieces transiently expressing MpHSL respond only to treatment with MpIDA1 (bright blue) and MpIDA2 (grey), but not to MpIDA3 (yellow) and MpIDA4 (red) with a ROS-burst. A N-terminal truncated version of MpIDA1 and MpIDA4 (MpIDA1-short, orange; MpIDA4-short, green) did not activate the receptor (**Table 17**). Concentrations used= 1 µM, except for the positive control (flg22, dark blue, 100 nM).

ID	Name	Activity	Sequence
Mapoly0251s0002	MpIDA1	yes	FQKLPRSSEVPPQGoSPIHN
Mapoly0251s0002	HBg-MpIDA1	yes	VSGWRLFKKISGFQKLPRSSEVPPQGoSPIHN
Mapoly0251s0002	MpIDA1-short	no	EVPPQGoSPIHN
Mapoly0003s0117	MpIDA2	yes	FERLPRGTTVPDSNoSPVHN

Mapoly0085s0063	MpIDA3	no	LQRLPRDTPVPPSG**o**SGPNR
Mapoly0003s0111	MpIDA4	no	FQMLPRNTRPPPRG**o**SPGSN
Mapoly0003s0111	MpIDA4-short	no	RPPPRG**o**SPGSN
	IDA3	yes	PKGV PIPPSAPSKRHN
	IDA9 (PiPPo)	no	PIPPSA**o**SKRHN
	IDL1	yes	FHSFSKRV IvPPSgPSmRHN
	IDA2	no	PKGV PIPPSA**o**SKRHN
	IDA4	yes	PKGV PIPPSAPSKRHN**-SY**
	IDA5	yes	**YS-**PKGV PIPPSAPSKRHN
	IDA6	yes	FGYLPKGV PIP**o**SAPSKRHN
	IDA7	no	FG**Y**LPKGV PIP**o**SA**o**SKRHN
	IDA8	yes	PIP**o**SAPSKRHN
	IDA10	yes	PIPPSAPSKRHN
	IDL5-DC	no	FsGFLPKTL PIP**h**SAPSRKHN**-DC**

Table 17: Overview of the activity of IDA peptides on MpHSL. The peptides (1 µM) were tested on leaf pieces of *N. benthamiana*, transiently expressing MpHSL, by ROS-burst assays. **o** indicates hydroxyproline.

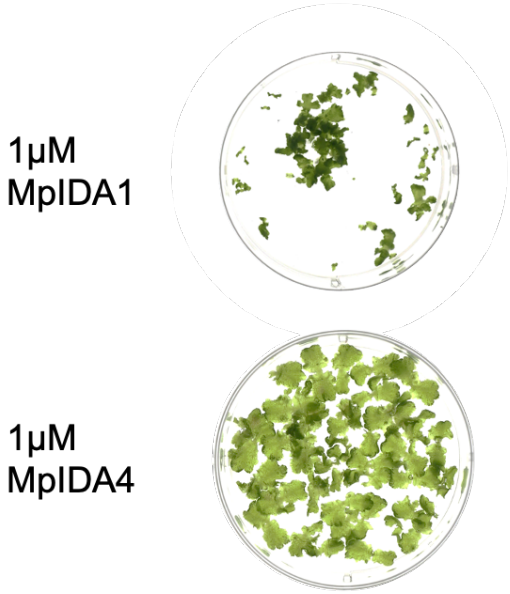

Figure 44: Exclusively an active MpIDA peptide is inhibiting the development of *M. polymorpha* gemmae. Gemmae after 22 days, treated on day 0 with active (MpIDA1) or inactive (MpIDA4) MpIDA peptide (**Table 17**), respectively.

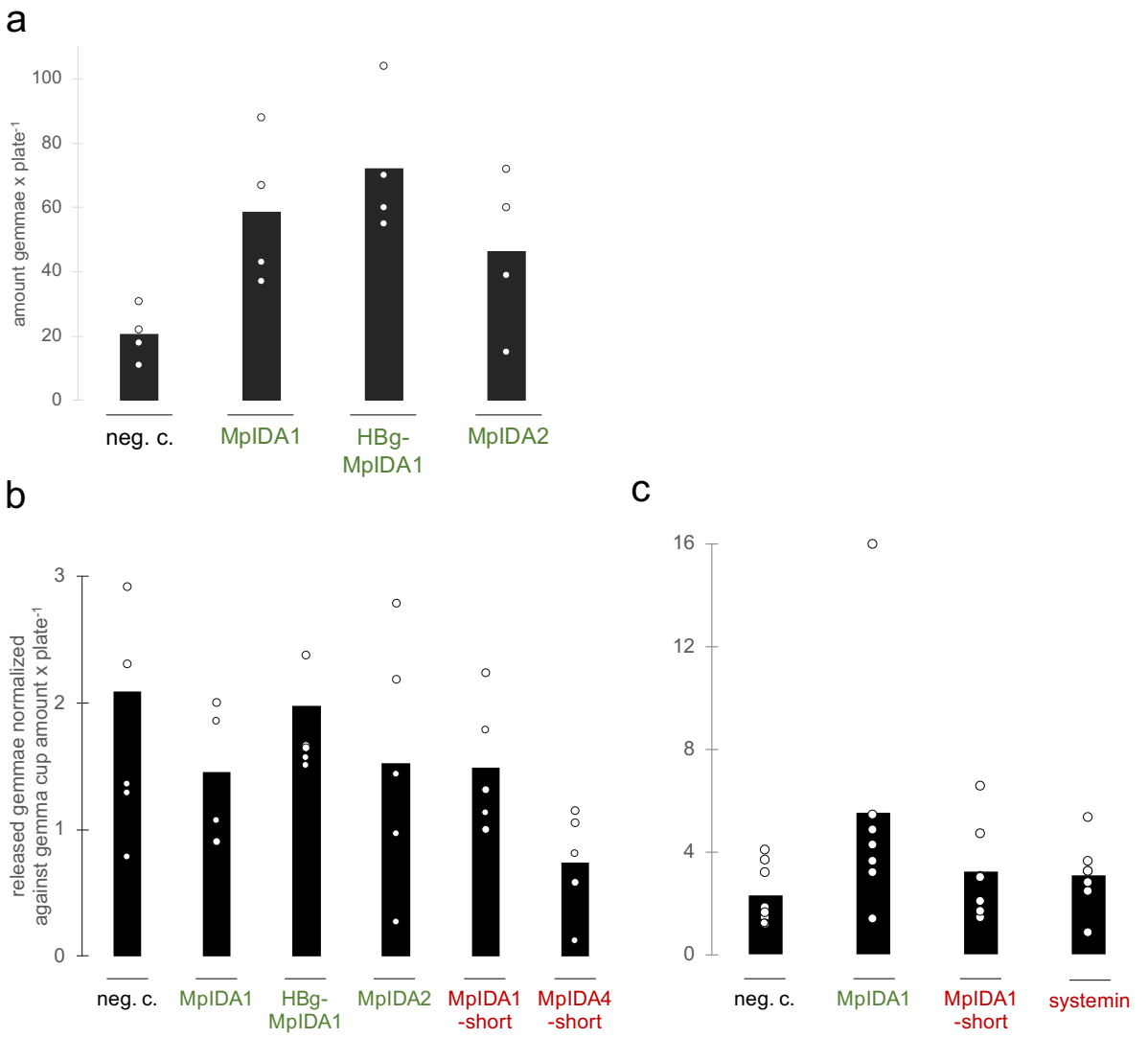

Figure 45: A gemmae release assay might hint at a function of MpIDA peptides in abscission. To test if the presence of MpIDA peptide is increasing the release of gemmae, a process which could involve the regulation of abscission via an endogenous signal, a gemmae release assay was performed (2.2.19.4). Peptides colored in red are inactive, peptides colored in green are active in immune response and growth inhibition assays. Plates or liquid cultures with no peptide represent negative controls (neg. c.) **a)** The first approach showed a trend towards a higher amount of gemmae from gemma cups grown on active MpIDA peptides. **b)** For the second approach, the amount of released gemmae was normalized against the amount of gemma cups. The trend could not be confirmed. **c)** The third approach showed the trend again, however, the single data are highly variable. Bars represent the average of replicates (circles).

7.4 MpSOBIR – as an adaptor kinase for RLPs in vascular plants?

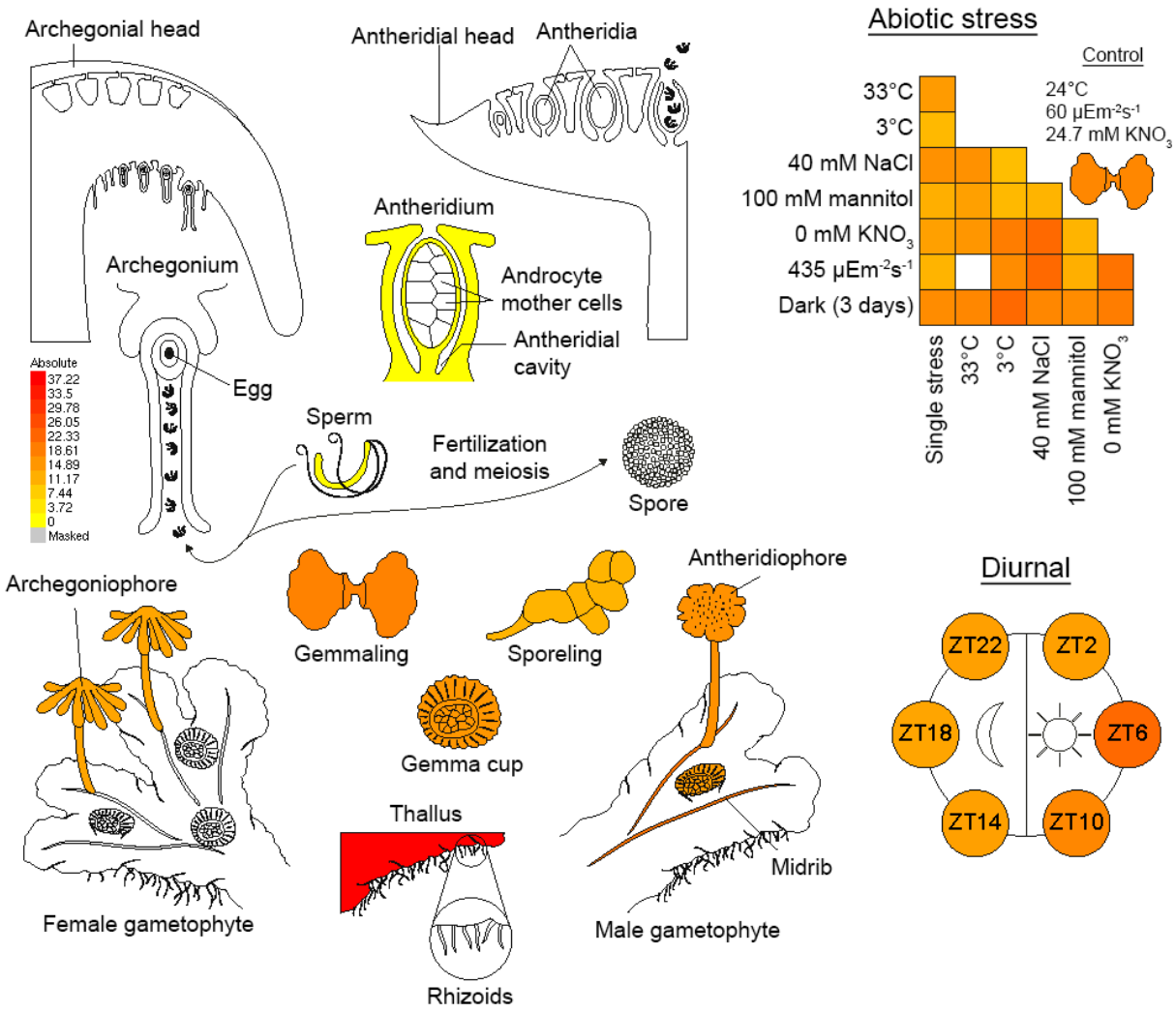

Figure 46: MpSOBIR is highly expressed in the thallus and present in reproductive tissues, but not in the antheridium and the sperm (Liverwort Atlas eFP Browser at bar.utoronto.ca).

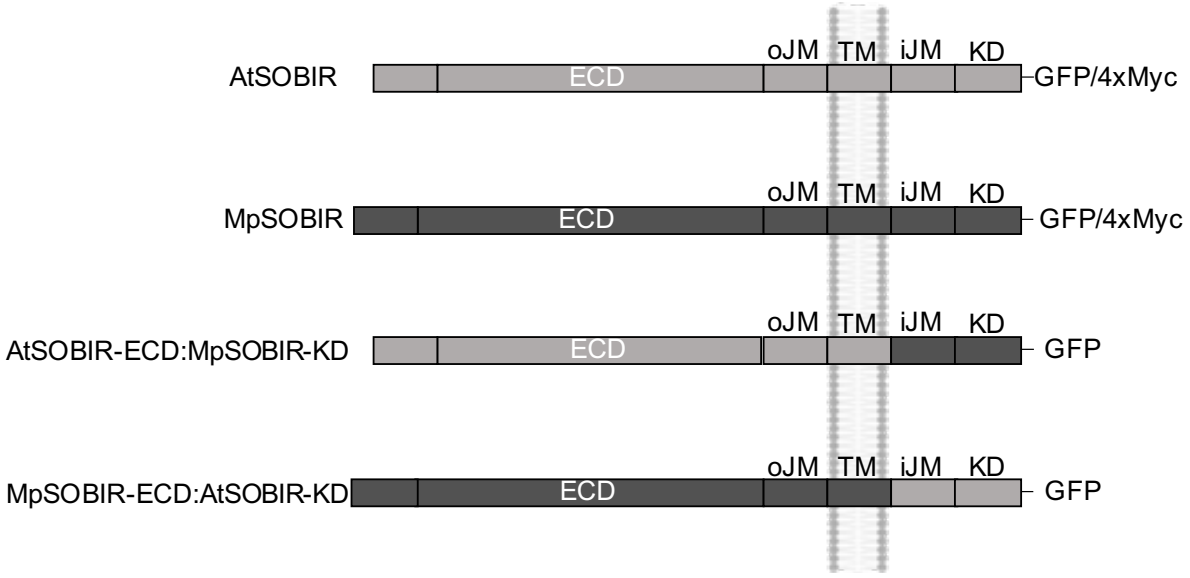

Figure 47: Chimeric receptors of MpSOBIR and AtSOBIR. To validate the functional substitution of MpSOBIR for AtSOBIR, chimeric receptors were generated. The ectodomain (ECD) contains the transmembrane domain (TM). kinase domain (KD), outer jaxtermembrane (oJM), inner jaxtermemebrane (iJM).

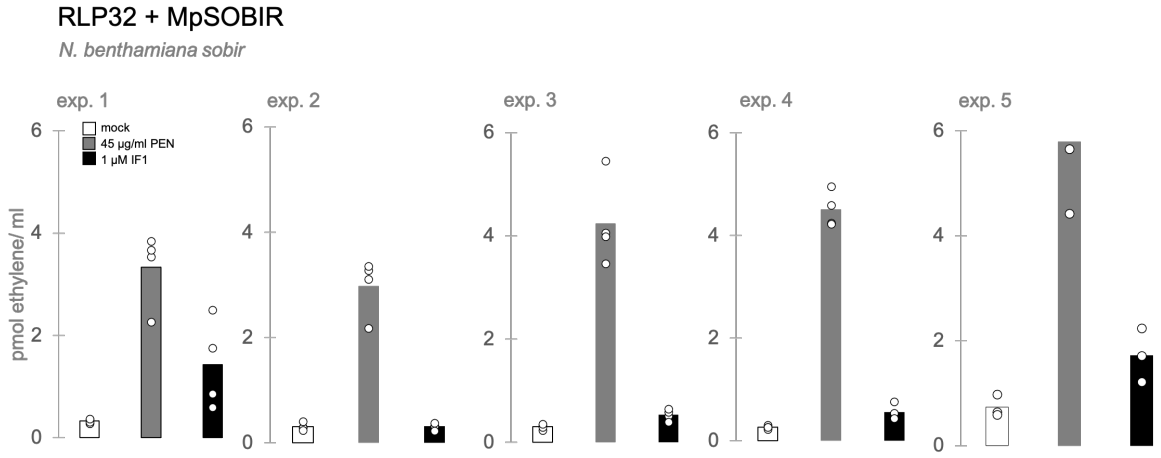

Figure 48: No complementation of *N. benthamiana sobir* with RLP32 and MpSOBIR. The co-transformation of RLP32 and MpSOBIR did not result in a clear biosynthesis of ethylene after treatment with IF1. Leaf pieces, however, responded to the positive control PEN. Insufficient production of ethylene (2-4) and high standard deviations of positive results (1,5) lead to the interpretation of an unsuccessful complementation of MpSOBIR for NbSOBIR in co-expression with RLP32. Expression of respective receptors was validated by Western blotting (data not shown). Bars represent the average of four replicates (circles).

7.5 MpBIR – a potential negative regulator

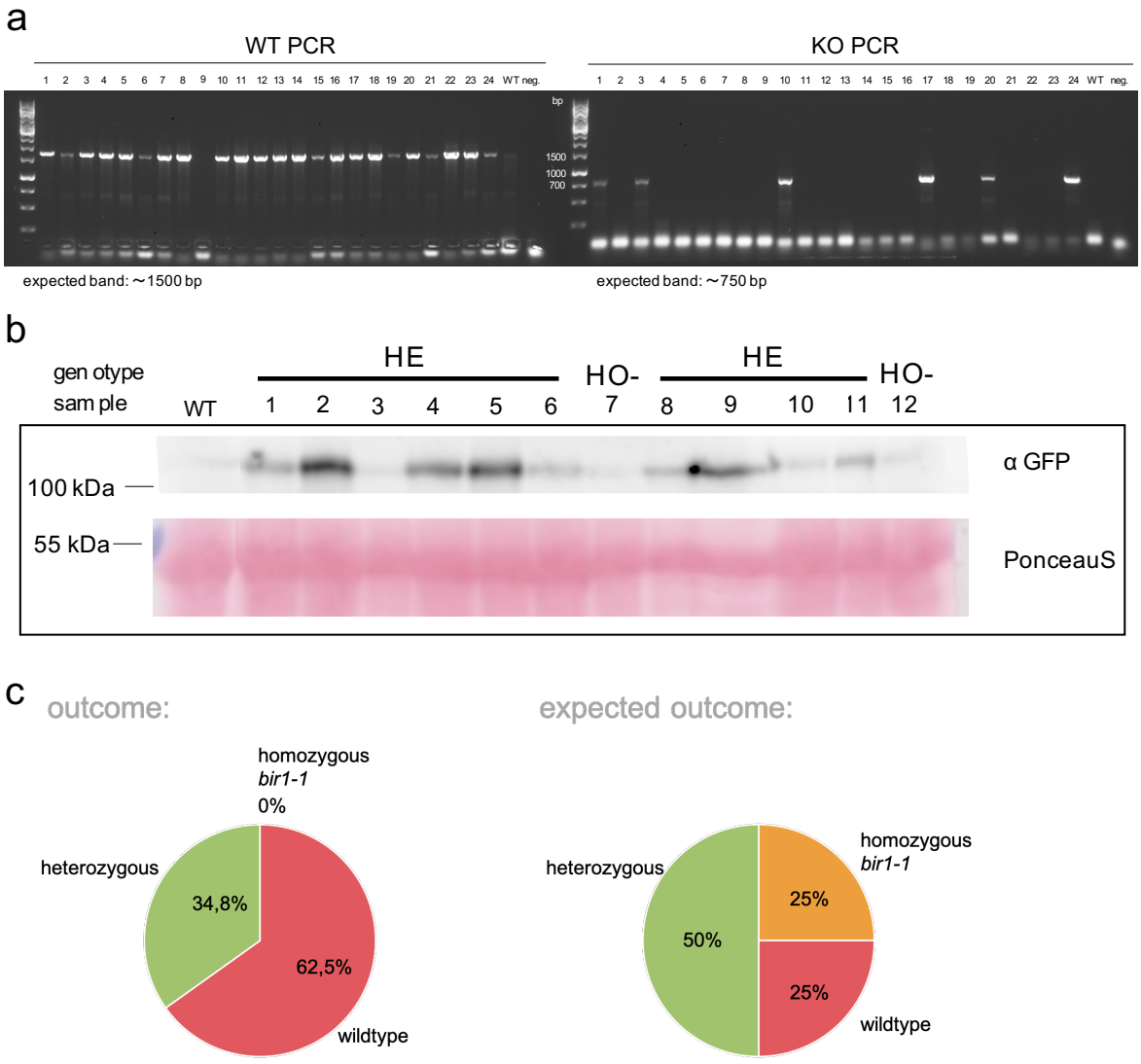

Figure 49: Genotyping stably transformed *A. thaliana bir1-1* heterozygous T-DNA-insertion lines with MpSERK. a) PCR amplification of a wildtype (WT)- and a T-DNA-insertion (KO)-fragment of 24 exemplary plant gDNA samples. The WT-fragment indicates the presence of *BIR1*. In case of a homozygous mutant line no fragment would be amplified for the WT PCR. The KO-fragment results out of a primer binding on the BIR1 T-DNA-insertion and is thus evidence for the successful ko of *BIR1*. Sample number 9 showed no amplification in any PCR reaction and was repeated at a later timepoint. **b)** Western blot of 12 randomly selected plants of different genotypes indicates the presence of a signal for the recombinant MpBIR:GFP at approximately 110 kDa. Seeds were previously screened by pFAST expression. HO-=homozygote/wildtype (lack of T-DNA-insertion), HE=heterozygous (PCR product with both primer pairs). **c)** Expected versus actual outcome of the genotyping, showing a reverse distribution of homozygous (wildtype) plants and heterozygous plants, as well as no homozygous plant for *bir1-1*.

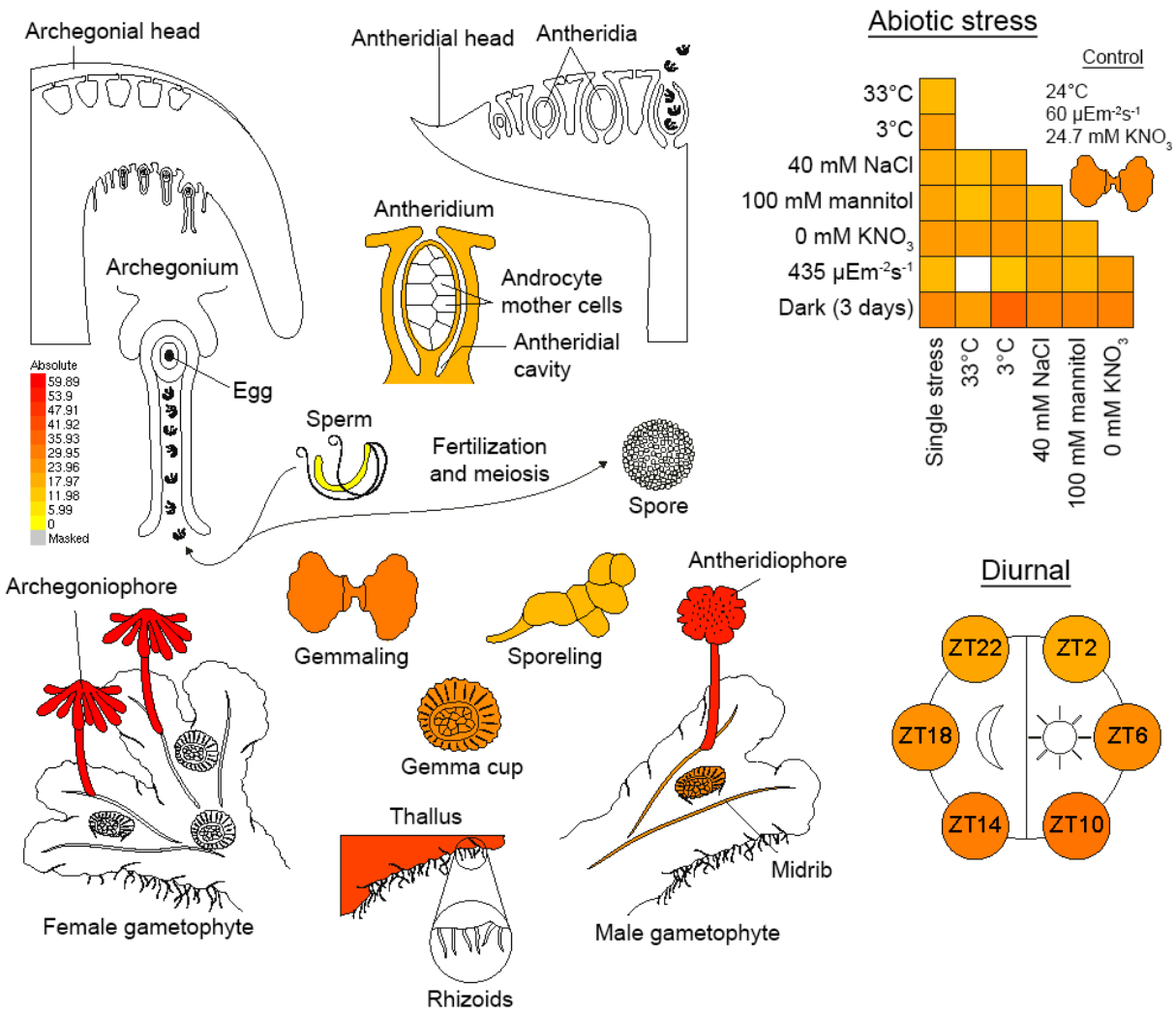

Figure 50: MpBIR is broadly expressed (Liverwort Atlas eFP Browser at bar.utoronto.ca). Main expression in the thallus and the gametophores, but not in the sperm.

8 References

Aalen, R.B., Wildhagen, M., Stø, I.M., and Butenko, M.A. (2013). IDA: a peptide ligand regulating cell separation processes in Arabidopsis. J. Exp. Bot. **64**: 5253–5261.

aan den Toorn, M., Albrecht, C., and de Vries, S. (2015). On the Origin of SERKs: Bioinformatics Analysis of the Somatic Embryogenesis Receptor Kinases. Mol. Plant **8**: 762–782.

Albert, I. et al. (2015). An RLP23–SOBIR1–BAK1 complex mediates NLP-triggered immunity. Nat. Plants **1**: 15140.

Albert, M. and Fürst, U. (2017). Quantitative Detection of Oxidative Burst upon Activation of Plant Receptor Kinases. In Plant Receptor Kinases, R.B. Aalen, ed, Methods in Molecular Biology. (Springer New York: New York, NY), pp. 69–76.

Albert, M., Jehle, A.K., Furst, U., Chinchilla, D., Boller, T., and Felix, G. (2013a). A Two-Hybrid-Receptor Assay Demonstrates Heteromer Formation as Switch-On for Plant Immune Receptors. PLANT Physiol. **163**: 1504–1509.

Albert, M., Jehle, A.K., Furst, U., Chinchilla, D., Boller, T., and Felix, G. (2013b). A Two-Hybrid-Receptor Assay Demonstrates Heteromer Formation as Switch-On for Plant Immune Receptors. PLANT Physiol. **163**: 1504–1509.

Albert, M., Jehle, A.K., Mueller, K., Eisele, C., Lipschis, M., and Felix, G. (2010a). *Arabidopsis thaliana* Pattern Recognition Receptors for Bacterial Elongation Factor Tu and Flagellin Can Be Combined to Form Functional Chimeric Receptors. J. Biol. Chem. **285**: 19035–19042.

Albert, M., K. Jehle, A., Lipschis, M., Mueller, K., Zeng, Y., and Felix, G. (2010b). Regulation of cell behaviour by plant receptor kinases: Pattern recognition receptors as prototypical models. Eur. J. Cell Biol. **89**: 200–207.

Alcaraz, L.D., Peimbert, M., Barajas, H.R., Dorantes-Acosta, A.E., Bowman, J.L., and Arteaga-Vázquez, M.A. (2018). Marchantia liverworts as a proxy to plants' basal microbiomes. Sci. Rep. **8**.

Althoff, F., Kopischke, S., Zobell, O., Ide, K., Ishizaki, K., Kohchi, T., and Zachgo, S. (2014). Comparison of the MpEF1α and CaMV35 promoters for application in Marchantia polymorpha overexpression studies. Transgenic Res. **23**: 235–244.

Amborella Genome Project et al. (2013). The *Amborella* Genome and the Evolution of Flowering Plants. Science **342**: 1241089.

Bi, G., Liebrand, T.W.H., Bye, R.R., Postma, J., van der Burgh, A.M., Robatzek, S., Xu, X., and Joosten, M.H.A.J. (2016). SOBIR1 requires the GxxxG dimerization

motif in its transmembrane domain to form constitutive complexes with receptor-like proteins: Functional analysis of SOBIR1. Mol. Plant Pathol. **17**: 96–107.

Blaum, B.S., Mazzotta, S., Nöldeke, E.R., Halter, T., Madlung, J., Kemmerling, B., and Stehle, T. (2014). Structure of the pseudokinase domain of BIR2, a regulator of BAK1-mediated immune signaling in Arabidopsis. J. Struct. Biol. **186**: 112–121.

Böhm, H., Albert, I., Fan, L., Reinhard, A., and Nürnberger, T. (2014a). Immune receptor complexes at the plant cell surface. Curr. Opin. Plant Biol. **20**: 47–54.

Böhm, H., Albert, I., Oome, S., Raaymakers, T.M., Van den Ackerveken, G., and Nürnberger, T. (2014b). A Conserved Peptide Pattern from a Widespread Microbial Virulence Factor Triggers Pattern-Induced Immunity in Arabidopsis. PLoS Pathog. **10**: e1004491.

Boller, T. and Felix, G. (2009). A Renaissance of Elicitors: Perception of Microbe-Associated Molecular Patterns and Danger Signals by Pattern-Recognition Receptors. Annu. Rev. Plant Biol. **60**: 379–406.

Boller, T. and He, S.Y. (2009). Innate Immunity in Plants: An Arms Race Between Pattern Recognition Receptors in Plants and Effectors in Microbial Pathogens. Science **324**: 742–744.

Bowman, J.L. et al. (2017a). Insights into Land Plant Evolution Garnered from the Marchantia polymorpha Genome. Cell **171**: 287-304.e15.

Bowman, J.L. et al. (2017b). Insights into Land Plant Evolution Garnered from the Marchantia polymorpha Genome. Cell **171**: 287-304.e15.

Bowman, J.L. (2011). Stomata: Active Portals for Flourishing on Land. Curr. Biol. **21**: R540–R541.

Bressendorff, S., Azevedo, R., Kenchappa, C.S., Ponce de León, I., Olsen, J.V., Rasmussen, M.W., Erbs, G., Newman, M.-A., Petersen, M., and Mundy, J. (2016). An Innate Immunity Pathway in the Moss *Physcomitrella patens*. Plant Cell **28**: 1328–1342.

Butenko, M.A. (2003). INFLORESCENCE DEFICIENT IN ABSCISSION Controls Floral Organ Abscission in Arabidopsis and Identifies a Novel Family of Putative Ligands in Plants. PLANT CELL ONLINE **15**: 2296–2307.

Butenko, M.A., Wildhagen, M., Albert, M., Jehle, A., Kalbacher, H., Aalen, R.B., and Felix, G. (2014a). Tools and Strategies to Match Peptide-Ligand Receptor Pairs. Plant Cell **26**: 1838–1847.

Butenko, M.A., Wildhagen, M., Albert, M., Jehle, A., Kalbacher, H., Aalen, R.B.,

and Felix, G. (2014b). Tools and Strategies to Match Peptide-Ligand Receptor Pairs. Plant Cell **26**: 1838–1847.

Cao, Y., Liang, Y., Tanaka, K., Nguyen, C.T., Jedrzejczak, R.P., Joachimiak, A., and Stacey, G. (2014). The kinase LYK5 is a major chitin receptor in Arabidopsis and forms a chitin-induced complex with related kinase CERK. Plant Biol.: 19.

Carella, P., Gogleva, A., Hoey, D.J., Bridgen, A.J., Stolze, S.C., Nakagami, H., and Schornack, S. (2019). Conserved Biochemical Defenses Underpin Host Responses to Oomycete Infection in an Early-Divergent Land Plant Lineage. Curr. Biol. **29**: 2282-2294.e5.

Carella, P., Gogleva, A., Tomaselli, M., Alfs, C., and Schornack, S. (2017). Phytophthora palmivora establishes tissue-specific intracellular infection structures in the earliest divergent land plant lineage.

Carella, P. and Schornack, S. (2018). Manipulation of Bryophyte Hosts by Pathogenic and Symbiotic Microbes. Plant Cell Physiol. **59**: 656–665.

Catanzariti, A., Do, H.T.T., Bru, P., Sain, M., Thatcher, L.F., Rep, M., and Jones, D.A. (2017). The tomato *I* gene for Fusarium wilt resistance encodes an atypical leucine-rich repeat receptor-like protein whose function is nevertheless dependent on SOBIR 1 and SERK 3/ BAK 1. Plant J. **89**: 1195–1209.

Chinchilla, D., Shan, L., He, P., de Vries, S., and Kemmerling, B. (2009). One for all: the receptor-associated kinase BAK1. Trends Plant Sci. **14**: 535–541.

Chinchilla, D., Zipfel, C., Robatzek, S., Kemmerling, B., Nürnberger, T., Jones, J.D.G., Felix, G., and Boller, T. (2007). A flagellin-induced complex of the receptor FLS2 and BAK1 initiates plant defence. Nature **448**: 497–500.

Chiyoda, S., Ishizaki, K., Kataoka, H., Yamato, K.T., and Kohchi, T. (2008). Direct transformation of the liverwort Marchantia polymorpha L. by particle bombardment using immature thalli developing from spores. Plant Cell Rep. **27**: 1467–1473.

Cho, S.K., Larue, C.T., Chevalier, D., Wang, H., Jinn, T.-L., Zhang, S., and Walker, J.C. (2008). Regulation of floral organ abscission in *Arabidopsis thaliana*. Proc. Natl. Acad. Sci. **105**: 15629–15634.

Coleman, A.D., Maroschek, J., Raasch, L., Takken, F.L.W., Ranf, S., and Hückelhoven, R. (2021). The Arabidopsis leucine-rich repeat receptor-like kinase MIK2 is a crucial component of early immune responses to a fungal-derived elicitor. New Phytol. **229**: 3453–3466.

Daudi, A. and O'Brien, J. (2012). Detection of Hydrogen Peroxide by DAB Staining

in Arabidopsis Leaves. BIO-Protoc. **2**.

Delaux, P.-M. et al. (2019). Reconstructing trait evolution in plant evo–devo studies. Curr. Biol. **29**: R1110–R1118.

Delaux, P.-M. and Schornack, S. (2021). Plant evolution driven by interactions with symbiotic and pathogenic microbes. Science **371**: eaba6605.

Delaux und Schornack - 2021 - Plant evolution driven by interactions with symbio.pdf.

Deveaux, Y., Peaucelle, A., Roberts, G.R., Coen, E., Simon, R., Mizukami, Y., Traas, J., Murray, J.A.H., Doonan, J.H., and Laufs, P. (2003). The ethanol switch: a tool for tissue-specific gene induction during plant development. Plant J. **36**: 918–930.

Domazakis, E., Wouters, D., Visser, R.G.F., Kamoun, S., Joosten, M.H.A.J., and Vleeshouwers, V.G.A.A. (2018). The ELR-SOBIR1 Complex Functions as a Two-Component Receptor-Like Kinase to Mount Defense Against *Phytophthora infestans*. Mol. Plant-Microbe Interactions® **31**: 795–802.

Domínguez-Ferreras, A., Kiss-Papp, M., Jehle, A.K., Felix, G., and Chinchilla, D. (2015). An Overdose of the Arabidopsis Coreceptor BRASSINOSTEROID INSENSITIVE1-ASSOCIATED RECEPTOR KINASE1 or Its Ectodomain Causes Autoimmunity in a SUPPRESSOR OF BIR1-1-Dependent Manner. Plant Physiol. **168**: 1106–1121.

Edwards, K., Johnstone, C., and Thompson, C. (1991). A simple and rapid method for the preparation of plant genomic DNA for PCR analysis. Nucleic Acids Res. **19**: 1349–1349.

Fan, L. et al. (2022). Genotyping-by-sequencing-based identification of Arabidopsis pattern recognition receptor RLP32 recognizing proteobacterial translation initiation factor IF1. Nat. Commun. **13**: 1294.

Fan, M., Wang, M., and Bai, M.-Y. (2016). Diverse roles of SERK family genes in plant growth, development and defense response. Sci. China Life Sci. **59**: 889–896.

Felix, G., Duran, J.D., Volko, S., and Boller, T. (1999). Plants have a sensitive perception system for the most conserved domain of bacterial flagellin: Plants perceive a conserved domain of bacterial flagellin. Plant J. **18**: 265–276.

Flores-Sandoval, E., Dierschke, T., Fisher, T.J., and Bowman, J.L. (2016). Efficient and Inducible Use of Artificial MicroRNAs in *Marchantia polymorpha*. Plant Cell Physiol. **57**: 281–290.

Flores-Sandoval, E., Eklund, D.M., and Bowman, J.L. (2015). A Simple Auxin

Transcriptional Response System Regulates Multiple Morphogenetic Processes in the Liverwort Marchantia polymorpha. PLOS Genet. **11**: e1005207.

Freeman (2008). An Overview of Plant Defenses against Pathogens and Herbivores. Plant Health Instr.

Fürst, U., Zeng, Y., Albert, M., Witte, A.K., Fliegmann, J., and Felix, G. (2020). Perception of Agrobacterium tumefaciens flagellin by FLS2XL confers resistance to crown gall disease. Nat. Plants **6**: 22–27.

Furumizu, C., Krabberød, A.K., Hammerstad, M., Alling, R.M., Wildhagen, M., Sawa, S., and Aalen, R.B. (2021). The sequenced genomes of nonflowering land plants reveal the innovative evolutionary history of peptide signaling. Plant Cell: koab173.

Gao, M., Wang, X., Wang, D., Xu, F., Ding, X., Zhang, Z., Bi, D., Cheng, Y.T., Chen, S., Li, X., and Zhang, Y. (2009). Regulation of Cell Death and Innate Immunity by Two Receptor-like Kinases in Arabidopsis. Cell Host Microbe **6**: 34–44.

Gimenez-Ibanez, S., Zamarreño, A.M., García-Mina, J.M., and Solano, R. (2019). An Evolutionarily Ancient Immune System Governs the Interactions between Pseudomonas syringae and an Early-Diverging Land Plant Lineage. Curr. Biol.: S0960982219306931.

Gou, X., Yin, H., He, K., Du, J., Yi, J., Xu, S., Lin, H., Clouse, S.D., and Li, J. (2012). Genetic Evidence for an Indispensable Role of Somatic Embryogenesis Receptor Kinases in Brassinosteroid Signaling. PLoS Genet. **8**: e1002452.

Großeholz, R., Feldman-Salit, A., Wanke, F., Schulze, S., Glöckner, N., Kemmerling, B., Harter, K., and Kummer, U. (2020). Specifying the role of BAK1-interacting receptor-like kinase 3 in brassinosteroid signaling. J. Integr. Plant Biol. **62**: 456–469.

Gust, A.A. and Felix, G. (2014). Receptor like proteins associate with SOBIR1-type of adaptors to form bimolecular receptor kinases. Curr. Opin. Plant Biol. **21**: 104–111.

Halter, T. et al. (2014a). The Leucine-Rich Repeat Receptor Kinase BIR2 Is a Negative Regulator of BAK1 in Plant Immunity. Curr. Biol. **24**: 134–143.

Halter, T. et al. (2014b). The Leucine-Rich Repeat Receptor Kinase BIR2 Is a Negative Regulator of BAK1 in Plant Immunity. Curr. Biol. **24**: 134–143.

Han, G. (2019). Origin and evolution of the plant immune system. New Phytol. **222**: 70–83.

Hayafune, M. et al. (2014). Chitin-induced activation of immune signaling by the rice

receptor CEBiP relies on a unique sandwich-type dimerization. Proc. Natl. Acad. Sci. **111**: E404–E413.

Higo, A. et al. (2018). Transcription factor DUO1 generated by neo-functionalization is associated with evolution of sperm differentiation in plants. Nat. Commun. **9**: 5283.

Hirakawa, Y., Fujimoto, T., Ishida, S., Uchida, N., Sawa, S., Kiyosue, T., Ishizaki, K., Nishihama, R., Kohchi, T., and Bowman, J.L. (2020). Induction of Multichotomous Branching by CLAVATA Peptide in Marchantia polymorpha. Curr. Biol. **30**: 3833-3840.e4.

Hirakawa, Y., Uchida, N., Yamaguchi, Y.L., Tabata, R., Ishida, S., Ishizaki, K., Nishihama, R., Kohchi, T., Sawa, S., and Bowman, J.L. (2019). Control of proliferation in the haploid meristem by CLE peptide signaling in Marchantia polymorpha. PLOS Genet. **15**: e1007997.

Hohmann, U., Lau, K., and Hothorn, M. (2017). The Structural Basis of Ligand Perception and Signal Activation by Receptor Kinases. Annu. Rev. Plant Biol. **68**: 109–137.

Hohmann, U., Nicolet, J., Moretti, A., Hothorn, L.A., and Hothorn, M. (2018). The SERK3 elongated allele defines a role for BIR ectodomains in brassinosteroid signalling. Nat. Plants **4**: 345–351.

Huang, W.R.H., Schol, C., Villanueva, S.L., Heidstra, R., and Joosten, M.H.A.J. (2020). Knocking out *SOBIR1* in *Nicotiana benthamiana* abolishes functionality of transgenic receptor-like protein Cf-4. Plant Physiol.: kiaa047.

Imkampe, J. et al. (2017). The Arabidopsis Leucine-Rich Repeat Receptor Kinase BIR3 Negatively Regulates BAK1 Receptor Complex Formation and Stabilizes BAK1. Plant Cell **29**: 2285–2303.

Ishizaki, K., Chiyoda, S., Yamato, K.T., and Kohchi, T. (2008). Agrobacterium-Mediated Transformation of the Haploid Liverwort Marchantia polymorpha L., an Emerging Model for Plant Biology. Plant Cell Physiol. **49**: 1084–1091.

J. J. Knack, Wilcox, L.W., Delaux, P.-M., Ané, J.-M., Piotrowski, M.J., Cook, M.E., Graham, J.M., and Graham, L.E. (2015). Microbiomes of Streptophyte Algae and Bryophytes Suggest That a Functional Suite of Microbiota Fostered Plant Colonization of Land. Int. J. Plant Sci. **176**: 405–420.

Jehle, A.K., Fürst, U., Lipschis, M., Albert, M., and Felix, G. (2013a). Perception of the novel MAMP eMax from different *Xanthomonas* species requires the *Arabidopsis* receptor-like protein ReMAX and the receptor kinase SOBIR. Plant Signal. Behav. **8**:

e27408.

Jehle, A.K., Lipschis, M., Albert, M., Fallahzadeh-Mamaghani, V., Fürst, U., Mueller, K., and Felix, G. (2013b). The Receptor-Like Protein ReMAX of *Arabidopsis* Detects the Microbe-Associated Molecular Pattern eMax from *Xanthomonas*. Plant Cell **25**: 2330–2340.

Jensen, S., Omarsdottir, S., Bwalya, A.G., Nielsen, M.A., Tasdemir, D., and Olafsdottir, E.S. (2012). Marchantin A, a macrocyclic bisbibenzyl ether, isolated from the liverwort Marchantia polymorpha, inhibits protozoal growth in vitro. Phytomedicine **19**: 1191–1195.

Johnson, M.A., Harper, J.F., and Palanivelu, R. (2019). A Fruitful Journey: Pollen Tube Navigation from Germination to Fertilization. Annu. Rev. Plant Biol. **70**: 809–837.

Kaku, H., Nishizawa, Y., Ishii-Minami, N., Akimoto-Tomiyama, C., Dohmae, N., Takio, K., Minami, E., and Shibuya, N. (2006). Plant cells recognize chitin fragments for defense signaling through a plasma membrane receptor. PLANT Biol.: 6.

Kato, H., Yasui, Y., and Ishizaki, K. (2020). Gemma cup and gemma development in *Marchantia polymorpha*. New Phytol. **228**: 459–465.

Kemmerling, B. et al. (2007). The BRI1-Associated Kinase 1, BAK1, Has a Brassinolide-Independent Role in Plant Cell-Death Control. Curr. Biol. **17**: 1116–1122.

Kim, E.-J. and Russinova, E. (2020). Brassinosteroid signalling. Curr. Biol. **30**: R294–R298.

Klepikova, A.V., Kasianov, A.S., Gerasimov, E.S., Logacheva, M.D., and Penin, A.A. (2016). A high resolution map of the *Arabidopsis thaliana* developmental transcriptome based on RNA-seq profiling. Plant J. **88**: 1058–1070.

Kobe, B. and Kajava, A.V. (2001). The leucine-rich repeat as a protein recognition motif. Curr. Opin. Struct. Biol. **11**: 725–735.

Kohchi, T., Yamato, K.T., Ishizaki, K., Yamaoka, S., and Nishihama, R. (2021a). Development and Molecular Genetics of *Marchantia polymorpha*. Annu. Rev. Plant Biol. **72**: annurev-arplant-082520-094256.

Kohchi, T., Yamato, K.T., Ishizaki, K., Yamaoka, S., and Nishihama, R. (2021b). Development and Molecular Genetics of *Marchantia polymorpha*. Annu. Rev. Plant Biol. **72**: annurev-arplant-082520-094256.

Kubota, A., Ishizaki, K., Hosaka, M., and Kohchi, T. (2013). Efficient *Agrobacterium* -Mediated Transformation of the Liverwort *Marchantia polymorpha* Using Regenerating Thalli. Biosci. Biotechnol. Biochem. **77**: 167–172.

Kumpf, R.P., Shi, C.-L., Larrieu, A., Sto, I.M., Butenko, M.A., Peret, B., Riiser, E.S., Bennett, M.J., and Aalen, R.B. (2013). Floral organ abscission peptide IDA and its HAE/HSL2 receptors control cell separation during lateral root emergence. Proc. Natl. Acad. Sci. **110**: 5235–5240.

Kunze, G., Zipfel, C., Robatzek, S., Niehaus, K., Boller, T., and Felix, G. (2004a). The N Terminus of Bacterial Elongation Factor Tu Elicits Innate Immunity in Arabidopsis Plants. Plant Cell **16**: 3496–3507.

Kunze, G., Zipfel, C., Robatzek, S., Niehaus, K., Boller, T., and Felix, G. (2004b). The N Terminus of Bacterial Elongation Factor Tu Elicits Innate Immunity in Arabidopsis Plants. Plant Cell **16**: 3496–3507.

Liebrand, T.W.H., van den Berg, G.C.M., Zhang, Z., Smit, P., Cordewener, J.H.G., America, A.H.P., Sklenar, J., Jones, A.M.E., Tameling, W.I.L., Robatzek, S., Thomma, B.P.H.J., and Joosten, M.H.A.J. (2013). Receptor-like kinase SOBIR1/EVR interacts with receptor-like proteins in plant immunity against fungal infection. Proc. Natl. Acad. Sci. **110**: 10010–10015.

Ligrone, R., Carafa, A., Lumini, E., Bianciotto, V., Bonfante, P., and Duckett, J.G. (2007). Glomeromycotean associations in liverworts: a molecular, cellular, and taxonomic analysis. Am. J. Bot. **94**: 1756–1777.

Liu, Simiao, Jizong Wang, Zhifu Han, Xinqi Gong, Heqiao Zhang, and Jijie Chai (2016). Molecular mechanism for fungal cell wall recognition by rice chitin receptor OsCEBiP. Structures: 1192–1200.

Liu, T., Liu, Z., Song, C., Hu, Y., Han, Z., She, J., Fan, F., Wang, J., Jin, C., Chang, J., Zhou, J.-M., and Chai, J. (2012). Chitin-Induced Dimerization Activates a Plant Immune Receptor. Science **336**: 1160–1164.

Liu, Y., Huang, X., Li, M., He, P., and Zhang, Y. (2016). Loss-of-function of *Arabidopsis* receptor-like kinase BIR 1 activates cell death and defense responses mediated by BAK 1 and SOBIR 1. New Phytol. **212**: 637–645.

Ma, C., Liu, Y., Bai, B., Han, Z., Tang, J., Zhang, H., Yaghmaiean, H., Zhang, Y., and Chai, J. (2017). Structural basis for BIR1-mediated negative regulation of plant immunity. Cell Res. **27**: 1521–1524.

Ma, X., Xu, G., He, P., and Shan, L. (2016). SERKing Coreceptors for Receptors. Trends Plant Sci. **21**: 1017–1033.

Matsui, H., Iwakawa, H., Hyon, G.-S., Yotsui, I., Katou, S., Monte, I., Nishihama, R., Franzen, R., Solano, R., and Nakagami, H. (2020). Isolation of Natural Fungal

Pathogens from Marchantia polymorpha Reveals Antagonism between Salicylic Acid and Jasmonate during Liverwort–Fungus Interactions. Plant Cell Physiol. **61**: 265–275.

Mecchia, M.A., Rövekamp, M., Giraldo-Fonseca, A., Meier, D., Gadient, P., Bowman, J.L., and Grossniklaus, U. (2020). Characterization of the single *FERONIA* homolog in *Marchantia polymorpha* reveals an ancestral role of *Cr* RLK1L receptor kinases in regulating cell expansion and morphological integrity (Evolutionary Biology).

Melotto, M., Zhang, L., Oblessuc, P.R., and He, S.Y. (2017). Stomatal Defense a Decade Later. Plant Physiol. **174**: 561–571.

Meng, X., Zhou, J., Tang, J., Li, B., de Oliveira, M.V.V., Chai, J., He, P., and Shan, L. (2016). Ligand-Induced Receptor-like Kinase Complex Regulates Floral Organ Abscission in Arabidopsis. Cell Rep. **14**: 1330–1338.

Mewari, N. and Kumar, P. (2011). Evaluation of antifungal potential of *Marchantia polymorpha* L. *, Dryopteris filix-mas* (L.) Schott and *Ephedra foliata* Boiss. against phyto fungal pathogens. Arch. Phytopathol. Plant Prot. **44**: 804–812.

Minamino, N., Norizuki, T., Mano, S., Ebine, K., and Ueda, T. (2021). Remodeling of organelles and microtubules during spermiogenesis in the liverwort *Marchantia polymorpha* (Plant Biology).

Monte, I. et al. (2018). Ligand-receptor co-evolution shaped the jasmonate pathway in land plants. Nat. Chem. Biol. **14**: 480–488.

Moussu, S., Broyart, C., Santos-Fernandez, G., Augustin, S., Wehrle, S., Grossniklaus, U., and Santiago, J. (2020). Structural basis for recognition of RALF peptides by LRX proteins during pollen tube growth. Proc. Natl. Acad. Sci. **117**: 7494–7503.

Mueller, K., Bittel, P., Chinchilla, D., Jehle, A.K., Albert, M., Boller, T., and Felix, G. (2012). Chimeric FLS2 Receptors Reveal the Basis for Differential Flagellin Perception in Arabidopsis and Tomato. Plant Cell **24**: 2213–2224.

Mueller, K., Felix, D.G., and Nürnberger, D.T. (2011). Molecular characterization of the flg22-interaction with FLS2.

Nelson, J. and Shaw, A.J. (2019). Exploring the natural microbiome of the model liverwort: fungal endophyte diversity in Marchantia polymorpha L. Symbiosis **78**: 45–59.

Nelson, J.M., Hauser, D.A., Hinson, R., and Shaw, A.J. (2018). A novel experimental system using the liverwort *Marchantia polymorpha* and its fungal endophytes reveals diverse and context-dependent effects. New Phytol. **218**: 1217–1232.

Nishihama, R., Ishida, S., Urawa, H., Kamei, Y., and Kohchi, T. (2016). Conditional Gene Expression/Deletion Systems for *Marchantia polymorpha* Using its Own Heat-Shock Promoter and Cre/ *lox* P-Mediated Site-Specific Recombination. Plant Cell Physiol. **57**: 271–280.

Pearce, G., Strydom, D., Johnson, S., and Ryan, C.A. (1991). A Polypeptide from Tomato Leaves Induces Wound-Inducible Proteinase Inhibitor Proteins. Science **253**: 895–897.

Ponce de León, I. and Montesano, M. (2017). Adaptation Mechanisms in the Evolution of Moss Defenses to Microbes. Front. Plant Sci. **8**.

Postma, J., Liebrand, T.W.H., Bi, G., Evrard, A., Bye, R.R., Mbengue, M., Kuhn, H., Joosten, M.H.A.J., and Robatzek, S. (2016). Avr4 promotes Cf-4 receptor-like protein association with the BAK1/SERK3 receptor-like kinase to initiate receptor endocytosis and plant immunity. New Phytol. **210**: 627–642.

Poveda, J. (2020). Marchantia polymorpha as a model plant in the evolutionary study of plant-microorganism interactions. Curr. Plant Biol. **23**: 100152.

Pruitt, R.N., Gust, A.A., and Nürnberger, T. (2021). Plant immunity unified. Nat. Plants **7**: 382–383.

Radhakrishnan, G.V. et al. (2020). An ancestral signalling pathway is conserved in intracellular symbioses-forming plant lineages. Nat. Plants **6**: 280–289.

Redecker, D., Kodner, R., and Graham, L.E. (2000). Glomalean Fungi from the Ordovician. Science **289**: 1920–1921.

Rich, M.K. et al. (2021). Lipid exchanges drove the evolution of mutualism during plant terrestrialization. Science **372**: 864–868.

Ron, M. and Avni, A. (2004). The Receptor for the Fungal Elicitor Ethylene-Inducing Xylanase Is a Member of a Resistance-Like Gene Family in Tomato. Plant Cell **16**: 1604–1615.

Saidi, Y., Finka, A., Chakhporanian, M., Zrÿd, J.-P., Schaefer, D.G., and Goloubinoff, P. (2005). Controlled Expression of Recombinant Proteins in Physcomitrella patens by a Conditional Heat-shock Promoter: a Tool for Plant Research and Biotechnology. Plant Mol. Biol. **59**: 697–711.

Santiago, J., Brandt, B., Wildhagen, M., Hohmann, U., Hothorn, L.A., Butenko, M.A., and Hothorn, M. (2016). Mechanistic insight into a peptide hormone signaling complex mediating floral organ abscission. eLife **5**: e15075.

Sasaki, G., Katoh, K., Hirose, N., Suga, H., Kuma, K., Miyata, T., and Su, Z.-H.

(2007). Multiple receptor-like kinase cDNAs from liverwort Marchantia polymorpha and two charophycean green algae, Closterium ehrenbergii and Nitella axillaris: Extensive gene duplications and gene shufflings in the early evolution of streptophytes. Gene **401**: 135–144.

Schwessinger, B., Roux, M., Kadota, Y., Ntoukakis, V., Sklenar, J., Jones, A., and Zipfel, C. (2011). Phosphorylation-Dependent Differential Regulation of Plant Growth, Cell Death, and Innate Immunity by the Regulatory Receptor-Like Kinase BAK1. PLoS Genet. **7**: e1002046.

Shi, C.-L. et al. (2018). The dynamics of root cap sloughing in Arabidopsis is regulated by peptide signalling. Nat. Plants **4**: 596–604.

Shi, C.-L., Alling, R.M., Hammerstad, M., and Aalen, R.B. (2019). Control of Organ Abscission and Other Cell Separation Processes by Evolutionary Conserved Peptide Signaling. Plants **8**: 225.

Shimada, T.L., Shimada, T., and Hara-Nishimura, I. (2010). A rapid and non-destructive screenable marker, FAST, for identifying transformed seeds of *Arabidopsis thaliana*. Plant J. **61**: 519–528.

Shimamura, M. (2016). *Marchantia polymorpha* : Taxonomy, Phylogeny and Morphology of a Model System. Plant Cell Physiol. **57**: 230–256.

Stegmann, M. and Zipfel, C. (2017). Complex regulation of plant sex by peptides. Science **358**: 1544–1545.

Stenvik, G.-E., Butenko, M.A., Urbanowicz, B.R., Rose, J.K.C., and Aalen, R.B. (2006). Overexpression of *INFLORESCENCE DEFICIENT IN ABSCISSION* Activates Cell Separation in Vestigial Abscission Zones in *Arabidopsis*. Plant Cell **18**: 1467–1476.

Stenvik, G.-E., Tandstad, N.M., Guo, Y., Shi, C.-L., Kristiansen, W., Holmgren, A., Clark, S.E., Aalen, R.B., and Butenko, M.A. (2008). The EPIP Peptide of INFLORESCENCE DEFICIENT IN ABSCISSION Is Sufficient to Induce Abscission in Arabidopsis through the Receptor-Like Kinases HAESA and HAESA-LIKE2. PLANT CELL ONLINE **20**: 1805–1817.

Stø, I.M., Orr, R.J.S., Fooyontphanich, K., Jin, X., Knutsen, J.M.B., Fischer, U., Tranbarger, T.J., Nordal, I., and Aalen, R.B. (2015). Conservation of the abscission signaling peptide IDA during Angiosperm evolution: withstanding genome duplications and gain and loss of the receptors HAE/HSL2. Front. Plant Sci. **6**.

Sun, Y., Li, L., Macho, A.P., Han, Z., Hu, Z., Zipfel, C., Zhou, J.-M., and Chai, J.

(2013). Structural Basis for flg22-Induced Activation of the *Arabidopsis* FLS2-BAK1 Immune Complex. Science **342**: 624–628.

Thuerig, B., Felix, G., Binder, A., Boller, T., and Tamm, L. (2005). An extract of Penicillium chrysogenum elicits early defense-related responses and induces resistance in Arabidopsis thaliana independently of known signalling pathways. Physiol. Mol. Plant Pathol. **67**: 180–193.

Voinnet, O., Rivas, S., Mestre, P., and Baulcombe, D. (2003). Retracted: An enhanced transient expression system in plants based on suppression of gene silencing by the p19 protein of tomato bushy stunt virus: *An enhanced transient expression system in* N. benthamiana. Plant J. **33**: 949–956.

de Vries, J. and Archibald, J.M. (2018). Plant evolution: landmarks on the path to terrestrial life. New Phytol. **217**: 1428–1434.

Wachsman, G. and Heidstra, R. (2010). The CRE/lox System as a Tool for Developmental Studies at the Cell and Tissue Level. In Plant Developmental Biology: Methods and Protocols, L. Hennig and C. Köhler, eds (Humana Press: Totowa, NJ), pp. 47–64.

Wang, Y., Li, Z., Liu, D., Xu, J., Wei, X., Yan, L., Yang, C., Lou, Z., and Shui, W. (2014). Assessment of BAK1 activity in different plant receptor-like kinase complexes by quantitative profiling of phosphorylation patterns. J. Proteomics **108**: 484–493.

Westermann, J., Koebke, E., Lentz, R., Hülskamp, M., and Boisson-Dernier, A. (2020). A Comprehensive Toolkit for Quick and Easy Visualization of Marker Proteins, Protein–Protein Interactions and Cell Morphology in Marchantia polymorpha. Front. Plant Sci. **11**: 569194.

Willmann, R. et al. (2011). *Arabidopsis* lysin-motif proteins LYM1 LYM3 CERK1 mediate bacterial peptidoglycan sensing and immunity to bacterial infection. Proc. Natl. Acad. Sci. **108**: 19824–19829.

Xie, C.-F. and Lou, H.-X. (2009). Secondary Metabolites in Bryophytes: An Ecological Aspect. Chem. Biodivers. **6**: 303–312.

Yoo, S.-D., Cho, Y.-H., and Sheen, J. (2007). Arabidopsis mesophyll protoplasts: a versatile cell system for transient gene expression analysis. Nat. Protoc. **2**: 1565–1572.

Yu, C.Y., Zhang, H.K., Wang, N., and Gao, X.-Q. (2021). Glycosylphosphatidylinositol-anchored proteins mediate the interactions between pollen/pollen tube and pistil tissues. Planta **253**: 19.

Yu, X., Feng, B., He, P., and Shan, L. (2017). From Chaos to Harmony: Responses

and Signaling upon Microbial Pattern Recognition. Annu. Rev. Phytopathol. **55**: 109–137.

Zhang, L., Hua, C., Pruitt, R.N., Qin, S., Wang, L., Albert, I., Albert, M., van Kan, J.A.L., and Nürnberger, T. (2021). Distinct immune sensor systems for fungal endopolygalacturonases in closely related Brassicaceae. Nat. Plants **7**: 1254–1263.

Zhang, L., Kars, I., Essenstam, B., Liebrand, T.W.H., Wagemakers, L., Elberse, J., Tagkalaki, P., Tjoitang, D., van den Ackerveken, G., and van Kan, J.A.L. (2014). Fungal Endopolygalacturonases Are Recognized as Microbe-Associated Molecular Patterns by the Arabidopsis Receptor-Like Protein RESPONSIVENESS TO BOTRYTIS POLYGALACTURONASES1. Plant Physiol. **164**: 352–364.

Zhang, W., Fraiture, M., Kolb, D., Löffelhardt, B., Desaki, Y., Boutrot, F.F.G., Tör, M., Zipfel, C., Gust, A.A., and Brunner, F. (2013). *Arabidopsis* RECEPTOR-LIKE PROTEIN30 and Receptor-Like Kinase SUPPRESSOR OF BIR1-1/EVERSHED Mediate Innate Immunity to Necrotrophic Fungi. Plant Cell **25**: 4227–4241.

Zhang, X., Henriques, R., Lin, S.-S., Niu, Q.-W., and Chua, N.-H. (2006). Agrobacterium-mediated transformation of Arabidopsis thaliana using the floral dip method. Nat. Protoc. **1**: 641–646.

Zhu, Q., Shao, Y., Ge, S., Zhang, M., Zhang, T., Hu, X., Liu, Y., Walker, J., Zhang, S., and Xu, J. (2019). A MAPK cascade downstream of IDA–HAE/HSL2 ligand–receptor pair in lateral root emergence. Nat. Plants **5**: 414–423.

Zipfel, C., Kunze, G., Chinchilla, D., Caniard, A., Jones, J.D.G., Boller, T., and Felix, G. (2006). Perception of the Bacterial PAMP EF-Tu by the Receptor EFR Restricts Agrobacterium-Mediated Transformation. Cell **125**: 749–760.

9 Acknowledgment

I would like to thank several people, who supported me during my time as a PhD at the ZMBP in Tübingen. Without their help and support I wouldn´t have enjoyed this experience as much as I did.

Thank you, Prof. Dr. Georg Felix to give me this great opportunity in 2018 and supervising my thesis. I enjoyed all the discussions we had and was able to learn a lot from it. But I also really apricate the fun conversations, which made this PhD very enjoyable and special.

Thank you, Prof. Dr. Rosa Lozano-Durán for joying my committee and being the second supervisor of my thesis.

I would also like to thank Dr. Farid El Kasmi and Dr. Andrea Guts for being part of my TAC and always giving me useful feedback and support.

Thank you, AG Felix. I am very fortunate to spend my time in such a collegial environment with lots of fruitful discussions and great fun. I did not only gain knowledge and experience but also great friends. I would particularly like to mention Luby and Loui, great friend with an open hear and advise, as well as Dr. Judith Fliegmann, who help me a lot with discussions and proofreading of this thesis.

A big Thank you to the whole plant biochemistry, great colleagues, friends and sense of community.

Last but not least, I would like to thank my husband, Kai, my family and my friends for their love, encouragement and confidence in me!

List of abbreviations

A

AM · *arbuscular mycorrhiza*

ANX1 · *ANXUR1*

approx · *approximately*

AZ · *abscission zone*

B

BAK1 · *BRI1-associated receptor Kinase 1*

BIR1 · *BAK1-interacting receptor-like kinase 1*

BUPS · *BUDDHA´S PAPER SEAL*

C

CEBiP · *chitin elicitor-binding protein*

CERK · *chitin elicitor receptor kinase*

*Cr*RLK1L · *Catharanthus roseus RLK1-like*

D

DAB · *3´-3´-Diaminoenzidine*

DAMPs · *damage associated molecular patterns*

E

ECD · *ectodomain*

EFR · *EF-Tu receptor*

EF-Tu · *elongation factor- Tu*

EGF · *epidermal growth factor*

Eix2 · *ethylene-inducing xylanase*

EPIP · *extended PIP*

ETI · effector-triggered immunity

F

FLS2 · *flagellin sensing 2*

G

GPI · glycosylphosphatidylinositol

H

HAE · *HAESA*

HSL2 · *HAE-like2*

I

IDA · *inflorescence deficient in abscission*

IDL · *IDA-like*

IP-MS · *Immuno precipitation-Mass Spectrometry*

L

LORELEI-like GLYCOLPHOSPHATIDYLINOSITOL (GPI)-ANCHORED PROTEINS2 · LORELEI-like GLYCOLPHOSPHATIDYLINOSITOL (GPI)-ANCHORED PROTEINS2

LRP · *lateral root primordia*

LRR · *leucine rich repeat*

LRR-RLKs · *LRR receptor-like protein*

LRR-RLP · LRR receptor-like protein

LRX · *leucine-rich repeat extensin protein*

LYKs · *LysM receptor kinases*

LYMs · *LysM-RLPs*, *LysM-RLPs*

LysM · *lysin motif*

M

MAMP · *microbe associated molecular pattern*

N

NaOAc · *Natriumacetate*

NGA · *N-acetyl-D-glucosamine*

NLR · *nucleotide-binding domain leucine-rich repeat*

O

oJM · *outer juxtamembrane*

P

PAMP · *pathogen associated molecular pattern*

PCR · *Polymerase-Chain-Reaction*

PEG · *Polyethylenglukol*

pFRK1 · *flg22-induced receptor-like kinase1*

PG · *endopolygalacturonases*

PRRs · *pattern recognition receptor*

PTI · PAMP-triggered immunity

R

RALF · *rapid alkalinization factor*

RBOHD · *respiratory burst oxidase homolog protein D*

RKs · receptor kinases

RLU · *relative light unit*

RP · *resistance proteins*

S

SB · *SDS sample buffer*

SEM · *scanning electron microscopy*

SERK · somatic embryogenesis receptor kinase

SOBIR · Suppressor of BIR1

SOBIR1 · *suppressor of BIR1-1*

T

TM · transmembrane domain

List of table

List of figures